

PHOTOSMOREGULATION: EVIDENCE OF HOST BEHAVIORAL PHOTOREGULATION  
OF AN ALGAL ENDOSYMBIONT BY THE ACOEL *CONVOLUTRILOBA RETROGEMMA*  
AS A MEANS OF NON-METABOLIC OSMOREGULATION

by

THOMAS SHANNON III

(Under the Direction of William K. Fitt)

ABSTRACT

This study examines the photobehaviors of the acoel *Convolutriloba retrogemma*, the factors affecting these behaviors, their regulatory functions, and how they affect or are affected by the acoel's algal endosymbiont. The first behavior detailed is a step-up, photophobic response to sudden increases in light. The variable response is blue-light-mediated and triggered by visual, photic stimuli. The second behavior detailed is a phototactic-photoaccumulative behavior responsible for observed mass basking formations. The photoaccumulative behavior is regulated by the photosynthetic activity of the algal endosymbiont. It is not exhibited by aposymbiotic animals. The effects of holozoic starvation are examined, particularly as they apply to host phototactic and photoaccumulative behavior. The data show that contrary to expected behavior, acoels denied prey for over 20 days do not seek out areas of high intensity light, but instead retreat to areas of lower intensity or to shadows. The results of this study support a hypothesis that the basking behaviors of these acoels serve as methods of photoregulating their algal endosymbionts. The results further suggest that starved acoels have diminished capabilities for processing translocated algal photosynthates and that under high-light

conditions a build-up of these compounds results in hyposmotic stress in the animals. It is suggested that the photoregulatory basking behaviors of *C. retrogemma* may function as a method of host osmoregulation and that intercellular change in osmotic pressure resulting from photosynthesis is the photoregulatory stimulus. The term “photosmoregulation” is offered to describe the process.

Presented is a novel method for detecting the movements of photosynthate *in vivo* in *C. retrogemma* utilizing differential weight change in animals subjected to light and dark treatments without holozoic feeding. Though successful in yielding desired results, the method was decidedly labor-intensive and an alternative method is suggested. Also presented is a refined method for the separation of algal symbionts from host tissue, and a method for determining accurate wet-weight of this and other soft-bodied, invertebrate species. Lastly, contained herein is a monograph describing a new species of acoel, *Convolutriloba macropyga*.

INDEX WORDS: *Convolutriloba retrogemma*, *Convolutriloba macropyga*, acoel, alga, symbiont, zoochlorellae, photosynthate, translocation, wet weight, photomovements, behavior, photoregulation, osmoregulation, photosmoregulation, nutrition, response, light emitting diode, halo

PHOTOSMOREGULATION: EVIDENCE OF HOST BEHAVIORAL PHOTOREGULATION  
OF AN ALGAL ENDOSYMBIONT BY THE ACOEL *CONVOLUTRILOBA RETROGEMMA*  
AS A MEANS OF NON-METABOLIC OSMOREGULATION

by

THOMAS SHANNON III

B.A., Saint Mary's College of Maryland, 2000

A Dissertation Submitted to the Graduate Faculty of The University of Georgia in Partial  
Fulfillment of the Requirements for the Degree

DOCTOR OF PHILOSOPHY

ATHENS, GEORGIA

2007

© 2007

Thomas Shannon III

All Rights Reserved

PHOTSMOREGULATION: EVIDENCE OF HOST BEHAVIORAL PHOTOREGULATION  
OF AN ALGAL ENDOSYMBIONT BY THE ACOEL *CONVOLUTRILOBA RETROGEMMA*  
AS A MEANS OF NON-METABOLIC OSMOREGULATION

by

THOMAS SHANNON III

Major Professor: William K. Fitt  
Committee: Mark A. Farmer  
Walter I. Hatch  
James W. Porter  
Gregory W. Schmidt

Electronic Version Approved:

Maureen Grasso  
Dean of the Graduate School  
The University of Georgia  
August 2007

For Tink

## TABLE OF CONTENTS

	Page
LIST OF FIGURES .....	vi
CHAPTER	
1 INTRODUCTION .....	1
2 LITERATURE REVIEW: AN OVERVIEW OF OSMOREGULATION IN ANIMALS AND THE POTENTIAL OSMOTIC IMPLICATIONS OF ALGAL-INVERTEBRATE SYMBIOSES .....	11
3 A NOVEL METHOD FOR THE DETERMINATION OF PHOTOSYNTHATE TRANSLOCATION IN AN ALGAL-ACOEL SYMBIOTIC SYSTEM: A QUALITATIVE APPROACH.....	41
4 PHOTOMOVEMENTS OF <i>CONVOLUTRILOBA RETROGEMMA</i> .....	67
5 PHOTOREGULATION AS A METHOD OF OSMOREGULATION IN THE SYMBIOTIC SYSTEM OF <i>CONVOLUTRILOBA RETROGEMMA</i> .....	93
6 <i>CONVOLUTRILOBA MACROPYGA</i> SP. NOV., AN UNCOMMONLY FECUND ACOEL (ACOELOMORPHA) DISCOVERED IN TROPICAL AQUARIA.....	122
7 CONCLUSION AND FUTURE DIRECTION .....	158

## LIST OF FIGURES

Figure 1.1. Photomicrograph of live <i>Convolutriloba</i> spp. Shown are representatives of the four described species: <i>C. retrogemma</i> , <i>C. hastifera</i> , <i>C. longifissura</i> , and <i>C. macropyga</i> . Specimens were viewed on a Wild M3Z stereomicroscope and photographed with a Sony DSC-P71 digital still camera.....	9
Figure 1.2. Comparative photomicrograph of live, sexually-immature <i>Convolutriloba</i> spp. A. <i>Convolutriloba retrogemma</i> B. <i>Convolutriloba hastifera</i> C. <i>Convolutriloba longifissura</i> D. <i>Convolutriloba macropyga</i> . Specimens were viewed on a Wild M3Z stereomicroscope and photographed with a Sony DSC-P71 digital still camera. ....	10
Figure 3.1. Schematic representation of the dewatering device used for the non-disruptive, vacuum-assisted, removal of water (external medium) from live acoels prior to weighing the animals. The device was fabricated from common PVC pipe and fittings.....	60
Figure 3.2. Photograph of apparatus used for removing water (external medium) from live acoels. A. Vacuum-assisted dewatering device. Vacuum source connects to barbed fitting. Valve allows for fine control of suction at the dewatering stage (top of device). B. Chamber used to hold acoels for PAM fluorometry. C. Underside of chamber designed to connect to dewatering stage to remove water from acoels. Center hole covered with 14 micron plankton net to support acoels during dewatering and fluorometry processes. D. Chamber connected to PAM fiber-optic cable. ....	61
Figure 3.3. Effective quantum yield of photosystem II in the zoochloellae endosymbionts ( <i>in vivo</i> ) of <i>Convolutriloba retrogemma</i> , determined by PAM fluorometry, as a function of DCMU concentration in the external medium. Error bars represent 95% confidence intervals. ....	62
Figure 3.4. Percent weight change (loss) of <i>Convolutriloba retrogemma</i> kept in total darkness for 7 days as a function of DCMU concentration in the external medium compared to control group (no DCMU). Error bars represent 95% confidence intervals. ....	63
Figure 3.5. Percent weight loss of <i>Convolutriloba retrogemma</i> subjected to 4 treatments (Light, Light with DCMU, Dark, and Dark with DCMU). Light was provided at an irradiance of 70 $\mu\text{mole}\cdot\text{m}^{-2}\cdot\text{s}^{-1}$ , [DCMU]=0.1 $\mu\text{M}$ , $n_{\text{LC}}=37$ , $n_{\text{LD}}=46$ , $n_{\text{DC}}=46$ , $n_{\text{DD}}=45$ . Error bars represent 95% confidence intervals. Results indicate positive photosynthetic carbon fixation and net transfer of photosynthate from algae to host. ....	64



Figure 3.6. Percent weight loss of *Convolutriloba retrogemma* subjected to 4 treatments. Same as previous figure, but with non-photosynthetic effects of DCMU removed from the data corresponding to the treatments utilizing DCMU. Error bars represent 95% confidence intervals. Data clearly show significantly higher weight loss in acoels kept in the dark and those treated with DCMU, indicating a net translocation of photosynthate from symbiont to host.....65

Figure 3.7. Post-test zoochlorellae densities in Light and Dark Control group acoels used in the carbon-translocation experiment. Density was measured as algal cells per milligram of host tissue. Error bars represent 95% confidence intervals.....66

Figure 4.1. Characteristic halo-formation resulting from the photoaccumulative behavior of basking *Convolutriloba retrogemma*. Aggregations, 2–5 cm wide, of the acoel generally form between 1 and 6 cm surrounding objects on flat substrate.....83

Figure 4.2. Schematic representation of light chamber and time-lapse photography apparatus utilized in the photomovement experiments.....84

Figure 4.3. Transmittance spectra of the filters used in determining and defining the short-term response of *Convolutriloba retrogemma* to a step-up, sudden increase in light intensity. These filters were used in conjunction with a halogen, fiber-optic light source.....85

Figure 4.4. Photographs of light chamber used in photomovement experiments. A. Chamber with camera and LED light-source attached. Thin tubing at top supplies moisture-saturated air, lower penetrations are cooling-water supply and return lines. Inset shows actual photograph taken during the photophobic response experiments. B. Top view of LED light-source showing interchangeable resistors, dimmer control and power switch. C. Bottom view of LED light-source showing array of six interchangeable LED lamps (470 nm peak  $\lambda$  shown).....86

Figure 4.5. Normalized output spectra of the five light emitting diodes used in the photophobic response experiments. Wavelength peaks were at 470, 525, 589, 610, and 630 nm respectively for the blue, green, yellow, orange, and red LED lamps.....87

Figure 4.6. Graphic representation of relative light intensity at substrate level with respect to distance from an object. The colored portion of the graph, between the dashed lines, corresponds to the approximate 2–5 cm area surrounding an object in which *Convolutriloba retrogemma* exhibit their halo-forming basking behavior.....88

Figure 4.7. Percentage of acoels remaining in lighted region vs. time. Open circles represent means of  $n = 5$  experimental trials under high intensity white-light ( $260 \mu\text{mole}\cdot\text{m}^{-2}\cdot\text{s}^{-1}$ ), shaded circles represent means under low intensity white-light ( $145 \mu\text{mole}\cdot\text{m}^{-2}\cdot\text{s}^{-1}$ ). 50 acoels were used in each trial. Error bars represent 95% confidence intervals at each time step. A marked step-up, photophobic response was evident under both light treatments, though somewhat slower and less-pronounced under low intensity light.....89

Figure 4.8. Percentage of acoels remaining in lighted region vs. time – photophobic response – Circle color represents color of filter used in each experiment. Each circle represents the mean of  $n = 5$  trials. Light-source intensity was constant over all treatments ( $260 \mu\text{mole}\cdot\text{m}^{-2}\cdot\text{s}^{-1}$ ); actual (colored) intensity at the water surface varied depending on the filter used (see fig. 4.4). 50 acoels were used in each trial. Error bars represent 95% confidence intervals at each time step. A step-up, photophobic response was evident under both blue and blue-green light treatments, whereas no response was observed under red light. ....90

Figure 4.9. Percentage of acoels remaining in lighted region vs. time – photophobic response – Circle color represents LED color used in each experiment. Each experiment consisted of  $n = 6$  trials. 50 acoels were used in each trial. Light intensity was kept equal across all experiments regardless of wavelength. Error bars are 95% confidence intervals at each time step. The data confirm that the step-up photophobic response, indicated in figures 4.5 and 4.6, was blue-light mediated. ....91

Figure 4.10. Percentage of acoels in lighted region vs. time – photoaccumulative response – Green circles represent means from control trials involving symbiotic acoels. Red circles represent means from trials involving aposymbiotic acoels. 15 acoels were used in each trial,  $n = 5$  trials per treatment. White-light intensity in all trials was  $1 \mu\text{mole}\cdot\text{m}^{-2}\cdot\text{s}^{-1}$ . Error bars represent 95% confidence intervals at each time step. The data indicate that the photoaccumulative response was mediated by a factor related to the photosynthetic activity of the algal endosymbiont. ....92

Figure 5.1. Functional relationship between wet weight (ww), dry weight (dw), and ash-free dry weight (afdww) of *Convolutriloba retrogemma*. The top line (closed circles) represents wet weight vs. dry weight ( $\text{dw} = 0.1111 \times \text{ww}$ ,  $R^2 = 0.98$ ). The bottom line (open circles) represents wet weight vs. ash-free dry weight ( $\text{afdww} = 0.0798 \times \text{ww}$ ,  $R^2 = 0.96$ ). ....113

Figure 5.2. Light preference of fed vs. starved *Convolutriloba retrogemma*. Independent axis corresponds to the irradiance levels measured in six sections of a test trough. Acoels were counted in each of the six sections after 10 days. Data were averaged from 10 trials each of fed and starved acoels; 30 individuals were used in each trial. Error bars represent 95% confidence intervals. ....114

Figure 5.3. Light preference of fed vs. starved *Convolutriloba retrogemma*. Independent axis corresponds to the combined results of the three lowest and the three highest irradiance levels shown in figure 5.1. Error bars represent 95% confidence intervals. ....115

Figure 5.4. Preliminary comparisons of chlorophyll *a*, protein, carbon, and nitrogen concentrations in Fed (F) vs. Starved (S) *Convolutriloba retrogemma* subjected to one of two irradiance treatments for 12 hours. Control (C) irradiance level was  $50 \mu\text{mole}\cdot\text{m}^{-2}\cdot\text{s}^{-1}$ , High (H) irradiance level was  $166 \mu\text{mole}\cdot\text{m}^{-2}\cdot\text{s}^{-1}$ . Error bars represent 95% confidence intervals. Though individual experiment results were inconclusive, concentrations of all substances tested decreased in starved acoels subjected to high light suggesting an influx of osmotic water into the animals' tissues. ....116

Figure 5.5. Comparison of carbon/nitrogen ratios in fed vs. starved *Convolutriloba retrogemma* subjected to one of three irradiance treatments. Error bars represent 95% confidence intervals. By examining the C:N ratio, the osmotic water effect in the starved groups is eliminated. The over-all higher averages seen in the starved groups suggest increased carbon levels (photosynthates) regardless of light intensity. The increase in C:N ratio in both fed and starved groups suggests an upper limit on the rate at which photosynthate can be transferred into, and metabolized by, host cells. ....117

Figure 5.6. Comparison of the differences in carbon/nitrogen ratios between control (50  $\mu\text{mole}\cdot\text{m}^{-2}\cdot\text{s}^{-1}$ ) and high (166  $\mu\text{mole}\cdot\text{m}^{-2}\cdot\text{s}^{-1}$ ) irradiance treatments on fed vs. starved *Convolutriloba retrogemma*. Error bars represent 95% confidence intervals. No statistical difference is shown, further suggesting a maximum limit on a host's ability to metabolize or otherwise utilize translocated endosymbiotic photosynthates. ....118

Figure 5.7. Percent weight change in dark-adapted *Convolutriloba retrogemma* weighed before and after being subjected to one hour of PAR irradiance (800  $\mu\text{mole}\cdot\text{m}^{-2}\cdot\text{s}^{-1}$ ) as measured over a one month starvation regimen. Each point represents the average of 24 acoels tested. Error bars represent 95% confidence intervals. A consistently positive, increasing weight gain was noticed in the animals beginning around the 10<sup>th</sup> day of starvation. A decreasing weight gain trend began after the 25<sup>th</sup> day of starvation, and no weight change was measured on day 31. The red data point at day 24 represents the average weight change of 24 acoels subjected to 50  $\mu\text{M}$  DCMU to inhibit photosynthesis. ....119

Figure 5.8. Percent weight change in *Convolutriloba retrogemma* as measured over a one month starvation regimen. The left-hand, blue, dependent axis and associated blue data points represent the same data shown in figure 5.5. The right-hand, red, dependent axis and associated red data points represent the average weight of acoels tested on each respective day of starvation as a percentage of the average weights measured on day zero. Pre-light-treatment weights were used. Smoothed lines represent a moving average of the corresponding data to better show the general trends. ....120

Figure 5.9. Percent water content of Fed (F) and Starved (S) *Convolutriloba retrogemma* subjected to PAR irradiance treatments: Control (C) = 50  $\mu\text{mole}\cdot\text{m}^{-2}\cdot\text{s}^{-1}$  and High (H) = 166  $\mu\text{mole}\cdot\text{m}^{-2}\cdot\text{s}^{-1}$ . Error bars represent 95% confidence intervals. Acoels were tested on the 32<sup>nd</sup> day of the starvation regimen. As shown, a significant difference was found between the fed and the starved treatments; however, no significant differences were found between irradiance treatments within fed or starved groups. ....121

Figure 6.1. *Convolutriloba macropyga* **sp. nov.**; photomicrographs of living, non-anaesthetized, non-squeezed specimens. A. Dorsal view of a large sub-adult with asexual buds and multiple median caudal lobes. B. Ventral view of smaller sub-adult exhibiting the characteristic “capturing funnel” leading to the mouth. Visible are the maturing false seminal vesicles terminating at the male gonopore forward of the central red-pigment spot. C. Dorsal view of an immature, asexually-produced progeny showing the characteristic two rounded lateral caudal lobes and single, longer, slender median caudal lobe. ....149

Figure 6.2. *Convolutriloba macropyga* sp. nov.; photomicrographs of living specimens. A. Dorsal view of whole anaesthetized specimen. Black arrowhead points to eyespot, black arrow to diamond-shaped spot of pigment cells. B. Ventral view of whole anaesthetized specimen. White arrowhead indicates mouth, white arrow seminal bursa and bursal nozzle tissue, black arrowhead ventral flap, and black arrow male gonopore. C. Dorsal view of cluster of three specimens showing refractive blue sheen. D. Dorsal body surface with blue concretions in incident light. E. Dorsal body surface with concretions in transmitted light. F. Rhabdoid glands of dorsal body wall. Arrow indicates refractile, uncolored rhabdoids; asterisk marks red rhabdoid gland cell; arrowhead indicates symbiotic algal cell. ....150

Figure 6.3. *Convolutriloba macropyga* sp. nov.; reconstructions to show arrangement of organs. A. Dorsal view. The gonads are paired but for clarity just the left testis and right ovary are shown. Arrows point to buds on lateral caudal lobes, arrowheads to paired ganglia and eyefields. B. Sagittal reconstruction of male copulatory organ. Peripheral parenchyma not shown. C. Sagittal reconstruction of female copulatory organ. Arrow points to female gonopore. Peripheral parenchyma not shown. ....151

Figure 6.4. *Convolutriloba macropyga* sp. nov.; whole mount stained with Alexa-488-labeled phalloidin and viewed with confocal microscopy. A. Optical section of ventral body-wall musculature. Anterior toward upper left corner. White arrows point to longitudinal muscles, white arrowheads to radial muscles, black arrowheads to U-shaped muscles. B. Projection of ventral and lateral body-wall musculature adjacent to the mouth (in upper left corner). ....152

Figure 6.5. *Convolutriloba macropyga* sp. nov.; reconstructions to show ventral body-wall musculature. For clarity just a few muscles are shown. Scale bar: 1 mm. A. All muscle components. B. Circular muscles. C. U-shaped muscles and longitudinal cross-over muscles. D. Special pore muscles and longitudinal muscles. ....153

Figure 6.6. *Convolutriloba macropyga* sp. nov.; photomicrographs of living specimens. A. Dorsal view of female copulatory organ with two bursal nozzles. Black arrowheads point to bursal nozzles. B. Dorsal view of female copulatory organ with three bursal nozzles. Black arrowheads point to bursal nozzles. ....154

Figure 6.7. *Convolutriloba macropyga* sp. nov.; photomicrographs of live juvenile. A. Dorsal view of whole specimen. Arrow points to statocyst, arrowhead to frontal pore. B. Frontal organ. Arrow points to frontal pore. C. Statocyst. Arrowheads point to nuclei of parietal cells; asterisk marks statolith. D. Rhabdoid gland cell. ....155

Figure 6.8. Light experiments in *Convolutriloba macropyga* sp. nov. and the *Convolutriloba* genus. A. Progeny release rates of *Convolutriloba macropyga* sp. nov. in response to light intensity. The experiment involved 24 adult specimens each in one of three light treatments: dark, low light, and high light. Trials ran for 15 days. Results are presented as average number of asexual progeny released per individual per day. Error bars are 95% confidence intervals. B. Comparison of dark-survival of species within the genus. Twenty-four adult animals of each species (*C. retrogemma*, *C. longifissura*, *C. hastifera*, and *C. macropyga*) were subjected to total darkness to determine and compare the extent of the obligate nature of algal symbiosis between the different host species. *Artemia* sp. prey was provided daily in superabundance to minimize the variable of holozoic starvation. Results are presented as percent survival over time.....156

Figure 6.9. Environmental tolerances of *Convolutriloba macropyga* sp. nov.; A. Salinity tolerance. Animals were subjected to a range of artificial seawater salinities,  $n = 6$  per salinity. Surviving numbers were recorded every 12 hours for three days. No change in survival percentages was noted after 60 hours. Second order polynomial regressions were fit to each data set;  $r^2 = 0.81$  for 60-hour regression line. Fifty percent lethality occurred at 24 and 44 ppt. B. Thermal tolerance. Animals were subjected to a range of temperatures,  $n = 20$  at each temperature tested. Surviving numbers were recorded every 24 hours for three days. ....157

## CHAPTER 1

### INTRODUCTION

Examples of symbioses with photosynthetic algae exist in many marine invertebrates including members of the Protista, Porifera, Cnidaria, Mollusca, Ascidia, and Acoelomorpha (Smith & Douglas 1987; Smith 1991; Trench 1993; Douglas 1994). Although the intricacies of these symbiotic relationships differ considerably between taxa, most are mutualistic to some extent with the algae providing products of photosynthesis to the host and the host maintaining the algae in the photic zone. In most instances, as in corals and their zooxanthellae, the host is heterotrophic and the symbiosis can be either obligate or facultative. In some symbioses, however, like that between the acoel *Symsagittifera (Convoluta) roscoffensis* Graff 1891, and the alga *Tetraselmis convolutae*, the host depends solely on its algae. In this particular relationship, the adult worm ceases to feed holozoically (Gamble & Keeble 1903; Keeble 1910) and derives all its nutritional and metabolic requirements from its endosymbionts.

Algal-invertebrate symbioses are thought to have evolved in adaptation to nutrient-poor environments such as reef systems where most nutrients are locked up in, and quickly recycled back into biomass (Muscatine & Porter 1977; Muscatine & Delia 1978). An interdependent relationship with a heterotrophic host benefits zooxanthellae or other algal endosymbionts by allowing them to become a part of the recycling process. By fitting into this process, the algae are afforded much higher concentrations of dissolved nutrients than they would encounter as phytoplankton. Comparisons of low phytoplankton densities in surface waters and high cellular densities of zooxanthellae in corals of tropical reef systems (Cook & Delia 1987), support the concept of tight nutrient cycling and illustrate the mutual benefit of symbioses between marine invertebrates and algae.

*Convolutriloba retrogemma* (Hendelberg & Åkesson 1988) is a heterotrophic, acoel in obligate symbiosis with an endosymbiotic, green alga. Hendelberg & Åkesson (1991) studied

the effect of light and feeding on the asexual reproduction rates of these acoels, and noted that an increase in photoperiod, or an increase in light intensity resulted in a higher reproductive rate. Furthermore, they showed that acoels allowed to feed holozoically on the larval nauplii of *Artemia* sp. had higher reproduction rates than those denied food. These observations suggested that both holozoic feeding and increased symbiont photosynthetic activity benefit the host. Any worm fed holozoically and deprived of light for 34-36 days, they found, lost its endosymbionts and died (Åkesson & Hendelberg 1989).

*C. retrogemma*, differs from *S. roscoffensis*, in that although it can survive extended periods without feeding holozoically, its full nutritional requirements cannot be met by the products of the endosymbiont. As evidence, Åkesson & Hendelberg (1989) noted that when *C. retrogemma* was denied holozoic feeding for extended periods, asexual budding ceased and body size decreased. The benefit of host metabolic processes to the symbiont was also illustrated in that host starvation resulted in decreased algal densities.

In a review of the symbiotic relationships between corals and their zooxanthellae, Muller-Parker & D'Elia (1997) note that corals must balance the benefits of photosynthate production and the costs of containing and maintaining their algae. Some of the costs they list include mechanisms necessary for coping with reactive oxygen species from photosynthesis, mechanisms for regulating the growth rates of their symbionts, and mechanisms for providing UV protection for the algae and their own tissues. They explain that exposures to environmental extremes in salinity, temperature or light levels tend to destabilize symbioses and can lead to bleaching, and even death, when the costs to sustain the symbionts are too high.

The symbiotic anemone *Anthopleura elegantissima*, like many other “sessile” cnidarians, contracts and expands its tentacles in response to visible light. In studying this animal, Pearse



(1974a) observed that the degree of expansion or contraction corresponded “with striking uniformity” to the relative intensity of light. Zooxanthellate animals, she noted, expanded in moderate light, and contracted in intense light or in darkness; this host behavior, she suggested, may serve as a mechanism of photoregulating the symbiont. In a related study, Pearse (1974b) observed phototactic behaviors exhibited by symbiotic *A. elegantissima*, but not by aposymbiotic animals. This behavior, dependent on the presence of the algal endosymbiont, varied according to the light intensity of the area from where the animal was collected, and appeared to serve a photoregulatory purpose as well.

*Convolutriloba retrogemma* spends most of its time flattened dorso-ventrally, basking, to provide light for its endosymbionts (Hendelberg & Åkesson 1988). I began studying this acoel, as an undergraduate, in 1999 when it was discovered in the research aquaria at St. Mary’s College of Maryland. One of the initial observations I made of the species was the peculiar, halo-shaped aggregations of hundreds of basking animals that would form around the bases of objects (see page 83, Fig. 4.1). Over a short period of time, two other basking behaviors were noted. The first of these behaviors was observed in animals that had settled on the vertical sides of the aquaria, whereby they would project the front half of their body away from the side and into the water column perpendicular to the directional light source. The other behavior, related to the halo-formations, occurred as the result of laying a yardstick across the top of a shallow, trough-style aquarium. Upon retrieving the stick ~ 20 hours later, a very distinct, eerily-straight aggregation of acoels was observed on the illuminated area of the substrate along the entire length of the shadow the yardstick had cast. Based entirely on this last formation, my initial hypothesis was formed; that the halo-formations of basking *Convolutriloba retrogemma* were either a method of photoregulation, a result of photoregulation, or a combination of the two.

Over the remainder of my undergraduate studies, I furthered my observations of this intriguing acoel and familiarized myself with the other two species in the genus, *Convolutriloba hastifera* Winsor 1990, and *Convolutriloba longifissura* Bartolomaeus & Balzer 1997. My interests in the genus, the symbioses, and the photobehaviors followed me into graduate school where I wasted no time converting an unused constant-temperature room into my own personal wet-lab and set about constructing an intricate, marine, tropical-reef mesocosm. I maintained mono-specific cultures and a mixed population of all three convolutrilobids over the duration of my doctoral studies, and in my final year discovered a fourth species, described it (Shannon & Achatz 2007), threw it into the mix (Fig. 1.1), and cultured it too.

The new species had me puzzled at first in that its mode of asexual reproduction was identical to the “unique” reverse-budding of *C. retrogemma*. It was, however, significantly larger (Fig. 1.2). In sharing my discovery with my acoelous peers and colleagues, I initially described it as best I could as “a big-ass retro!”; samples were sent out for DNA analysis labeled acronymically as BAR1, BAR2, etc., and the moniker stuck. In chapter 6 of this dissertation, and in the published description, I explain the etymology of the specific epithet as a derivation of the Greek *macro-* (large) and *pyga* (rump), and claim that it “reflects the extensive expansion of the posterior region of the body, especially while basking”. If you are reading *this* paragraph, you are one of the privileged few who know the true story behind the name *Convolutriloba macropyga*... lucky you.

The primary focus of my doctoral research was to determine what, if any, regulatory processes influenced the basking behaviors, as well as an observed photophobic behavior, of *C. retrogemma*. The lay-out of this dissertation does not follow the chronology of my experiments

or discoveries, but was designed instead to follow what a *normal* person would consider a logical progression; ergo, of the three core chapters:

The first – Chapter 3 – describes the design and results of a qualitative experiment for detecting photosynthate translocation from the algal endosymbiont to the host tissues in *C. retrogemma*. As it was so eloquently pointed out by Ruth Gates when I pitched her my hypotheses... “do you know for sure if there’s any carbon movement? You can’t base your entire Ph.D. on a bloody assumption.” Also in this chapter, related to the translocation experiment, is the design for a device used to prepare soft-bodied, aquatic animals (like acoels) for weighing without harming them, and a method for separating algal cells from host tissue without the use of mechanical homogenizers.

The second – Chapter 4 – defines the photobehaviors of *C. retrogemma* and outlines the experiments utilized to determine the qualitative and quantitative nature of light that leads to these behaviors. The two behaviors examined are a step-up photophobic response, hypothesized to be visually-mediated; and a photoaccumulative behavior, hypothesized to be photosynthetically-mediated, regulated, and responsible for the observed basking formations.

The third – Chapter 5 – focuses on the photoaccumulative behavior of *C. retrogemma* through experiments designed to determine the extent to which algal photosynthesis affects, and is affected by, the behavior. A series of experiments are conducted to determine the effect of light on the symbiosis as a function of host nutritional status (fed or starved). These and additional experiments are utilized to determine the possible stimuli(us) responsible for regulating the host’s photoaccumulative behavior.

## Literature cited

- Åkesson B, Hendelberg J (1989) Nutrition and asexual reproduction in *Convolutriloba retrogemma*, an acoelous turbellarian in obligate symbiosis with algal cells. In: Ryland JS, Tyler PA (eds) *Reproduction, genetics and distributions of marine organisms*. Olsen & Olsen, Fredensborg, Denmark, pp 13-21
- Bartolomeaus T, Balzer I (1997) *Convolutriloba longifissura*, nov. spec. (Acoela) - first case of longitudinal fission in Plathelminthes. *Microfauna Marina* 11:7-18
- Cook CB, Delia CF (1987) Are natural populations of zooxanthellae ever nutrient-limited? *Symbiosis* 4(1-3):199-211
- Douglas AE (1994) *Symbiotic Interactions*. Oxford University Press, Oxford, 148 pp.
- Gamble FW, Keeble F (1903) The bionomics of *Convoluta roscoffensis*, with special reference to its green cells. *Proceedings of the Royal Society of London Series B-Biological Sciences* 72:93-98
- Graff L (1891) *Die Organisation der Turbellaria Acoela*. Verlag Von Wilhelm Engelmann, Leipzig, 90 pp.
- Hendelberg J, Åkesson B (1988) *Convolutriloba retrogemma* gen. et sp.n., a turbellarian (Acoela, Platyhelminthes) with reversed polarity of reproductive buds. *Fortschritte der Zoologie* 36:321-327
- Hendelberg J, Åkesson B (1991) Studies of the budding process in *Convolutriloba retrogemma* (Acoela, Platyhelminthes). *Hydrobiologia* 227:11-17
- Keeble F (1910) *Plant-Animals: A Study in Symbiosis*. Cambridge University Press, London, 163 pp.
- Muller-Parker G, D'Elia CF (1997) Interactions between corals and their symbiotic algae. In: Birkeland C (ed) *Life and Death of Coral Reefs*. Chapman and Hall, New York, pp 96-113
- Muscatine L, Delia CF (1978) The uptake, retention, and release of ammonium by reef corals. *Limnology and Oceanography* 23(4):725-734
- Muscatine L, Porter JW (1977) Reef corals: Mutualistic symbioses adapted to nutrient-poor environments. *Bioscience* 27(7):454-460
- Pearse VB (1974a) Modification of sea anemone behavior by symbiotic zooxanthellae: Expansion and contraction. *Biological Bulletin* 147(3):641-651
- Pearse VB (1974b) Modification of sea anemone behavior by symbiotic zooxanthellae: Phototaxis. *Biological Bulletin* 147(3):630-640

Shannon T, Achatz JG (2007) *Convolutriloba macropyga* sp.nov., an uncommonly fecund acoel (Acoelomorpha) discovered in tropical aquaria. *Zootaxa* 1525:1-17

Smith DC (1991) Why do so few animals form endosymbiotic associations with photosynthetic microbes? *Philosophical Transactions of the Royal Society of London Series B-Biological Sciences* 333(1267):225-230

Smith DC, Douglas AE (1987) *The Biology of Symbiosis. Contemporary Biology*. Edward Arnold Ltd, London, 302 pp.

Trench RK (1993) Microalgal-invertebrate symbioses: A review. *Endocytobiosis and Cell Research* 9(2-3):135-175

Winsor L (1990) Marine Turbellaria (Acoela) from North Queensland. *Memoirs of the Queensland Museum* 28(2):785-800

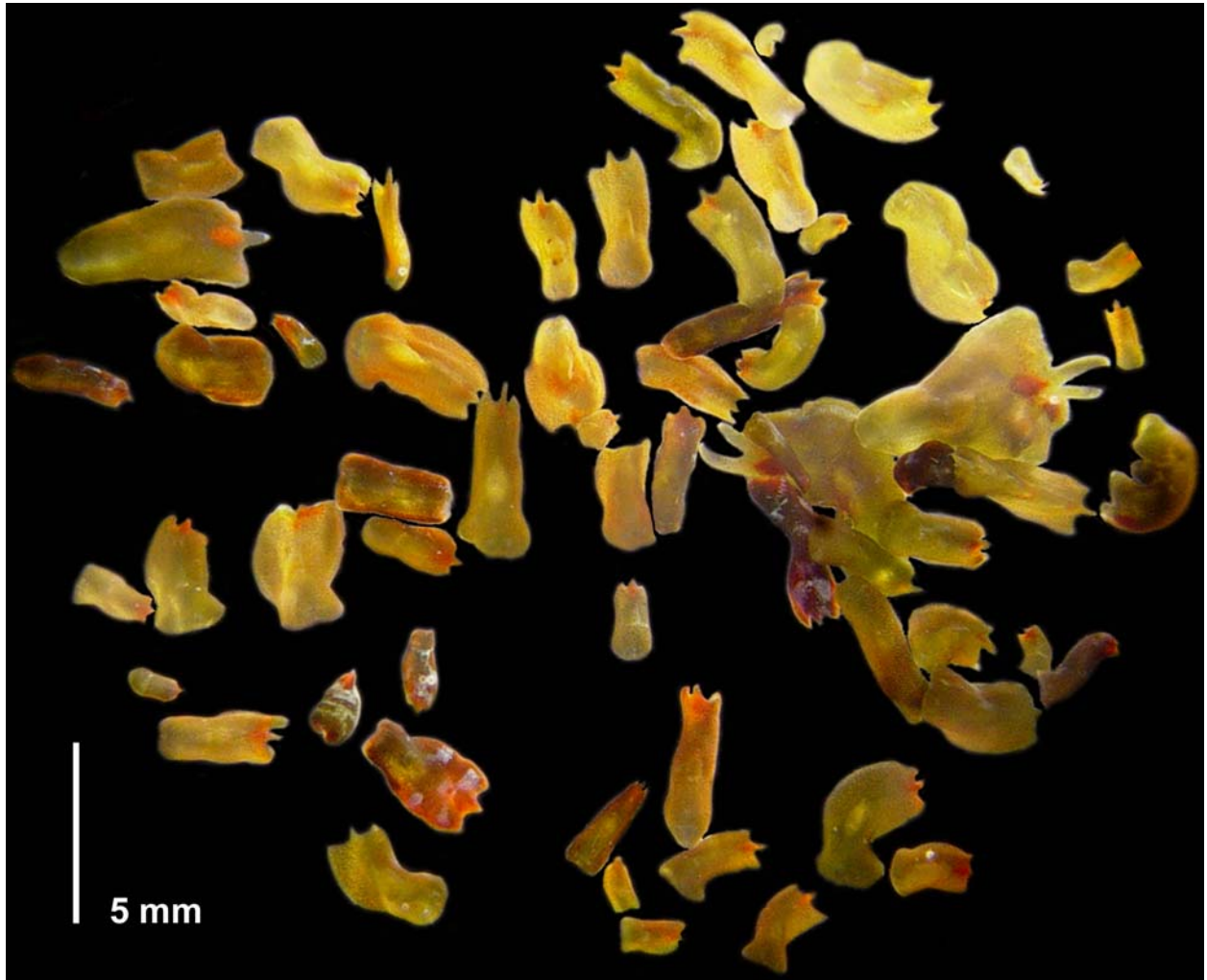


Figure 1.1. Photomicrograph of live *Convolutriloba* spp. Shown are representatives of the four described species: *C. retrogemma*, *C. hastifera*, *C. longifissura*, and *C. macropyga*. Specimens were viewed on a Wild M3Z stereomicroscope and photographed with a Sony DSC-P71 digital still camera.



Figure 1.2. Comparative photomicrograph of live, sexually-immature *Convolutriloba* spp. A. *Convolutriloba retrogemma* B. *Convolutriloba hastifera* C. *Convolutriloba longifissura* D. *Convolutriloba macropyga*. Specimens were viewed on a Wild M3Z stereomicroscope and photographed with a Sony DSC-P71 digital still camera.

## CHAPTER 2

### LITERATURE REVIEW:

#### AN OVERVIEW OF OSMOREGULATION IN ANIMALS AND THE POTENTIAL OSMOTIC IMPLICATIONS OF ALGAL-INVERTEBRATE SYMBIOSES



Life as we know it on this planet permeates most every environment, regardless of abiotic constraints. From the thriving communities clustered around hydrothermal vents sprouting from an otherwise barren, desolate deep-sea floor, to mealworms eking out a seemingly parched existence in a bag of flour, animals have managed to carve out ecological niches under even the most inhospitable conditions. Every animal however, from amoebae to elephant, despite the physical and chemical parameters of the environment that surrounds it, must maintain biological homeostasis. Whether marine, aquatic, or terrestrial; equatorial, temperate or polar, each species must maintain a physical and chemical balance of its cellular and intercellular fluids irrespective of external parameters. For most all species, deviation of internal parameters outside of narrow tolerances is not conducive of life.

In observing and studying an animal's maintenance of internal solute concentrations, one needs to view the organism as a compartmentalized system and define regulatory mechanisms at each compartmental interface. In unicellular animals the interface is between the cytosol and the surrounding, external environment; in multicellular animals there are two or more interfaces. In simpler, multicellular animals there is an interface between cellular cytosol and extracellular fluids as well as an additional interface between the extracellular fluids and the surrounding environment. As animals become more complex, the number of interfaces increase as tissues specialize into organs and functional systems evolve that require specific solute concentrations that differ from those in other systems within the same animal.

## Cell Volume Regulation

On a cellular level, the selective permeability of the plasma membrane coupled with specific, passive and active transmembranous transport proteins allows for the regulation of an extensive interchange of nutrient and waste molecules, respiratory gasses, and inorganic ions. Such regulation is necessary to maintain a relatively constant, total intracellular solute concentration, or osmolality, required of dynamic biochemical activities of all cellular processes. It is further required to balance the osmotic diffusion of water into and out of a cell. Inadequate regulation of cellular solute concentrations results in a change in the osmolality or osmotic pressure of the cytosol which in turn leads to cellular osmotic stress. Hypoosmotic stress, whereby the osmolality of the extracellular fluid is *less* than that of the cytosol, results in osmotic diffusion of water into the cell leading to cellular swelling or lysis (turgidity in walled cells); hyperosmotic stress, on the other hand, whereby the osmolality of the extracellular fluid is *greater* than that of the cytosol, results in osmotic diffusion of water out of the cell leading to cellular shrinking (plasmolysis in walled cells). Equal intracellular and extracellular osmolality results in an isosmotic condition, whereby osmotic loss and gain of water in a cell is balanced. Although the total intracellular and extracellular solute concentrations are equal in this situation, the ionic and molecular constituencies differ significantly (e.g., Campbell *et al.* 1999b).

The science of cell volume regulation is not yet fully understood, but relatively recent research and discoveries have added significant insight to a paradigm that has held court for over 100 years. The chemical nature of osmolytes was first studied at the turn of the 20<sup>th</sup> century with the introduction of the concept of organic substances, in addition to inorganic ions, playing a major role as osmotic effectors. It wasn't until a half century later that intracellular, free amino acid concentrations were shown to increase in response to hyperosmotic stress in several

euryhaline crustaceans (e.g., Gilles 1997). Since then, the importance of free amino acids in the function of cell volume control has been shown in salinity-stressed organisms of almost every phyla whereby through protein synthesis and degradation, intracellular concentrations of amino acids decrease and increase in response to hypoosmotic and hyperosmotic stress respectively (e.g., Schmidt-Nielsen 1997b). Numerous studies involving the regulation of cell volume in a variety of tissues in both vertebrates and invertebrates conclude that in addition to certain amino acids and their derivatives, a limited *core* group of organic substances are routinely utilized as osmotic effectors across all phyla. These substances include polyhydric alcohols, sugars, quaternary ammonium compounds, urea and methylamines (Yancey *et al.* 1982; Law 1991; Yancey 2001). Unlike inorganic ions, many of the molecules in these groups have little or no perturbing effects on enzymatic or other macromolecular-mediated cellular processes. In several instances, anisotomically driven increases in the concentration of certain organic osmolytes can even *counteract* the perturbing effects of other organic substances and/or inorganic ions by stabilizing the native state of cellular proteins and protein assemblies (Yancey *et al.* 1982; Courtenay *et al.* 2000; Yancey 2001).

Certain nitrogenous substances are routinely utilized as cellular osmolytes while the intracellular levels of similar molecules, though present, remain unchanged during anisotomotic episodes. Among the amino acids, glycine, alanine, and proline (nonpolar), serine (polar), and taurine (decarboxylated leucine) are generally found in high concentrations in most marine invertebrate cells and in certain vertebrate cells. On the other hand, electrically charged amino acids such as arginine and lysine (those with a cationic, or basic, side chain) have a significant perturbing effect on cellular enzymatic functions and do not appear to change in response to osmotic stress (Bowlus & Somero 1979; Schmidt-Nielsen 1997b; Yancey 2001). Other

nitrogenous substances such as betaine (trimethylglycine), trimethylamine oxide, and glutamate can offset the perturbing effects of high intracellular concentrations of inorganic cations ( $K^+$  &  $Na^+$ ) as well as those of organic protein denaturants. Trimethylamine oxide (TMAO), with betaine and sarcosine (N-methyl glycine) to lesser degrees, is found in very high concentrations in the urea-rich tissues of elasmobranchs and coelacanth. With cellular concentration ratios ranging from 3:2 to 2:1 (urea:TMAO), trimethylamine oxide acts as an *osmoprotectant* to counteract protein denaturation by urea (a metabolic waste product) thereby allowing both substances to act as osmolytes (Lin & Timasheff 1994; Wang & Bolen 1997). Lastly, some of the aforementioned, and other, nitrogenous osmolytes are preferentially utilized as osmoprotectants to stabilize proteins in the cells of organisms subjected to environmental extremes. Glycerol, along with mannitol and sucrose are common algal osmolytes; it is also utilized by most insect species exposed to freezing temperatures (Yancey *et al.* 1982). Glucose production (gluconeogenesis) occurs in most vertebrates and invertebrates and is purported (along with glycerol) to function as a cellular osmolyte in several crustaceans (primarily euryhaline decapods) in response to osmotic stress, and also as a possible osmoprotectant as noted by seasonal (temperature) variations in gluco- and glyceroneogenetic activities (Schein *et al.* 2005). Methylamines, like those in elasmobranchs, function similarly in many other phyla. They accumulate as osmoprotectants/osmolytes in such taxonomically-diverse, urea-rich tissues as those of mammalian kidney medullae to those of the crab-eating, mangrove frog *Rana cancrivora* (Gordon *et al.* 1961; Schmidt-Nielsen 1997b). Variants of these osmolytes, i.e., methyltaurine and glycine betaine, are further hypothesized to stabilize proteins against high pressures, and are found as dominant osmolytes, along with taurine and hypotaurine in

vestimentiferan worms and other organisms associated with deep-sea hydrothermal vents and cold hydrocarbon seeps (Yin *et al.* 2000).

As previously stated, recent work has vastly increased our understanding of the phenomenon of cell volume regulation. This work has introduced some expected changes in our perception of the mechanisms involved in cellular osmotic homeostasis, and some, such as the discovery of aquaporins, have not only solved the riddles of historically observed idiosyncrasies, but have generated an explosion of new studies and created a shift in the archetypical paradigm of membrane permeability. With many of the questions surrounding the roles of organic osmolytes in cell volume regulation answered and widely accepted, contemporary studies are now focusing on the *combined* roles of organic *and* inorganic-ionic osmolytes, sensing and control mechanisms, and the influence of aquaporins (membrane water channels) as they relate to cellular water stress.

Cell volume regulation in invertebrates and vertebrates appears to occur by similar mechanisms and discoveries of specific osmolytes, osmolyte transport systems, and/or signal transduction pathways in specific tissues of one organism are generally *rediscovered* in subsequent studies of similar or different tissues in *different* species, phyla, and/or kingdoms. Regulatory mechanisms can be divided into two general categories; regulatory volume increase (RVI) whereby cells regain osmotically *lost* water in response to hyperosmotic stress, and regulatory volume decrease (RVD) whereby cells rid themselves of osmotically *gained* water in response to hypoosmotic stress. The objective of both strategies is to re-adjust intracellular solute concentrations, in respect to changes in either external or internal osmolality, to levels conducive to the maintenance of a constant cellular volume, and in a manner that minimizes interference of vital cellular metabolic processes (e.g., Wehner *et al.* 2004).

Early studies of cell volume regulation focused mainly on the movements of the primary intracellular inorganic osmolytes  $K^+$  and  $Cl^-$  and indicated that compensatory changes in their intracellular concentrations resulted from osmotic stress in almost all cells. In many studies, however, these changes did not account for the *total* cytosolic osmolyte concentration changes required to restore optimal cellular volume. Based on the results of more recent studies, it has become clear that the movement of inorganic osmolytes, alone, *can* exact requisite intracellular volumetric recovery, but only in response to relatively small osmotic perturbations. In one such representative example, that of volume regulation in the epithelial cells of freshwater mussels (Dietz *et al.* 1998), a limited ability for cell volume regulation was observed involving the transmembrane movements of  $K^+$  and  $Na^+$  ions. Under hyperosmotic conditions an immediate loss of osmotic water was followed by a slow, passive diffusion of  $Na^+$  and  $K^+$  down their concentration gradients into the cell followed concomitantly by obligatory osmotic water resulting in partial cell volume restoration. Upon return to normal, hypoosmotic, medium,  $Na^+/K^+$  ATPase activity coupled with  $Na^+$  and  $K^+$  diffusion out of the cell resulted in a rapid restoration of original cell volume and  $[K^+]_i$ . This limited cell volume regulatory mechanism is presumed by the authors to explain the mussel's stenohaline nature. In most cells, inorganic osmolyte translocation is the first response to hyper- and hypoosmotic stress. During RVI, cells tend to take up primarily  $Na^+$  since electrochemical and biochemical driving forces across the plasma membrane are greatest for this cation. As in the example above, subsequent activation of  $Na^+/K^+$  ATPase restores the original  $Na^+$  gradient. During RVD, rapid efflux of  $K^+$  and  $Cl^-$  follows cellular swelling upon the activation of ionic transmembrane transport systems. By rapidly eliminating both cations *and* anions, cell lysis is avoided and membrane electrical potential is maintained (Pierce 1982; Lang *et al.* 1998; Wehner *et al.* 2004). Pierce (1982; 2001)

notes that, *in general*, cells that exist in extracellular environments up to approximately 400 mosm (milliosmoles, full seawater ~1000 mosm) rely primarily on inorganic ions for volume regulation. These would include, as noted above, those of many freshwater animals and the majority of non-excretory cells of terrestrial vertebrates. Cells existing in higher extracellular environments, he notes, like those of marine and brackish water animals and those affiliated with excretory organs, i.e., vertebrate kidneys, rely more on organic osmolytes.

Due to the perturbing effects of inorganic ions, their usefulness in volume regulation is limited to small changes in osmotic pressures. In most euryhaline organisms and certain terrestrial vertebrate cells this rapid, ion-transfer mechanism via a variety of activated ion channels and/or KCl symport (Lang *et al.* 1998) is utilized to counteract *initial* volumetric changes to a point that will minimize the probability of cellular metabolic dysfunction or lysis, but it is the slower augmentation and transmembrane movements of non-perturbing organic osmolytes that is instrumental in RVI and RVD (Pierce 1982; Law 1991; Dragolovich & Pierce 1992). In one example, that of one of the best understood invertebrate cell types, the red blood cell of the bivalve, *Noetia ponderosa*, hypoosmotic stress is followed by an immediate influx of osmotic water causing a volumetric increase and cellular swelling. Two distinct responses result concurrently: 1) the immediate efflux of intracellular  $K^+$  and  $Cl^-$ , likely via a PKC (protein kinase C) activated channel, followed by obligatory osmotic water prevents cell lysis, and 2) the activation of a transmembrane protein channel mediating the passive efflux of taurine coupled with  $Cl^-$  ions further regulates a volumetric decrease to the pre-stress cellular volume (Pierce & Warren 2001). As shown in this example, cellular release of both organic and inorganic osmolytes immediately follows exposure to hypoosmotic media. Though efflux of cellular osmolytes are apparently triggered by membrane stretch resulting from volumetric increase, the

specificity of translocated molecules in any given cell type indicates that organic osmolyte efflux is not a consequence of increased membrane permeability, but involves dedicated pathways and/or specific channel activation. The organic to inorganic ratio of total osmolytes responsible for RVD varies by cell type and can be as high as 0.5 thereby affirming the importance of organic molecules in the process. The role of organic osmolytes in RVI, however, appears to be far *less* important. In most studies, RVI occurs rapidly (generally within minutes) and seems to involve only inorganic ions but a decrease in membrane permeability to organic osmolytes is observed. This decreased permeability ameliorates the increase (by transport or metabolic synthesis) of intracellular organic osmolytes necessary to replace the augmented inorganic ions by minimizing “leakage” of the osmolytes out of the cell. It is in this post-RVI regard that the importance of organic osmolytes becomes apparent (e.g., Wehner *et al.* 2004).

A major focus today in the field of cellular volume regulation is in advancing and refining our understanding of the mechanisms by which cells sense osmotic stress and transduce those signals to generate osmolyte movements. Several chemical and physical parameters likely to modulate a volumetric regulatory response include changes in: intra- or extracellular chemical activity and/or signal molecule concentrations, intracellular hydrostatic pressure, cytoplasmic volume, and the physical state of the plasma membrane (e.g., van der Heide & Poolman 2000). Membrane swelling in response to volumetric increases during hypoosmotic stress and RVD is considered the primary activating mechanism in the cells of many eukaryotes. The transmembrane proteins activated by membrane swelling have been termed *volume-sensitive, organic osmolyte-anion channels* (VSOAC). Research, thus far, has implicated two general activation mechanisms of these, and similar, channels: 1) conformational changes in a channel due directly to membrane swelling, and 2) the increase in intracellular signaling molecule



concentrations due to their influx across an initially distended membrane (Pierce *et al.* 1989; Kirk 1997; Pena-Rasgado *et al.* 2001). The former, though discovered in a prokaryotic organism, has implications of processes that likely exist in eukaryotes as well. The glycine betaine transport system of *Lactococcus lactis* is activated under hyperosmotic stress and inhibited under hypoosmotic stress conditions. Results of the study indicate that asymmetrical physical changes in the lipid bilayer due to inherent membrane curvature may be coupled to conformational changes necessary to activate and deactivate the transport protein. As such, the transport system acts as both osmosensor *and* osmoregulator (van der Heide & Poolman 2000). The latter mechanism is involved in the aforementioned example of RVD in the red blood cells of *Noetia ponderosa*. In these cells the influx of  $\text{Ca}^{2+}$  (a signaling ion), which occurs simultaneously with the efflux of  $\text{K}^+$  and  $\text{Cl}^-$ , raises  $[\text{Ca}^{2+}]_i$ ; thereby activating calmodulin (a calcium-activated messenger protein). Calmodulin activation, in turn, is believed to result in the phosphorylation and activation of the taurine/ $\text{Cl}^-$  VSOAC (Pierce & Warren 2001).

The role of organic osmolytes in RVI, as mentioned earlier, is not so much one of translocation, but of intracellular, metabolic synthesis and accumulation. Our understanding of this system stems from research of the hyperosmotic stress response of *Saccharomyces cerevisiae*. These studies reveal that hyperosmotic stress induces, in this yeast, the transcription of glycerol-3-phosphate dehydrogenase (GPD) through the activation of the HOG (high osmolarity glycerol) MAP (mitogen-activated protein) kinase pathway. The transcription of GPD, a key enzyme in the synthesis of glycerol results in the production and intracellular accumulation of the osmolyte (Albertyn *et al.* 1994; Gilles 1997; Wojda *et al.* 2003). The discovery and subsequent research of the HOG pathway in yeast has had a direct application to our understanding of osmotic stress sensing and transcription control by similar MAP kinase

pathways in other organisms as well (e.g., de Nadal *et al.* 2002; Jimenez *et al.* 2004; Westfall *et al.* 2004).

By far, of all recent discoveries, that of aquaporins has had the most profound influence on our understanding of membrane permeability and osmosis. First identified in 1991 in human erythrocytes, aquaporins are transmembrane proteins that function as passive, osmotically-driven, bidirectional, transmembrane water channels (e.g., Agre *et al.* 1993; Agre 1997; Shapiguzov 2004). Now numbering well over 200 discovered types, they have been found in every cell in which they've been sought, and their structure is surprisingly conserved across all phyla. They are instrumental in the movement of osmotic water into and out of cells at rates far greater than by transmembrane diffusion alone (the measured rate in one species of  $3.9 \times 10^9$  water molecules·subunit<sup>-1</sup>·s<sup>-1</sup>) and are responsible for the selective permeability of membranes (Sanders & Bethke 2000; Ren *et al.* 2001). Shapiguzov (2004) states in the *Regulation* section of his review on aquaporins that, overall, “the regulated operation of aquaporins ensures the control over permeability of certain membranes to water... [and that] this regulation occurs at the transcriptional or posttranslational stages.” He lists several options/criteria for the expression of aquaporin genes including: constitutive expression, response to hormones, response to blue-light, response to salt and osmotic stress, and response to drought.

The regulation of membrane permeability by the transcription (increase) and degradation (decrease) of aquaporins has finally explained the variability often observed in many cells throughout scientific history. The increase in water permeability in the epithelial cells of renal collecting ducts in the mammalian kidney, for instance, has long been attributed to increased levels of the hormone vasopressin in response to dehydration. It is now known that vasopressin

regulates the water permeability by inducing exocytosis of aquaporin-laden vesicles towards the epithelial cell surfaces (Nielsen *et al.* 1995).

### **Osmotic Regulation and Homeostasis**

Homeostasis, or an organism's maintenance of a constant internal environment is required for the efficient and continued operation of all cellular and organismal functions independent of changes in the external environment. The evolutionary histories of today's animals can be traced in observing the interactions of extant animals with the environments that surround them. It is presumed that the earliest organisms were entirely dependent on the medium in which they lived and that over time, fluctuations in a given internal parameters occurred. Concomitant changes in the metabolic processes dependent on these internal parameters were the likely motive force driving the evolution of osmotic and ionic regulation. Single celled marine protozoa, like many found today, would have been the first to regulate intracellular ionic concentrations in association with maintaining cell volume. As these organisms evolved to multicellular forms, similar to the simple, metazoan marine invertebrates of contemporary oceans, the internal cells would be maintained within an internal body fluid whose ionic composition would, in turn, be maintained at different concentrations than the surrounding seawater. Further evolution would add more cells to more specialized tissues eventually exceeding the surface-to-volume limits for passive diffusion of respiratory gasses and nitrogenous wastes (metabolic by-products of protein and nucleic acid breakdown). Concurrent with exceeding these limits would be the development of excretory organs to maintain homeostatic internal environments under even greater external changes allowing organisms to expand their ranges to the edges of the sea and into estuarine waters. The development and

modifications of these organs would lead to respiratory systems, which in conjunction with modifications to other tissues would eventually lead to an organism's ability to invade extreme environmental conditions and ultimately to its ability to move freely from one environment to another (e.g., Prusch 1983).

For many marine invertebrates osmotic homeostasis is primarily passive in that the osmolality of internal fluids vary little from that of the external media. As most of these animals must remain in full strength seawater to maintain homeostasis, they are deemed *stenohaline*. Some marine invertebrates, however, can maintain homeostasis over a greater range of external salinities and are *euryhaline*. Of the euryhaline species, many can tolerate the large changes in external salinities because they have evolved metabolic processes capable of functioning under a wide range of internal osmolality. As these animals move within their optimal range, their internal osmolality conforms to that of the external medium. These euryhaline, and most stenohaline, animals, are *osmoconformers*. The other euryhaline species tolerate changes in salinity by actively regulating their internal osmotic parameters and maintaining a more "constant" osmolality of their body fluids. These animals are *osmoregulators*. It should be noted, though, that whether an osmoconformer or osmoregulator, all animals must actively regulate ions in order to maintain optimal cellular functions and membrane potentials.

As already alluded to, as the surface-to-volume ratio of an animal decreases, the ability to release waste ammonium from, and move respiratory gasses into and out of all cells by diffusion alone also decreases. As such, many organisms have evolved excretory organs for the removal of nitrogenous wastes and respiratory organs for the uptake and release of respiratory gasses; in some instances, such as in the gills of bivalves, these processes occur within the same tissues. Furthermore, since the nitrogenous, metabolic wastes (primarily ammonia and urea) behave as

osmolytes, their accumulation in, and subsequent release from, these organisms will have osmotic consequences. Hence, osmoregulation and nitrogenous waste removal are, *generally*, inextricably linked. The osmoregulatory substances and nitrogenous waste products are carried throughout these organisms by the hemolymph or interstitial fluid that bathes the body's cells and physiological adjustments, usually involving feedback mechanisms, continually adjust their levels. These physiological adjustments of osmoregulation and waste excretion both occur across layers of transport epithelial cells. Osmoregulation, itself, is usually accomplished by the transport of salts across a transport epithelium, followed by the obligatory osmotic flow of water.

As in the volumetric regulation of cells, water uptake by an animal must balance water loss. The mechanisms of organismal osmoregulation vary according to the evolutionary history of the particular species, but more so, according to the challenges inherent to the osmotic pressure differences between that species and its environment. When an animal is hyperosmotic to its environment, i.e., freshwater organisms, there is a net osmotic influx of water and solutes are lost by diffusion and by the excretion of osmotically gained water. These problems are generally countered by direct uptake of ions from the environment through active transport and food, and the reabsorption of solutes in the production of dilute urine. In low metabolism animals, such as freshwater clams, the problems can be minimized by maintaining a low blood concentration of ions. Protozoa utilize contractile vacuoles to pump out excess water. When an animal is hypoosmotic to its environment, i.e., marine bony fish and *Artemia* sp., there is a net osmotic water loss and a diffusive influx of ions. These problems are generally countered by continuous drinking, active excretion of ions, and the reabsorption of water in the production of concentrated urine.

## Osmoregulatory Strategies

The following, though not all-inclusive, is a break-down of osmoregulatory strategies utilized by representative animal groups according to their environment. Euryhaline animals are not represented as such. Euryhaline taxa are often able to tolerate large osmotic changes in their environments by altering their osmoregulatory mechanisms, i.e., they behave as a hyperosmotic animal in fresh water and as a hypoosmotic animal in seawater. Since there are stenohaline representatives of most euryhaline taxa, these will be described. All information in this section has been combined from several general sources (e.g., Prosser 1973; Brusca & Brusca 1990; Rupert & Barnes 1994; Schmidt-Nielsen 1997a; Campbell *et al.* 1999a).

**Marine invertebrates.** Most are isosmotic. Nitrogenous waste in the form of ammonium is released by diffusion in smaller species, and diffused from gill epithelia by others. Donnan effect of proteins (dialysis) in those with excretory organs ensures minimal supply of osmotic water for nitrogenous waste removal. All organisms exhibit active ion regulation; almost all are osmoconformers.

**Freshwater invertebrates.** All are hyperosmotic and constantly take in water from their environment. Protozoa pump out excess water with contractile vacuoles, and others excrete copious amounts of dilute urine. Salt loss is replaced by eating and/or uptake across gill epithelia. Many groups have evolved low permeability coverings.

*Cnidarians* – Periodic expulsion of fluids from gastrovascular cavity, which is kept hyperosmotic to other tissues.

*Flatworms, nemerteans, rotifers, gastrotrichs, and kinorhynchs* – Extracellular fluid is filtered into the protonephridia of the flame-cell system. These blind-end tubules excrete

a dilute fluid and function primarily in osmoregulation. Nitrogenous waste, though excreted partly by the protonephridial system, is mostly lost by diffusion.

*Nematodes* – Unique, plesiomorphic excretory structures called renette cells are assumed to serve an excretory function and may represent a primitive, non-ciliated protonephridia.

*Annelids* – Each segment has a pair of open-ended, tubular excretory organs, called metanephridia, closely associated with capillaries. The metanephridia collect coelomic fluid, the transport epithelial linings pump out salts for reabsorption, and dilute urine is excreted through nephridiopores. Being ammonotelic, freshwater species also eliminate ammonium by diffusion.

*Crustaceans* – Ammonium is released by nephridia and through gills. Nephridial organs are either antennal or maxillary glands the inner end of which is called the sacculus. Blood-filled channels surround the sacculus epithelium across which filtration occurs. The sacculus epithelia actively take up and secrete substances from the blood into the nephridial organs. These processes are instrumental in both removal of wastes and osmotic/ionic regulation.

*Mollusks* – Most species have paired, tubular metanephridia with the nephrostome opening into the pericardial cavity and nephridiopore discharging to the mantle cavity. Selective, active reabsorption of solutes from the pericardial fluids result in the production of a hypoosmotic urine.

**Marine vertebrates.** Most marine vertebrates are hypoosmotic to their environment, and therefore, osmoregulators. As such, these animals experience a net efflux of osmotic water and influx of ions. Several groups, however, including the hagfish, elasmobranchs, coelacanth, and crab-eating frogs tend to be slightly hyperosmotic to seawater.

*Elasmobranchs* – Sharks and their relatives maintain an osmolarity slightly higher than seawater by retaining urea. Body fluid salt concentration, however, is approximately 1/3 that of full seawater. Retention of urea by kidney reabsorption and the production of the requisite TMAO, betaine and/or sarcosine to counteract the perturbing effects of the stored urea makes these animals slightly hyperosmotic. Extensive ionic regulation is noted in this group, particularly sodium excretion by the kidneys and rectal gland. Active transport of salts in gills occurs to a lesser degree. The slight hyperosmolarity allows for osmotic inflow of water in gills. This water is utilized in urine formation and rectal gland excretion.

*Hagfish* – Similar to elasmobranchs, their body fluids are nearly isosmotic to seawater but with pronounced ionic regulation. They are all stenohaline.

*Coelacanth* – Also retain urea – osmoregulation assumed similar to elasmobranchs.

*Crab-eating frog* – Similar to elasmobranchs, (slightly hyperosmotic) but water influx occurs through the skin. Unlike sharks, their kidney does not reabsorb urea, and retention is by decreased urine production only while in seawater. Tadpoles osmoregulate as teleost fish (see below) and adopt elasmobranch pattern as adults.

*Teleosts* – Marine bony fishes lose water to their environment, primarily across the gills and must compensate by drinking large quantities of seawater. Kidneys remove divalent ions  $Mg^{2+}$  and  $SO_4^{2-}$ . Excretion of  $Na^+$  and  $Cl^-$  is accomplished by active transport in gill epithelia.

*Mammals* – Whales and other cetaceans, manatees, seals and other pinnipeds, unlike “true” marine animals, have no respiratory epithelia in contact with seawater and therefore do not contend with osmotic water loss to the same degree. The kidneys of



these animals are capable of producing urine hyperosmotic to full seawater allowing them to cope with high salt loads.

*Reptiles and birds* – Neither of these animal groups can produce urine hyperosmotic to seawater. Excess salts are excreted through specialized nasal salt glands.

**Freshwater vertebrates.** All are hyperosmotic; they therefore experience problems similar to freshwater invertebrates.

*Teleosts* – These animals, of course, are all hyperosmotic to their environments but are less permeable to ions than their marine counterparts. They experience excessive osmotic inflow of water across gills. Excess water is continually removed as very dilute urine, but due to large volumes, solute loss is inevitable. Solutes are taken in with food, but primary replacement is by active uptake in the gills.

*Elasmobranchs* – Part-time freshwater species tend to retain about 1/3 the concentration of urea of their marine counterparts, but still maintain very low levels of solutes. This results in less osmotic inflow (compared to that of a marine species subjected to freshwater) and concomitant urinary salt loss. Full time freshwater species maintain a blood urea concentration similar to freshwater teleosts and are presumed to utilize similar osmoregulatory mechanisms.

*Amphibians* – Frogs, toads, and newts all utilize mechanisms similar to teleost fish. Although some species retain gills as adults, all species must also contend with solute-permeable skin. Osmotic inflow of water is removed as dilute urine, which combined with increased skin permeability is responsible for most solute losses. Solute uptake is through food and active transport across the epidermis.

**Terrestrial invertebrates.** Terrestrial animals face the ever-present danger of desiccation due to water loss across respiratory tissues and/or by evaporation/perspiration from skin and mucous membranes. These animals combat desiccation through the production of metabolic water, through the nervous and hormonal control of thirst, through behavioral adaptations, and through water-conserving excretory organs. Most species, however, maintain hydration by drinking and eating food with high water content.

*Annelids* – Though not true terrestrials since they cannot live outside of a saturated, moist environment, they differ from their aquatic counterparts in being partly ureotelic.

Osmoregulation and solute retention is almost identical to that of freshwater species.

*Insects and spiders* – Malpighian tubules, blind tubules arising from the gut wall and extending into the hemocoel function in osmoregulation and removal of nitrogenous wastes from the hemolymph. These animals generally produce a relatively dry waste matter, some spiders, however, store nitrogenous waste as uric acid and void *no* waste product. The water-conserving strategies utilized by insects are partially responsible for the adaptive success of this group on land.

**Terrestrial vertebrates.** Almost all terrestrial vertebrates utilize the same strategies for the prevention of desiccation. The degree, however, to which each strategy is used depends on the evolutionary history of the particular species and the environment in which it lives. The primary strategies for maintaining water balance, as outlined above, are through food, drink, metabolic water production, reabsorption in the kidney and intestines, and through behavioral modifications. Solute replacement (lost through urine production and perspiration) is through food intake and reabsorption in the kidney as well. While some animals, like humans, require a continual replenishment of water through drinking, others, like the desert mouse, depend solely

on the water content of its food, metabolic water production, and behavioral activities that minimize its water loss. In many instances, this animal can live its entire life without ever drinking water.

*Amphibians* – This group is comprised of moist-skinned species susceptible to high evaporative water losses from the skin. Behavioral adaptations are utilized by most members in that many live in moist environments or near water. In water they osmoregulate as freshwater vertebrates. Those living in arid environments also rely on behavioral adaptations such as in-ground estivation and retention of very dilute urine during dry seasons.

## **Symbioses**

Many stenohaline, marine, osmoconforming invertebrates, and several freshwater species, are host to photosynthetic, symbiotic algae. Primarily consisting of members of the Porifera, Cnidaria, Platyhelminthes, and Mollusca phyla (Smith 1991), these symbioses involve both intra- and intercellular zoochlorellae (green algae) and zooxanthellae (dinoflagellates). Although the intricacies of these symbiotic relationships differ considerably between taxa, they are all mutualistic to some extent. Algal-invertebrate symbioses are thought to have evolved in adaptation to nutrient-poor environments such as reef systems where most nutrients are locked up in, and quickly recycled back into biomass (Muscatine & Porter 1977; Muscatine & Delia 1978). An interdependent relationship with a heterotrophic host receiving translocated photosynthates would also benefit a zooxanthellae or other alga by allowing it to become a part of a nutrient recycling process. By fitting itself into the process, the alga is maintained in the photic zone and afforded much higher concentrations of dissolved organics (ammonium and

urea) than it would encounter as a free-swimming phytoplankton. A comparison of low phytoplankton densities in surface waters and high cellular densities of zooxanthellae in corals of tropical reef systems (Cook & Delia 1987), further supports the concept of tight nutrient cycling and the mutual benefit of symbiosis between marine invertebrates and algae.

In the evolutionary process of symbiogenesis with an algal endosymbiont, the host animal must contend with novel conditions inherent to the “encapsulation” of a photosynthetic organism. Mechanisms must evolve in the host to minimize the negative effects of low pH and reactive oxygen species production as a consequence of photosynthetic activities. Moreover, in order to benefit from the symbiosis, the host must evolve mechanisms to not only transport photosynthates across its membranes, but it must be able to utilize those photosynthates through respiration or metabolization into larger molecules or lipids at a rate consistent with translocation from the alga. Conservative estimates of translocated photosynthates in a variety of symbiotic systems range from between 10 and 60 percent of total carbon fixed by the alga (Taylor 1974; Douglas 1994). This reflects not only the scale of translocation, but the differences in the associations. The identity of translocated photosynthate substrates also differs between systems, and although work continues into the true nature of many of these substrates, due their rapid utilization by host cells, it is often the derivatives or metabolic products of the photosynthates that are identified. The nutritive pathways of several algal-invertebrate systems have been studied more than others and generalizations have been made as to the substrates and products involved in each. It has been shown that *Chlorella* species translocate maltose to cells in *Hydra* sp., and that *Symbiodinium* sp. translocates several substrates including glycerol and triglyceride. In both systems the photosynthate is either respired or rapidly metabolized to glycogen in *Hydra* sp. or lipids in *Symbiodinium* sp. hosts (e.g., Douglas 1994).

The intertidal, acoelous turbellarian, *Convoluta roscoffensis*, and its endosymbiotic, prasinophyte alga, *Tetraselmis convolutae*, is a system that has been studied for over a century. First identified by Graff (1891), and later described by Gamble & Keeble (1903) and at length by Keeble (1910), the symbiosis is considered obligate in the adult worm whereby the acoel ceases to feed holozoically and relies solely on its endosymbiont for nutrition. Sequential nutritional studies on the worm and its symbiont revealed, first, that the main product of fixation in the algae is mannitol, but that it was amino acids (primarily alanine) that were released by the algae to the acoel (Muscatine *et al.* 1974). The second study by Boyle and Smith (1975) revealed that at least half of the carbon fixed in photosynthesis moved from alga to animal. They also suggested an amino acid substrate but hypothesized that ammonia produced by uric acid catabolism in the algae was assimilated into glutamine and that *this* was the main amino acid released back to the animal. Meyer *et al.* (1979) revealed, in the third study, the host's inability to synthesize *de novo* long-chain saturated and unsaturated fatty acids, as well as sterols. Sterols found in *C. roscoffensis*, they discovered, were host-modified and its polyunsaturated fatty acids were plant-derived ( $\omega$ 3) suggesting algal-synthesized and translocated precursors.

### **Photosynthate Identification**

Given the examples above, it is clear that a substantial margin of error exists when attempting to isolate and identify the *virgin* translocated photosynthate. Symbiont photosynthate translocation studies abound, and methods for the detection and identification of potential algal-produced, nitrogen and carbon substrates vary from the use of pre-formulated test kits to the more, all-inclusive approach utilizing  $\text{NaH}^{14}\text{CO}_2$  incubations and subsequent analyses of the radio-labeled contents of the host cytosol. Translocation studies in isolated algae have failed to

identify substrates as it is only through the evolution of a symbiosis that not only does the alga allocate a proportion of its fixed carbon and nitrogen to the host, but it does it out, usually, as a molecule different from the one it would produce *outside* the host. Bearing this and evolutionary pressures in mind, it is logical to assume that any translocated molecule is one *specifically* beneficial to the host, and, as mentioned before, is likely metabolized as soon as, or very shortly after, it enters the host cytosol.

A recent paper by Whitehead and Douglas (Whitehead & Douglas 2003) addresses these issues and offers a modifiable method similar to one proposed three decades earlier (Taylor 1974) that circumvents the necessity to isolate, or even detect, the virgin “mobile compounds”, i.e., photosynthates, by comparatively analyzing the downstream, metabolic products instead.

The *in vivo* method utilizes two groups, an experimental and control. In the control group, the holobiont is incubated in  $\text{NaH}^{14}\text{CO}_2$  and allowed to photosynthesize. The algal and host tissues are separated and fractionated into lipids, proteins/nucleic acids, and trichloroacetic acid-soluble acidic, basic and neutral fractions. Identities of the fractions’ constituents are determined by HPLC and thin layer chromatography/thin layer electrophoresis. This identifies the metabolic products of the unknown mobile compound.

The experimental group treatment consists of an array of substrates from glucose to citrate, all labeled with  $^{14}\text{C}$ . Each experimental group is incubated in DCMU; organisms injected with one of the radio-labeled substrates, and allowed time to metabolize the substrate. Host tissues are separated and analyzed as above.

Control and experimental results are compared. If the metabolites found in any of the experimental groups match those in the control group, the experimental substrate indicates the identity of the unknown mobile compound.

## Osmotic Implications of Algal-Invertebrate Symbioses

In a review of the symbiotic relationships between corals and their zooxanthellae endosymbionts, Muller-Parker & D'Elia (1997) note that corals must balance the benefits of photosynthate production/use and the costs of containing and maintaining their algae. Some of the costs they list include mechanisms necessary for the coral to cope with high oxygen tension resulting from the symbiosis, mechanisms for regulating the growth rates of the zooxanthellae, and mechanisms for providing the algae with UV protection. They explain that exposures to environmental extremes in salinity, temperature or light levels tend to destabilize symbioses in corals and cause the algae to be ejected since the cost to sustain them is too high. Surprisingly absent is the potential for osmotic stress as a result of photosynthate production in an otherwise compromised system.

Several studies have investigated the effects of symbioses on the behavior of hosts, primarily as they relate to phototactic movements. Keeble (1910) referred to the natural “desire” of the algal symbionts to bask in the sun as the possible reason for the photoaccumulative behavior of *C. roscoffensis*. Zahl and McLaughlin (1959) compared the phototactic/photoaccumulative behaviors of symbiotic and aposymbiotic *Condylactis gigantea* and discovered a positive phototactic behavior in the symbiotic complex only. Pearse (1974b; 1974a) observed the behaviors of *Anthopleura elegantissima* and noted a correlation between the zooxanthellate condition and positive phototaxis as well as tentacle expansion and contraction.

In each of these studies, the researcher has alluded to the importance that photosynthesis plays in exacting the host responses. They suggest a mechanism of behavioral photoregulation, but they stop short of defining the mechanism by which photosynthesis mediates the behavioral response. It was my initial intention, during the course of the studies contained herein, to

examine closely the apparent osmoregulatory function of observed photomovements in the *Convolutriloba retrogemma* symbiotic complex; this I have accomplished. And although, like the previously mentioned researchers, I have shown that some aspect of the photochemical processes in the algal endosymbiont mediates these behaviors, the exact mechanism eludes me... and thereby keeps me humble.



## Literature Cited

- Agre P (1997) Molecular physiology of water transport: Aquaporin nomenclature workshop. Mammalian aquaporins. *Biology of the Cell* 89(5-6):255-257
- Agre P, Preston GM, Smith BL, Jung JS, Raina S, Moon C, Guggino WB, Nielsen S (1993) Aquaporin CHIP: the archetypal molecular water channel. *American Journal of Physiology* 265(4):F463-F476
- Albertyn J, Hohmann S, Thevelein JM, Prior BA (1994) GPD1, which encodes glycerol-3-phosphate dehydrogenase, is essential for growth under osmotic stress in *Saccharomyces cerevisiae*, and its expression is regulated by the high-osmolarity glycerol response pathway. *Molecular and Cellular Biology* 14(6):4135-4144
- Bowlus RD, Somero GN (1979) Solute compatibility with enzyme function and structure: rationales for the selection of osmotic agents and end-products of anaerobic metabolism in marine invertebrates. *Journal of Experimental Zoology* 208(2):137-151
- Boyle JE, Smith DC (1975) Biochemical interactions between the symbionts of *Convoluta roscoffensis*. *Proceedings of the Royal Society of London. Series B, Biological Sciences* 189(1094):121-135
- Brusca RC, Brusca GJ (1990) *Invertebrates*. Sinauer Associates, Inc., Sunderland, 922 pp.
- Campbell NA, Reece JB, Mitchell LG (1999a) *Biology*. Benjamin/Cummings, Menlo Park, CA, 1175 pp.
- Campbell NA, Reece JB, Mitchell LG (1999b) Membrane Structure and Function. In: Mulligan E (ed) *Biology*. Benjamin/Cummings, Menlo Park, CA, pp 130-146
- Cook CB, Delia CF (1987) Are natural populations of zooxanthellae ever nutrient-limited? *Symbiosis* 4(1-3):199-211
- Courtenay ES, Capp MW, Anderson CF, Record MT (2000) Vapor pressure osmometry studies of osmolyte-protein interactions: Implications for the action of osmoprotectants in vivo and for the interpretation of "osmotic stress" experiments in vitro. *Biochemistry* 39(15):4455-4471
- de Nadal E, Alepuz PM, Posas F (2002) Dealing with osmostress through MAP kinase activation. *Embo Reports* 3(8):735-740
- Dietz TH, Neufeld DH, Silverman H, Wright SH (1998) Cellular volume regulation in freshwater bivalves. *Journal of Comparative Physiology B-Biochemical Systemic and Environmental Physiology* 168(2):87-95
- Douglas AE (1994) Nutritional interactions in symbiosis. In: *Symbiotic Interactions*. Oxford University Press, Oxford, pp 56-77

- Dragolovich J, Pierce SK (1992) Comparative time courses of inorganic and organic osmolyte accumulation as horseshoe crabs (*Limulus polyphemus*) adapt to high salinity. *Comparative Biochemistry and Physiology a-Physiology* 102(1):79-84
- Gamble FW, Keeble F (1903) The bionomics of *Convoluta roscoffensis*, with special reference to its green cells. *Proceedings of the Royal Society of London Series B-Biological Sciences* 72:93-98
- Gilles R (1997) "Compensatory" organic osmolytes in high osmolarity and dehydration stresses: History and perspectives. *Comparative Biochemistry and Physiology a-Physiology* 117(3):279-290
- Gordon MS, Schmidt-Neilsen K, Kelly HM (1961) Osmotic regulation in the crab-eating frog (*Rana cancrivora*). *Journal of Experimental Biology* 38(3):659-678
- Graff L (1891) *Die Organisation der Turbellaria Acoela*. Verlag Von Wilhelm Engelmann, Leipzig, 90 pp.
- Jimenez C, Berl T, Rivard CJ, Edelstein CL, Capasso JM (2004) Phosphorylation of MAP kinase-like proteins mediate the response of the halotolerant alga *Dunaliella viridis* to hypertonic shock. *Biochimica Et Biophysica Acta-Molecular Cell Research* 1644(1):61-69
- Keeble F (1910) *Plant-Animals: A Study in Symbiosis*. Cambridge University Press, London, 163 pp.
- Kirk K (1997) Swelling-activated organic osmolyte channels. *Journal of Membrane Biology* 158(1):1-16
- Lang F, Busch GL, Volkl H (1998) The diversity of volume regulatory mechanisms. *Cellular Physiology and Biochemistry* 8(1-2):1-45
- Law RO (1991) Amino acids as volume-regulatory osmolytes in mammalian cells. *Comparative Biochemistry and Physiology a-Physiology* 99(3):263-277
- Lin TY, Timasheff SN (1994) Why do some organisms use a urea-methylamine mixture as osmolyte? Thermodynamic compensation of urea and trimethylamine N-oxide interactions with protein. *Biochemistry* 33(42):12695-12701
- Meyer H, Provasoli L, Meyer F (1979) Lipid biosynthesis in the marine flatworm *Convoluta roscoffensis* and its algal symbiont *Platymonas convoluta*. *Biochimica Et Biophysica Acta* 573(3):464-480
- Muller-Parker G, D'Elia CF (1997) Interactions between corals and their symbiotic algae. In: Birkeland C (ed) *Life and Death of Coral Reefs*. Chapman and Hall, New York, pp 96-113
- Muscatine L, Boyle JE, Smith DC (1974) Symbiosis of acoel flatworm *Convoluta roscoffensis* with alga *Platymonas convolutae*. *Proceedings of the Royal Society of London Series B-Biological Sciences* 187(1087):221-234

- Muscatine L, Delia CF (1978) The uptake, retention, and release of ammonium by reef corals. *Limnology and Oceanography* 23(4):725-734
- Muscatine L, Porter JW (1977) Reef corals: Mutualistic symbioses adapted to nutrient-poor environments. *Bioscience* 27(7):454-460
- Nielsen S, Chou CL, Marples D, Christensen EI, Kishore BK, Knepper MA (1995) Vasopressin increases water permeability of kidney collecting duct by inducing translocation of aquaporin-CD water channels to plasma membrane. *Proceedings of the National Academy of Sciences of the United States of America* 92(4):1013-1017
- Pearse VB (1974a) Modification of sea anemone behavior by symbiotic zooxanthellae: Expansion and contraction. *Biological Bulletin* 147(3):641-651
- Pearse VB (1974b) Modification of sea anemone behavior by symbiotic zooxanthellae: Phototaxis. *Biological Bulletin* 147(3):630-640
- Pena-Rasgado C, Pierce SK, Rasgado-Flores H (2001) Osmolytes responsible for volume reduction under isosmotic or hypoosmotic conditions in barnacle muscle cells. *Cellular and Molecular Biology* 47(5):841-853
- Pierce SK (1982) Invertebrate cell volume control mechanisms: a coordinated use of intracellular amino acids and inorganic ions as osmotic solute. *Biological Bulletin* 163(3):405-419
- Pierce SK, Politis AD, Cronkite DH, Rowland LM, Smith LH (1989) Evidence of calmodulin involvement in cell-volume recovery following hypo-osmotic stress. *Cell Calcium* 10(3):159-169
- Pierce SK, Warren JW (2001) The taurine efflux portal used to regulate cell volume in response to hypoosmotic stress seems to be similar in many cell types: Lessons to be learned from molluscan red blood cells. *American Zoologist* 41(4):710-720
- Prosser CL (1973) *Comparative Animal Physiology*. W. B. Saunders Company, Philadelphia, 966 pp.
- Prusch RD (1983) Evolution of invertebrate homeostasis: Osmotic and ionic regulation. *Comparative Biochemistry and Physiology a-Physiology* 76(4):753-761
- Ren G, Reddy VS, Cheng A, Melnyk P, Mitra AK (2001) Visualization of a water-selective pore by electron crystallography in vitreous ice. *Proceedings of the National Academy of Sciences of the United States of America* 98(4):1398-1403
- Rupert EE, Barnes RD (1994) *Invertebrate Zoology*. Saunders College Publishing, New York, 1056 pp.
- Sanders D, Bethke P (2000) Membrane Transport. In: Buchanan BB, Gruissem W, Jones RL (eds) *Biochemistry & Molecular Biology of Plants*. American Society of Plant Biologists, Rockville, MD, pp 110-158

- Schein V, Chitto ALF, Etges R, Kucharski LC, van Wormhoudt A, Da Silva RSM (2005) Effects of hypo- or hyperosmotic stress on gluconeogenesis, phosphoenolpyruvate carboxykinase activity, and gene expression in jaw muscle of the crab *Chasmagnathus granulata*: seasonal differences. *Journal of Experimental Marine Biology and Ecology* 316(2):203-212
- Schmidt-Nielsen K (1997a) *Animal physiology: adaptation and environment*. Cambridge University Press, Cambridge, 607 pp.
- Schmidt-Nielsen K (1997b) Water and osmotic regulation. In: *Animal physiology: adaptation and environment*. Cambridge University Press, Cambridge, pp 301-354
- Shapiguzov AY (2004) Aquaporins: Structure, systematics, and regulatory features. *Russian Journal of Plant Physiology* 51(1):127-137
- Smith DC (1991) Why do so few animals form endosymbiotic associations with photosynthetic microbes? *Philosophical Transactions of the Royal Society of London Series B-Biological Sciences* 333(1267):225-230
- Taylor DL (1974) Nutrition of algal-invertebrate symbiosis. I. Utilization of soluble organic nutrients by symbiont-free hosts. *Proceedings of the Royal Society of London. Series B, Biological Sciences* 186(1085):357-368
- van der Heide T, Poolman B (2000) Osmoregulated ABC-transport system of *Lactococcus lactis* senses water stress via changes in the physical state of the membrane. *Proceedings of the National Academy of Sciences of the United States of America* 97(13):7102-7106
- Wang AJ, Bolen DW (1997) A naturally occurring protective system in urea-rich cells: Mechanism of osmolyte protection of proteins against urea denaturation. *Biochemistry* 36(30):9101-9108
- Wehner F, Olsen H, Tinel H, Kinne-Saffran E, Kinne RKH (2004) Cell volume regulation: osmolytes, osmolyte transport, and signal transduction. In: *Reviews of Physiology, Biochemistry and Pharmacology*, 148. Springer-Verlag, Berlin, pp 1-80
- Westfall PJ, Ballou DR, Thorner J (2004) When the stress of your environment makes you go HOG wild. *Science* 306(5701):1511-1512
- Whitehead LF, Douglas AE (2003) Metabolite comparisons and the identity of nutrients translocated from symbiotic algae to an animal host. *Journal of Experimental Biology* 206(18):3149-3157
- Wojda I, Alonso-Monge R, Bebelman JP, Mager WH, Siderius M (2003) Response to high osmotic conditions and elevated temperature in *Saccharomyces cerevisiae* is controlled by intracellular glycerol and involves coordinate activity of MAP kinase pathways. *Microbiology-Sgm* 149:1193-1204
- Yancey PH (2001) Water stress, osmolytes and proteins. *American Zoologist* 41(4):699-709

Yancey PH, Clark ME, Hand SC, Bowlus RD, Somero GN (1982) Living with water stress: Evolution of osmolyte systems. *Science* 217(4566):1214-1222

Yin M, Palmer HR, Fyfe-Johnson AL, Bedford JJ, Smith RAJ, Yancey PH (2000) Hypotaurine, N-methyltaurine, taurine, and glycine betaine as dominant osmolytes of vestimentiferan tubeworms from hydrothermal vents and cold seeps. *Physiological and Biochemical Zoology* 73(5):629-637

Zahl PA, McLaughlin JJA (1959) Studies in marine biology. IV. On the role of algal cells in the tissues of marine invertebrates. *Journal of Protozoology* 6(4):344-352

## CHAPTER 3

# A NOVEL METHOD FOR THE DETERMINATION OF PHOTOSYNTHATE TRANSLOCATION IN AN ALGAL-ACOEL SYMBIOTIC SYSTEM: A QUALITATIVE APPROACH<sup>1</sup>

---

<sup>1</sup> Shannon, T. To be submitted to *Limnology and Oceanography*.

## **Abstract**

Owing to the fragile nature of its green algal symbiont, *Convolutriloba retrogemma*, like other members of the genus and other symbiotic acoels, does not lend itself well to established methods for the detection and quantification of photosynthate translocation from symbiont to host. Herein is described a novel method for detecting the movements of photosynthate *in vivo* in the species utilizing differential weight change in animals subjected to light and dark treatments without holozoic feeding. Though successful in yielding desired results, the method was decidedly labor-intensive and an alternative method is suggested in light of a new-found technique to induce sexual reproduction in the genus. Also described is a refined method for the separation of algal symbionts from host tissue in the species, and a method for determining accurate wet-weight of this and other soft-bodied, invertebrate species.

**Key words:** *Convolutriloba*, photosynthate, translocation, acoel, wet-weight, zoochlorellae, symbiont, *in vivo*

## Introduction

Though the following chapters of this study focus primarily on the osmotic dynamic between *Convolutriloba retrogemma* and its algal endosymbiont, and the photobehavioral regulatory mechanisms that affect the relationship. The arguments set forth would be for naught without evidence of a net translocation of photosynthetically fixed carbon from symbiont to host.

A handful of standard methods have been used for the detection and quantification of photosynthate translocation in a multitude of algal-invertebrate systems, and have been instrumental in the identification of the carbon species involved. The use of radioactively labeled  $\text{NaH}^{14}\text{CO}_3$  is by far the most common method (Steemann Nielsen 1952) whereby  $^{14}\text{C}$  is photosynthetically fixed by the algal symbiont and following the separation of host tissue from the algae, is tested for in the host tissues (e.g. Muscatine & Hand 1958; Trench 1971). Stable carbon isotope ( $^{13}\text{C}$ ) analysis has also been utilized, as in zooxanthellate tridacnids (Johnston *et al.* 1995), and the measurement of respiratory quotients (Gattuso & Jaubert 1990) has been used in *Stylophora* corals.

*C. retrogemma* poses several challenges to each of these methods. First and foremost is the difficulty in separating the algal symbionts, intact, from the host tissue. Muscatine *et al.* (1974) noted in *Symsagittifera (Convoluta) roscoffensis* Graff 1891, an algal-acoel system studied for over a century, similar difficulties in separating the host from its prasinophyte alga; like other researchers (Taylor 1974; Boyle & Smith 1975; Kremer 1975; Meyer *et al.* 1979), they utilized instead, aposymbiotic hatchlings and/or adults as well as cultures of the isolated symbiont in their  $^{14}\text{C}$  methods. The separation of the zoochlorellae from *C. retrogemma* has proven even more difficult than in *S. roscoffensis*. The main problem experienced in both systems is the fragile nature of the alga in symbiosis. Unlike the dinoflagellate *Symbiodinium* in



corals, the chlorophyta are not protected by a rigid cell wall and are easily disintegrated by most mechanical homogenization techniques. Separation is further hampered in *C. retrogemma* by a reactive toxin released from specialized rhabdoid gland cells in the host during homogenization (Hendelberg & Åkesson 1988; Shannon & Achatz 2007). Upon release, the toxin appears to disrupt the membrane integrity of any cell it contacts.

The second challenge posed by *C. retrogemma* is the difficulty in producing aposymbiotic adults even by methods successful with *S. roscoffensis* and other symbiotic acoels, i.e., bubbling CO<sub>2</sub> through the medium (Bohn & Drzewina 1928; Boyle & Smith 1975), or incubating the animals in DCMU in light (Trench & Winsor 1987). This, coupled with the rarity of sexual reproduction in the species and thereby the difficulty in securing eggs and aposymbiotic hatchlings, precludes the use of most methods used on other acoels.

The measurement of respiratory quotients, though amenable to *Symbiodinium*-scleractinian symbioses, would be impractical for use on *C. retrogemma*. Gattuso & Jaubert (1990) based the accuracy of their coral respiration ratio (host:holobiont) estimates on an assumption (respiration is proportional to the corresponding biomass ratio) that is strongly supported by extensive research on similar scleractinian symbiotic systems. Though much work has been done on *S. roscoffensis* relating to carbon fixation and translocation within the symbiosis, including respiratory studies (Nozawa *et al.* 1972), the ecology of *C. retrogemma* differs to such a degree that similar assumptive practices would likely yield erroneous and misleading data.

The idiosyncrasies involved in working with *C. retrogemma* and the inefficacy of established methods to verify photosynthate translocation within this system necessitated the development of the method described herein. This non-destructive, *in vivo* method compared the

weight change over time of individual animals subjected to a light regimen to that of animals kept in the dark. It was hypothesized that if there was a net carbon translocation in the symbiosis, the animals kept in the dark would be denied the photosynthates and would therefore lose more weight than those in the light.

In order to ensure the validity of this method, any variability due to activity or chance metabolic differences between the two groups had to be eliminated. DCMU, 3-(3,4-dichlorophenyl)-1,1-dimethylurea, a photosystem II inhibitor (Mattoo *et al.* 1981) used in many studies to determine photosynthetic carbon-fixation rates by acting as a chemical equivalent to the traditional “dark bottle” (Legendre *et al.* 1983) was utilized for this purpose. DCMU was used in the light to inhibit photosynthesis without affecting potential, visually-mediated diel behaviors; it was used in the dark for comparative purposes to identify any non-photosynthetic effects it may have on the acoel host.

*Convolutriloba retrogemma*, like most acoels, is a relatively small (~ 5–6 mm) and exceedingly fragile animal. The most daunting aspect of formulating this method was the challenge of obtaining an accurate and reproducible weight on the same live animal at the onset and completion of the experiment, i.e., removal of all but a thin layer of water coating the epidermis, and without injuring the animal.

## **Materials and Methods**

Populations of *Convolutriloba retrogemma* were maintained in trough-style research aquaria in both a mixed-species population with other convolutrilobids (*C. hastifera*, *C. longifissura* & *C. macropyga*) and in a monospecific culture tank separate from other *Convolutriloba* spp. The aquaria were housed in a constant temperature room maintained at

25°C. Artificial seawater (ASW, Instant Ocean<sup>®</sup>) was maintained at a salinity of 34±1 ppt as measured with an Atago S/Mill hand-held refractometer. The mixed-species tank was illuminated by four Philips 40W 5000°K Ultralume fluorescent lamps providing an average PAR irradiance of ~100  $\mu\text{mole}\cdot\text{m}^{-2}\cdot\text{s}^{-1}$  at the water's surface. Culture tanks were illuminated by two URI Super Actinic and two URI Aquasun-4 VHO 110W fluorescent lamps powered by an IceCap 660 ballast providing ~200  $\mu\text{mole}\cdot\text{m}^{-2}\cdot\text{s}^{-1}$ . All tanks were maintained on a 14h:10h light-dark cycle. Irradiance measurements were made with an LI-190SA quantum sensor and registered with a Li-Cor Model LI-1400 Data Logger. *Artemia* sp. nauplii were provided daily in superabundance to supplement the acoels' diet of rotifers, copepods, and crustacean larvae already present in the aquaria.

Central to this study was the ability to determine the accurate weight of the same live animals at different stages of the experiments. In order to accomplish this task with minimal negative effect to the animals, a dewatering device (Figs 3.1 and 3.2A) was designed and built to remove all but a thin layer of water covering the epidermis of an animal by applying gentle suction. For initial set up of the device, a pre-tared patch of 14-micron, nylon plankton-net (1 cm x 1 cm) was placed atop the 200-micron netting platform, the dewatering stage of the device, and the device was connected to a vacuum source via the barbed connection. Vacuum to the stage via a 3 mm hole was minimized at this point by fully opening the 1/4" valve. A live acoel was then placed, along with a drop of water, atop the pre-tared patch using a plastic disposable pipette. To remove the water in which the specimen was contained, the valve was slowly closed until the droplet began to recede through the patch and into the dewatering device. With the patch and specimen dewatered, they were removed as one and the underside of the patch was blotted against a circle of filter paper (Whatman No.1) to ensure the removal of any remaining,

excess water then weighed using a Mettler AG245 5-place balance. With the weight determined, the specimen and patch were placed gently, upside-down (to minimize the possibility of tearing the animal from the netting) into a culture dish of filtered ASW and the animal allowed to swim off the patch before collecting it for further experimentation. The pre-tared patch was then rinsed in DI H<sub>2</sub>O to remove any salts and polar contaminants followed by a rinse in acetone to remove any non-polar contaminants then placed on the dewatering stage to dry. The valve on the dewatering device was left in the position that resulted in the initial dewatering ensuring consistent suction on subsequent samples. Additional suction for the rapid drying of the cleaned patch was easily obtained by temporarily covering the valve opening with a finger.

Animals selected for all experiments were preconditioned to ensure similar nutrition levels of each holobiont prior to the onset of experimentation. As such, specimens were collected from the culture tanks and placed in shallow plastic tubs for 15 days and maintained at 25°C on a 14h:10h light-dark cycle with a surface irradiance of 70  $\mu\text{mole}\cdot\text{m}^{-2}\cdot\text{s}^{-1}$  provided by two Philips 5000°K Ultralume and two Philips cool white 40W fluorescent lamps. *Artemia* sp. nauplii were added daily in superabundance and water was changed every other day. This regimen was followed by 7 days under the same conditions, but with food removed, to allow for the evacuation of all digested matter from the animals, and to ensure that any nutrition gained during experimentation was photosynthetically derived.

Two preliminary experiments were run concurrently to ascertain an optimal concentration of DCMU with minimal non-photosynthetic, negative effects for use in the photosynthate translocation experiment. For each of these experiments, 6 treatments were employed: Control (no DCMU), 1, 0.5, 0.1, 0.05, and 0.01  $\mu\text{M}$  DCMU. DCMU crystals were initially mixed in small volumes of ethanol to allow for complete dissolution. Stock solution was then added to 34

ppt ASW to the desired final DCMU concentrations. Ethanol with no DCMU was added to controls. DCMU solutions were transferred to open beakers and placed on heated stir plates at 40°C and medium stir speeds overnight to evaporate the ethanol. DCMU solutions were restored to their original volumes and salinity by adding DI H<sub>2</sub>O.

The first experiment involved the use of Pulse Amplitude Modulation (PAM) fluorometry to determine the DCMU concentration corresponding to the minimum effective quantum yield of photosystem II ( $Y$ ), above which no significant change occurred. The method used was modified from that of Warner, *et al.*, (1996). Preconditioned animals were placed at random in six 4½” glass culture dishes, 20 per dish. Each dish contained 100 ml ASW with a DCMU concentration corresponding to one of the 6 treatments. Dishes were subjected to an irradiance of 70  $\mu\text{mole}\cdot\text{m}^{-2}\cdot\text{s}^{-1}$ , as outlined above, for 8 hours then placed in the dark for 1 hour. Following dark acclimation  $F_o$ ,  $F_m$ , and  $Y$  values were determined for 5 replicate samples (4 randomly chosen animals per replicate) for each treatment by PAM fluorometry (Diving PAM, Walz, Germany). Each sample was placed in a chamber, open at one end (Fig. 3.2B) and covered with 14-micron plankton-net at the other (Fig. 3.2C), designed to fit over the end of the PAM fiber-optic cable. Excess water was removed from the animals by placing the net end of the chamber atop the stage platform of the dewatering device, described earlier, and applying vacuum as previously outlined. The chamber containing the dewatered animals was then slipped onto the end of the fiber-optic cable (Fig. 3.2D) such that the animals were ~1.5 mm from the fiber-optic tip. Readings were taken, recorded and charted.

The second experiment involved subjecting animals to the dark to determine a DCMU concentration with minimal negative, non-photosynthetic effects, i.e., a concentration above which weight loss over time, and death rate exceed that of the control group. The pre-test weight

of all preconditioned animals was determined as previously outlined. Animals were then placed in Costar (Corning Inc.) 24-well cell-culture trays, one animal per well. Each well contained 2.5 ml ASW with a DCMU concentration, chosen at random, corresponding to one of the 6 treatments, 10 replicates per treatment. Trays were then placed in the dark for 1 week. Water was changed daily. Following dark treatment, the post-test weight of all animals was determined and percent weight change calculated. Results were compared to those of the dark control group and the results of the PAM experiment to determine the optimal DCMU concentration for use in the photosynthate translocation experiment.

Four treatments were used in the photosynthate translocation experiment: Light Control (LC), Light with DCMU (LD), Dark Control (DC), and Dark with DCMU (DD). Light irradiance was  $70 \mu\text{mole}\cdot\text{m}^{-2}\cdot\text{s}^{-1}$ , as previously outlined, DCMU concentration was  $0.1 \mu\text{M}$ . The pre-test weight ( $W_o$ ) of all preconditioned animals was determined as previously outlined. Animals were then placed in eight 24-well cell-culture trays, one animal per well. Four trays each were assigned to either light or dark treatment. Each well contained 2.5 ml ASW with or without DCMU, chosen at random such that  $n = 48$  for each treatment. The experiment was carried out over a 10-day period with no holozoic feeding. Water was changed daily. The post-test weight ( $W_f$ ) of all animals was determined and 24 animals each from the LC and DC groups were set aside for algal counts. Average percent weight change was calculated for each treatment as:

$$100 \left( \sum_{i=1}^n (W_{o_i} - W_{f_i}) / n \right)_T$$

Where  $T$  = treatment and  $n$  = number of replicates for treatment  $T$  surviving through the end of the experiment. Non-photosynthetic effect of DCMU was determined as the difference in average percent weight change between the DC and DD groups, i.e.,

$$100 \left( \left( \sum_{i=1}^n (W_{o_i} - W_{f_i}) / n \right)_{DD} - \left( \sum_{i=1}^n (W_{o_i} - W_{f_i}) / n \right)_{DC} \right)$$

This average difference was then subtracted from the calculated difference of each replicate in the LD and DD treatments before averaging the percent weight change for each group in order to eliminate the non-photosynthetic effect of DCMU variability. Results were graphed and treatment groups compared.

Algal counts, calculated as algal cells per mg host tissue, were determined for post-test animals in both the light and dark control groups. For each group, the 24 animals of known weight were divided into 4 replicates of 6 randomly assigned animals each. The animals of each replicate were transferred to a culture dish containing 31 ppt ASW buffered to pH 9.0 (necessary to prevent activation of host toxins, personal communication with Walter Hatch) then transferred in aliquots of 1300  $\mu$ l into 1.5 ml microfuge tubes and chilled at 4°C for ~2–3 hours (a regimen ascertained to compromise the integrity of the host cell membranes, but not those of the algal cells). Following refrigeration, the tubes were vortexed for 120 seconds to disrupt and homogenize the host cells, subjected to a centrifuge “burst”, i.e., ~5–10 seconds to concentrate algal cells without over-compacting them, and 1240  $\mu$ l of supernatant was pipetted out. Algal pellets were rinsed by adding 600  $\mu$ l of chilled, buffered ASW, gently shaking the tubes by hand, subjecting the tubes to a centrifuge burst and pipetting off 600  $\mu$ l of supernatant. A final 600  $\mu$ l of chilled, buffered ASW was added to each tube along with 40  $\mu$ l of 37% formaldehyde to preserve the algal cells. Tubes were vortexed for 60 seconds to resuspend the algal cells and refrigerated at 4°C to await counting. Cell counts were determined for each replicate using a Neubauer brightline hemacytometer (Fisher Scientific) on a Zeiss Axioskop-2 phase-contrast compound microscope. Six fields (1 mm x 1 mm x 0.1mm) were counted per replicate.

## Results

**DCMU concentration.** Two preliminary experiments were carried out to determine an optimal DCMU concentration for use in photosynthate translocation experiments. In the first of these, PAM fluorometry of acoels incubated in ASW with DCMU (Fig. 3.3), a marked decrease in effective quantum yield of photosystem II ( $Y$ ) of the algal endosymbiont was evident as DCMU concentration increased from 0  $\mu\text{M}$  in the control group ( $Y=0.673$ ) to 0.1  $\mu\text{M}$  ( $Y=0.403$ ). No further statistical change in quantum yield was noted in acoel groups incubated at or above 0.1  $\mu\text{M}$  DCMU (one-way ANOVA with [DCMU] as the independent variable, 0.1, 0.5, and 1.0  $\mu\text{M}$  tested,  $\alpha=0.05$ ,  $p=0.543$ ).

Over the course of the 7-day, dark-incubation period in the second of the two preliminary experiments, acoel death occurred in all DCMU treatment groups with the exception of the control group. Of the 10 animals in each group, 9 died in 1.0  $\mu\text{M}$ , 8 died in 0.5  $\mu\text{M}$ , and 2, 3, and 2 of 10 died in 0.1, 0.05, and 0.01  $\mu\text{M}$  DCMU respectively. Of the latter three treatment groups (Fig. 3.4), there were no statistical differences in weight change over the course of the experiment compared to that of the control group (one-way ANOVA with [DCMU] as the independent variable,  $\alpha = 0.05$ ,  $p = 0.164$ ).

A DCMU concentration of 0.1  $\mu\text{M}$  corresponded to the asymptotic onset of quantum yield along the independent axis of  $Y$  vs. [DCMU] in the fluorometry experiment. This concentration was also the highest of those tested in the dark/weight-loss experiment to produce a statistically similar weight change compared to the control group while maintaining a relatively low death rate. As such, 0.1  $\mu\text{M}$  DCMU was the concentration chosen for use in the photosynthate translocation experiment.



**Photosynthate translocation.** Of the 48 acoels used in each treatment of the translocation experiment, 11 died in the LC group, 2 each died in the LD and DC groups, and 3 died in the DD group. Initial calculations of average weight-loss (Fig. 3.5) indicated a greater loss in animals subjected to either dark or DCMU (LD, DC, and DD) than in those of the light control group (LC). Among these three groups, on average, animals subjected to DCMU (LD and DD) experienced slightly higher weight-loss than those of the dark control.

With the non-photosynthetic effect of DCMU calculated and subtracted from the data of the LD and DD groups (Fig. 3.6), the average weight-loss is nearly identical among groups LD, DC, and DD (one-way ANOVA,  $\alpha = 0.05$ ,  $p = 0.923$  compared to  $p = 0.137$  among same groups before removal of DCMU non-photosynthetic effect). A one-way ANOVA ( $\alpha = 0.05$ ) run on all four treatment groups after DCMU effect removal yielded a  $p$ -value  $< 0.001$ , a post-hoc Tukey HSD test for comparison of means confirmed that the average percent weight-loss of animals in the light control was significantly lower than that of animals in the other three groups, and that no significant differences in average percent weight-loss existed between those three. A subsequent one-tail t-test comparing the means of the light and dark controls indicated a highly significant difference between the two groups ( $\alpha = 0.05$ ,  $p < 0.001$ ).

**Zoochlorellae density.** The average post-experimental density of algal endosymbionts in acoels from the light control (LC) group was ~19,000 cells per milligram (wet weight) of host tissue. The density in acoels from the dark control (DC) group was ~29,000 cells/mg. A two-tail t-test comparing the means indicated a highly significant difference between the two groups ( $\alpha = 0.05$ ,  $p < 0.001$ ).

## Conclusions

**Efficacy of the dewatering device.** Central to the success of this method was the need to obtain an accurate wet-weight of *Convolutriloba retrogemma* in such a way as to inflict little or no harm on the animal. Unlike other small invertebrates with exoskeletons, cuticle, tegument, or other epidermal structural protection or support, i.e., arthropods, annelids, nemerteans, nematodes, trematodes, etc., most acoels are far more delicate and cannot withstand even the gentlest of drying techniques. Whereas copepods are easily blotted dry on filter-paper discs, weighed, and returned to their medium “no worse for the wear”, placing most acoels on filter-paper generally results not only in the disintegration of the animals, but the inability to weigh them since both animal and water-of-transfer absorb into the disc. *Convolutriloba* spp., like most acoels, have no epidermal sclerotic elements and lack even a sub-epidermal basement membrane (e.g., Tyler & Hooge 2004). It is likely the absence of this connective tissue layer, coupled with the large number of mucus, and other, gland cells penetrating from the underlying musculature through the epidermal cells that makes these animals highly susceptible to “intercellular failure”, or whole-body disintegration when removed from the protection of their aqueous environment.

In earlier experiments leading up to this study, acoels were dewatered simply by placing them suspended in a drop of water atop the same 14-micron plankton-net patch described in the methods section, and placing the patch directly onto a filter-paper disc (Whatman No.1). Although effective in removing the extraneous water by “wicking” it through the net into the paper, this method proved far less efficient and inaccurate in that the water was absorbed too rapidly into the paper. In doing so, the kinetic energy of the water flowing along the dorsal epidermis to the lateral margins of the animal was sufficient to pull some of the animal through

the net with it. More often than not, residual stains of animal tissue were left on the filter-paper; in some instances the net-movement of water was great enough to compromise the integrity of the entire animal. By removing tissue, the method yielded lower than actual weights, altered the physical state and health of the animal, and in doing so added undesirable variability to any experiment in which that animal was used. Since many of the earlier studies, like this one, required preconditioning of the animals over a given time, and long experimental trials, the potential for numerous fatalities added uncertainty to obtaining sufficient data.

The design of the dewatering device used in this study allows for operator control over the velocity of the water being removed. As shown in figure 3.1, the small hole leading from the main chamber of the device to the underside of the dewatering stage is approximately 2 mm below the 200-micron net covering the stage; this provides several control factors: 1. By using a single small hole, the suction source is minimalized and centralized. 2. The small gap below the stage-net allows for the dissipation of the vacuum over a larger area, i.e., suction will be strongest near the small hole and will decrease radially and outward from the hole. 3. The space of the gap and the underlying surface area of the top of the plug act in slowing the velocity of the water by increasing distance and friction.

When the acoel/water/patch combination is placed on the stage and the valve is fully open, there is negligible suction at the hole, and the water remains as a drop due to its surface tension. As the valve is slowly closed the suction increases at a corresponding rate under the specimen until it is high enough to *just* overcome the surface tension of the drop and begin pulling the water through the 14-micron pores of the plankton-net patch. With a new water droplet forming on the underside of the 200-micron net stage, the animal is now completely surrounded by water and the surface tension remains intact (if placed on filter-paper directly, it is

at this point that the surface tension of the water is disrupted as it contacts the paper and leads to the increased velocity of the water above the animal as the droplet collapses). Since the surface tension is unbroken, the water drop slowly “sinks” through the plankton-net thereby minimizing velocities along the lateral margin of the animal. With most of the water now below the animal, the drop contacts the top of the plug and slowly spreads out surrounding the top of the hole and down its sides; since the plug is non-absorptive, surface tension remains intact but is now spread over a larger, solid surface thereby adding friction. It is this friction over a relatively large area that *keeps* the water moving slowly around the animal while at the same time increasing in velocity as it nears and enters the restriction and smaller area of the hole where suction is greatest. With no break in surface tension, all the water is pulled down from around the animal in one continuous, controllable movement leaving only a thin film coating the epidermis. Of the hundreds of acoels weighed (many repeatedly) during the course of these and other experiments, less than ten left any residual spots of tissue on the filter-paper during the blotting step that precedes weighing, and none were killed by the process.

**Photosynthate translocation.** This method was designed around the specific difficulties experienced in working with members of the *Convolutriloba* genus, and was developed over several years in combination with, and borrowing from, other methodologies developed for other experiments. The ultimate intention was to develop a method that did not require the separation of host tissues and symbiont cells, and would therefore be tested *in vivo* and not require the use of  $^{14}\text{C}$  or  $^{13}\text{C}$ . To this extent, the method was a success. The results clearly showed, with metabolic and diel variability accounted for, that *C. retrogemma* in the dark, physically or chemically, experienced a relatively high weight-loss for the lack of something afforded to their counterparts in the light. Given the lower weight loss experienced by *C. retrogemma* in the light

with both groups denied holozoic feeding, only one variable was left unaccounted for, symbiont mass.

Åkesson & Hendelberg (1989) note that unlike other symbiotic acoels, such as *Symsagittifera roscoffensis*, *C. retrogemma* routinely consume and digest their own symbionts. Given this information, it would seem likely that the weight lost by animals in the dark, above that lost by those in the light, could be accounted for by algae consumed and digested in lieu of unavailable photosynthates. The zoochlorellae separation technique used on the post-test animals of this study came about as a long series of trials and error, and by sheer coincidence was finalized (by its first satisfactory results) half way into the photosynthate translocation experiment. As can be seen in the results of these post-test comparisons of algal densities in acoels of the light and dark controls (Fig. 3.7), the significantly higher densities found in the dark control animals does not support the idea of increased consumption of endosymbionts when denied photosynthates. Such a hypothesis is further unwarranted in that only minute particles of digested matter were found in both treatments, indicating that any algal mass consumed would at least in part be converted to host mass; which does not appear to be the case. Algal cells in *C. retrogemma* were found to survive for over 30 days in the dark (Åkesson & Hendelberg 1989); since the dark treatment lasted only 10 days, it appears that the higher densities of algae in the dark controls is likely the result of little or no loss of algal numbers coupled with an accelerated loss of host mass.

Although the photosynthate translocation experiment was successful in showing a net transfer from the symbiont to the host, it proved to be exceedingly labor-intensive as a method for merely showing movement without quantifying it. Muscatine *et al.*, (1974) offer a simpler method in which they incubated adult specimens of *S. roscoffensis* in  $\text{NaH}^{14}\text{CO}_3$  in the light;

with the acoels removed from the  $^{14}\text{C}$  incubation and washed, their eggs and mucus were collected and tested for the labeled carbon. The same methodology using  $^{14}\text{C}$  or  $^{13}\text{C}$  would be far more amenable, than that used in this study, for use on all the convolutrilobids given the recent discovery of how to induce sexual reproduction in these otherwise primarily-asexual acoels (Shannon & Achatz 2007).

**Future direction.** The zoochloellae separation method outlined in this study, though not entirely perfected, resulted in an “acceptable”, small percentage of algal cell lyses, and shows great potential for use in future, quantitative translocation experiments – with minor modifications. The most valuable and utile information, however, to emerge from this study is the design of the dewatering device. It performed beyond expectations in preparing an exceedingly fragile, small, soft-bodied animal for wet-weighing without injury, and yielded surprisingly accurate and reproducible results. It was very inexpensive and simple to build from parts available at most hardware stores (with the exception of the plankton-netting). With little or no modification it has the potential to be used on any number of taxa.

### **Acknowledgements**

Thanks to Bill Fitt and Walter Hatch for their continued support of my work. This research was supported by the U.S. Environmental Protection Agency under STAR Fellowship No. FP-91636501-0

## Literature Cited

- Åkesson B, Hendelberg J (1989) Nutrition and asexual reproduction in *Convolutriloba retrogemma*, an acoelous turbellarian in obligate symbiosis with algal cells. In: Ryland JS, Tyler PA (eds) *Reproduction, genetics and distributions of marine organisms*. Olsen & Olsen, Fredensborg, Denmark, pp 13-21
- Bohn G, Drzewina A (1928) Les 'Convoluta'. Introduction à l'étude des processus physico-chimiques chez l'être vivant. *Annales des sciences naturelles. (Zoologie)* 11:299-398
- Boyle JE, Smith DC (1975) Biochemical interactions between the symbionts of *Convoluta roscoffensis*. *Proceedings of the Royal Society of London. Series B, Biological Sciences* 189(1094):121-135
- Gattuso JP, Jaubert J (1990) Effect of light on oxygen and carbon dioxide fluxes and on metabolic quotients measured *in situ* in a zooxanthellate coral. *Limnology and Oceanography* 35(8):1796-1804
- Graff L (1891) *Die Organisation der Turbellaria Acoela*. Verlag Von Wilhelm Engelmann, Leipzig, 90 pp.
- Hendelberg J, Åkesson B (1988) *Convolutriloba retrogemma* gen. et sp.n., a turbellarian (Acoela, Platyhelminthes) with reversed polarity of reproductive buds. *Fortschritte der Zoologie* 36:321-327
- Johnston M, Yellowlees D, Gilmour I (1995) Carbon isotopic analysis of the free fatty acids in a tridacnid-algal symbiosis: interpretation and implications for the symbiotic association. *Proceedings of the Royal Society of London Series B-Biological Sciences* 260(1359):293-297
- Kremer BP (1975)  $^{14}\text{CO}_2$  fixation by endosymbiotic alga *Platymonas convolutae* within turbellarian *Convoluta roscoffensis*. *Marine Biology* 31(3):219-226
- Legendre L, Demers S, Yentsch CM, Yentsch CS (1983) The  $^{14}\text{C}$  method: Patterns of dark  $\text{CO}_2$  fixation and DCMU correction to replace the dark bottle. *Limnology and Oceanography* 28(5):996-1003
- Mattoo AK, Pick U, Hoffmanfalk H, Edelman M (1981) The rapidly metabolized 32,000-dalton polypeptide of the chloroplast is the "proteinaceous shield" regulating photosystem II electron transport and mediating diuron herbicide sensitivity. *Proceedings of the National Academy of Sciences of the United States of America-Biological Sciences* 78(3):1572-1576
- Meyer H, Provasoli L, Meyer F (1979) Lipid biosynthesis in the marine flatworm *Convoluta roscoffensis* and its algal symbiont *Platymonas convoluta*. *Biochimica Et Biophysica Acta* 573(3):464-480
- Muscatine L, Boyle JE, Smith DC (1974) Symbiosis of acoel flatworm *Convoluta roscoffensis* with alga *Platymonas convolutae*. *Proceedings of the Royal Society of London Series B-Biological Sciences* 187(1087):221-234

- Muscatine L, Hand C (1958) Direct evidence for the transfer of materials from symbiotic algae to the tissues of a coelenterate. *Proceedings of the National Academy of Sciences of the United States of America* 44(12):1259-1263
- Nozawa K, Taylor DL, Provasol L (1972) Respiration and photosynthesis in *Convoluta roscoffensis* Graff, infected with various symbionts. *Biological Bulletin* 143(2):420-430
- Shannon T, Achatz JG (2007) *Convolutriloba macropyga* sp.nov., an uncommonly fecund acoel (Acoelomorpha) discovered in tropical aquaria. *Zootaxa* 1525:1-17
- Stemann Nielsen E (1952) The use of radio-active carbon ( $C^{14}$ ) for measuring organic production in the sea. *ICES Journal of Marine Science* 18(2):117-140
- Taylor DL (1974) Nutrition of algal-invertebrate symbiosis. I. Utilization of soluble organic nutrients by symbiont-free hosts. *Proceedings of the Royal Society of London. Series B, Biological Sciences* 186(1085):357-368
- Trench RK (1971) The physiology and biochemistry of zooxanthellae symbiotic with marine coelenterates. I. The assimilation of photosynthetic products of zooxanthellae by two marine coelenterates. *Proceedings of the Royal Society of London Series B-Biological Sciences* 177(1047):225-235
- Trench RK, Winsor H (1987) Symbiosis with dinoflagellates in two pelagic flatworms, *Amphiscolops* sp. and *Haplodiscus* sp. *Symbiosis* 3(1):1-22
- Tyler S, Hooge M (2004) Comparative morphology of the body wall in flatworms (Platyhelminthes). *Canadian Journal of Zoology-Revue Canadienne De Zoologie* 82(2):194-210
- Warner ME, Fitt WK, Schmidt GW (1996) The effects of elevated temperature on the photosynthetic efficiency of zooxanthellae in hospite from four different species of reef coral: A novel approach. *Plant Cell and Environment* 19(3):291-299



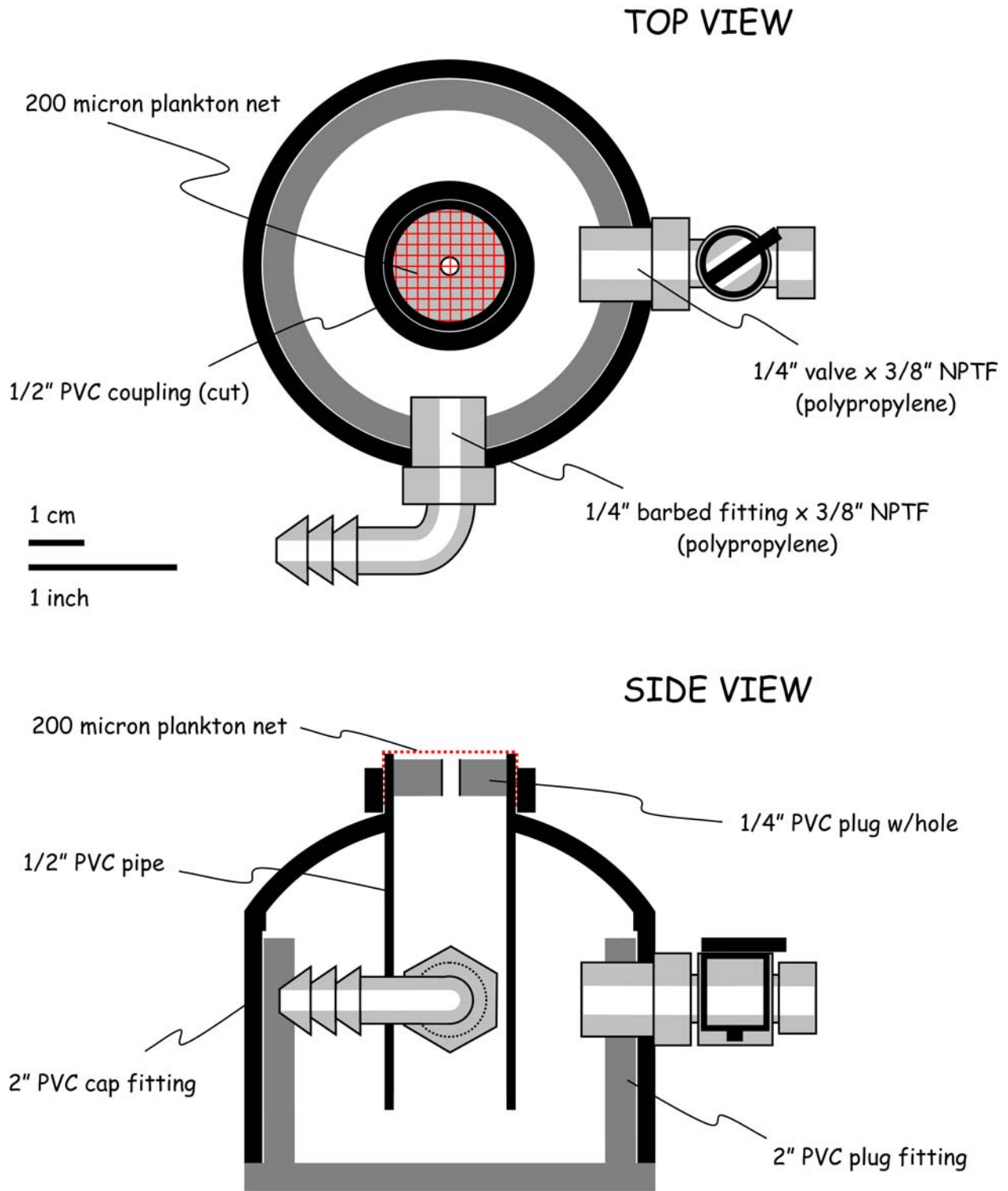


Figure 3.1. Schematic representation of the dewatering device used for the non-disruptive, vacuum-assisted, removal of water (external medium) from live acoels prior to weighing the animals. The device was fabricated from common PVC pipe and fittings.

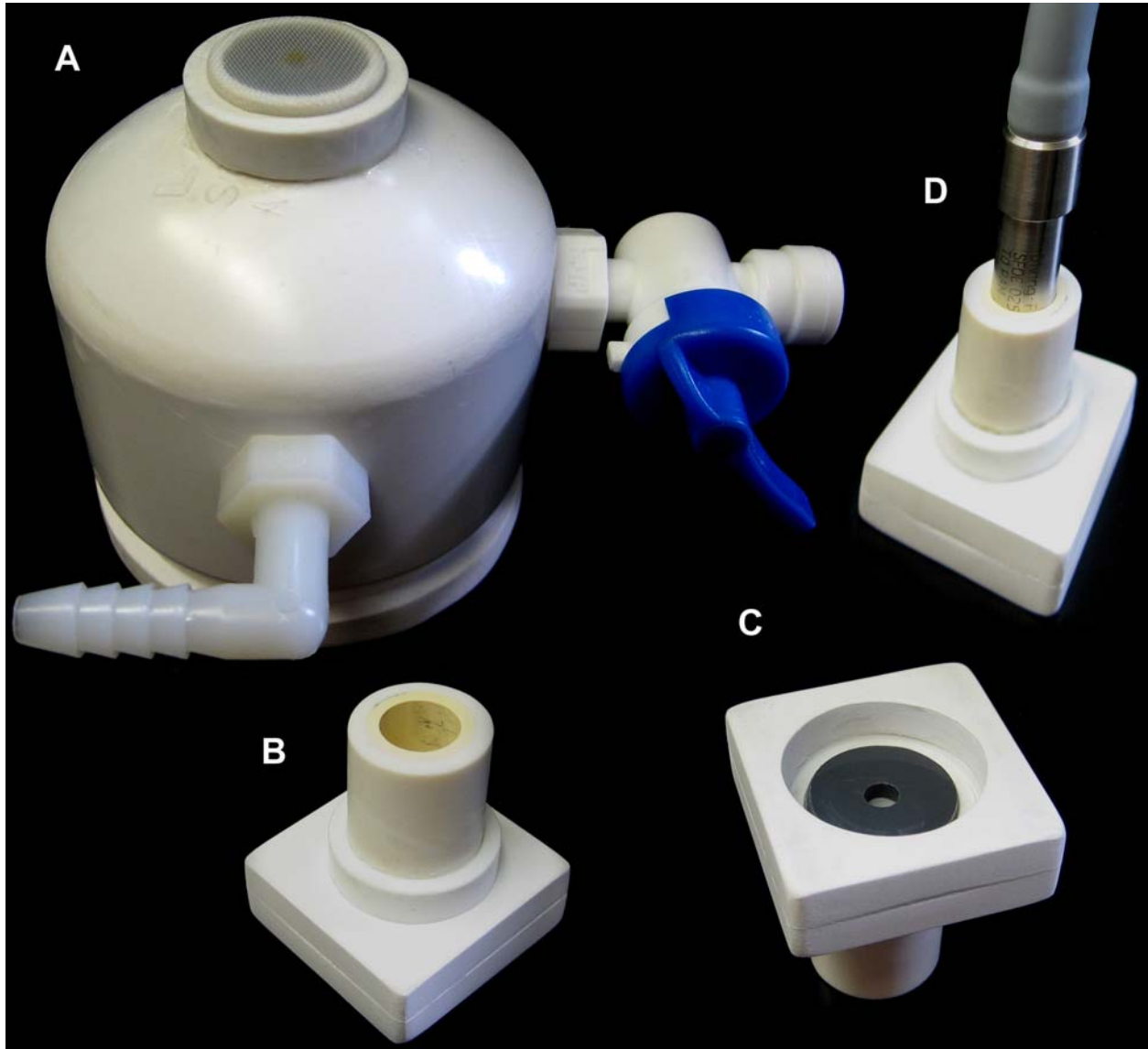


Figure 3.2. Photograph of apparatus used for removing water (external medium) from live acoels. A. Vacuum-assisted dewatering device. Vacuum source connects to barbed fitting. Valve allows for fine control of suction at the dewatering stage (top of device). B. Chamber used to hold acoels for PAM fluorometry. C. Underside of chamber designed to connect to dewatering stage to remove water from acoels. Center hole covered with 14 micron plankton net to support acoels during dewatering and fluorometry processes. D. Chamber connected to PAM fiber-optic cable.

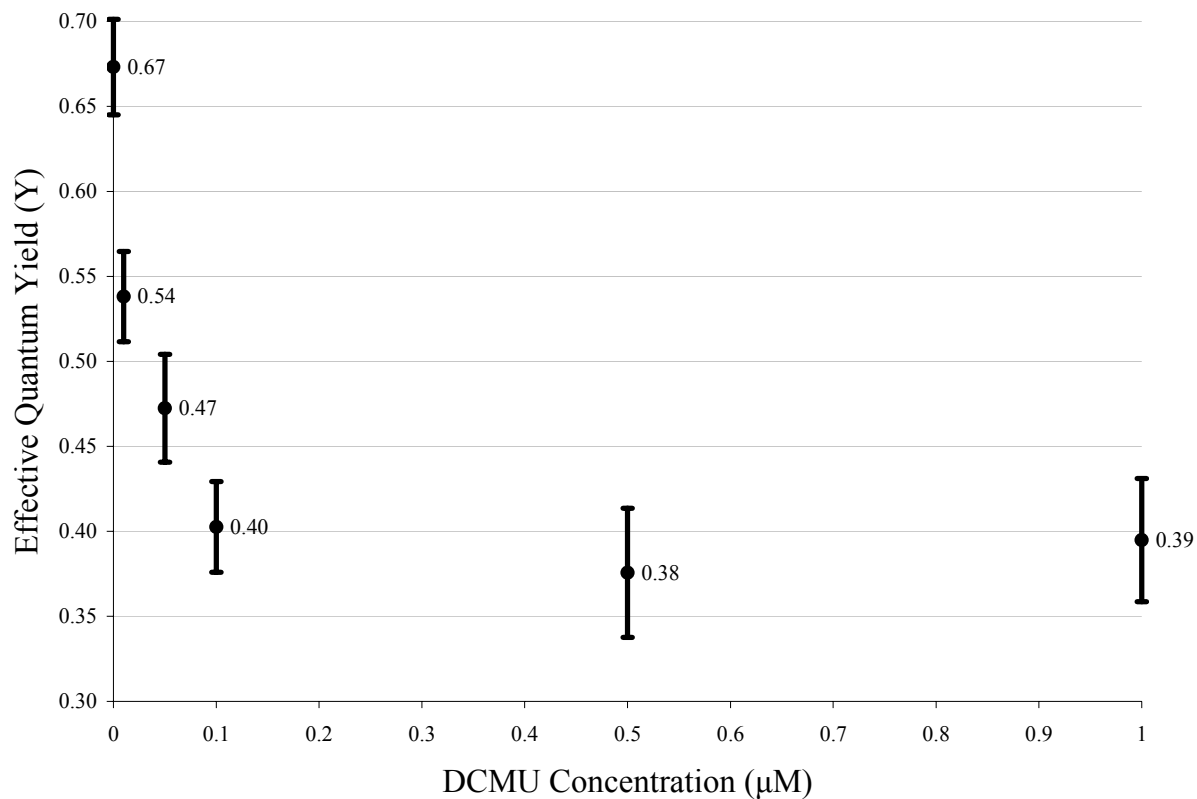


Figure 3.3. Effective quantum yield of photosystem II in the zoochlorellae endosymbionts (*in vivo*) of *Convolutriloba retrogemma*, determined by PAM fluorometry, as a function of DCMU concentration in the external medium. Error bars represent 95% confidence intervals.

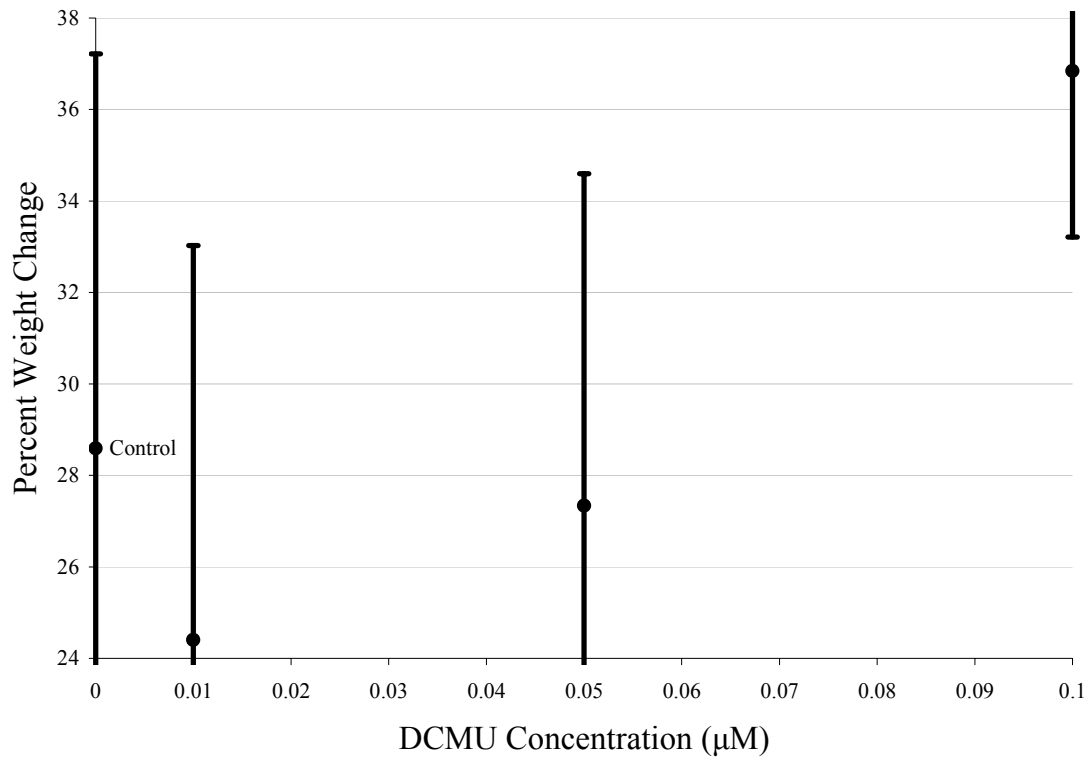


Figure 3.4. Percent weight change (loss) of *Convolutriloba retrogemma* kept in total darkness for 7 days as a function of DCMU concentration in the external medium compared to control group (no DCMU). Error bars represent 95% confidence intervals.

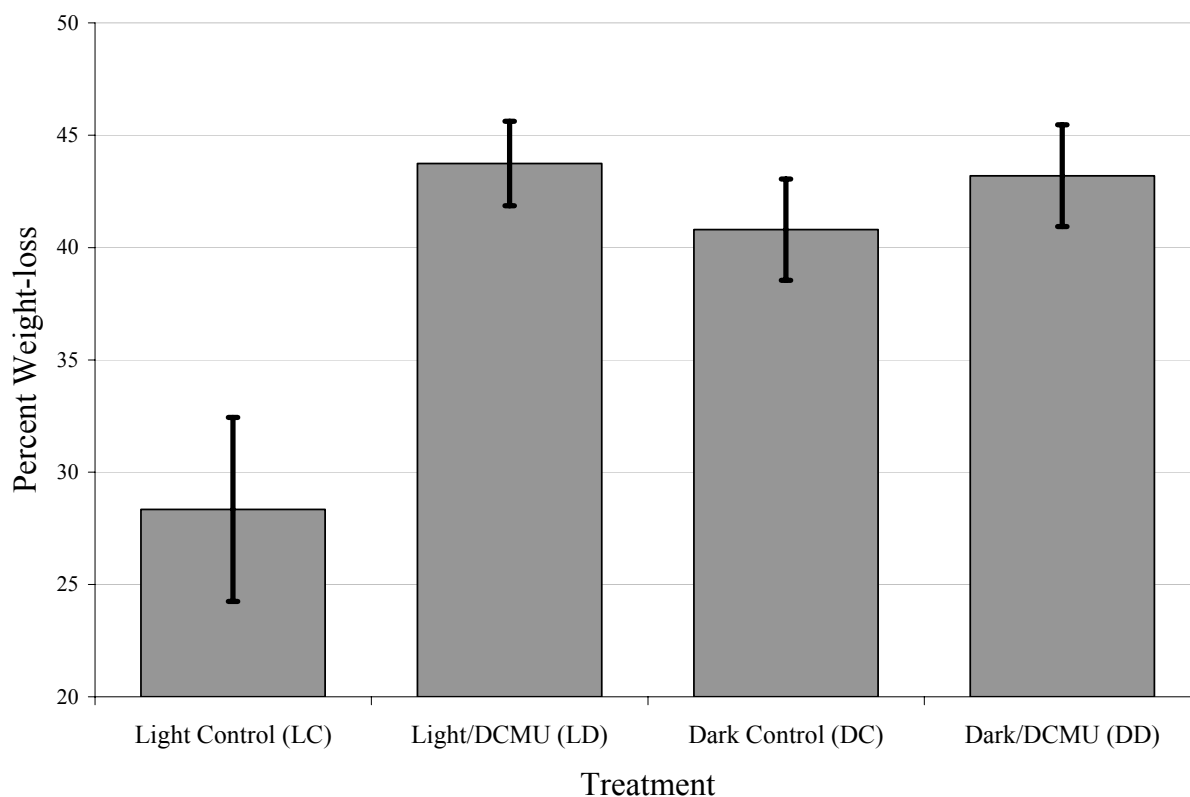


Figure 3.5. Percent weight loss of *Convolutriloba retrogemma* subjected to 4 treatments (Light, Light with DCMU, Dark, and Dark with DCMU). Light was provided at an irradiance of  $70 \mu\text{mole}\cdot\text{m}^{-2}\cdot\text{s}^{-1}$ ,  $[\text{DCMU}] = 0.1 \mu\text{M}$ ,  $n_{\text{LC}} = 37$ ,  $n_{\text{LD}} = 46$ ,  $n_{\text{DC}} = 46$ ,  $n_{\text{DD}} = 45$ . Error bars represent 95% confidence intervals. Results indicate positive photosynthetic carbon fixation and net transfer of photosynthate from algae to host.

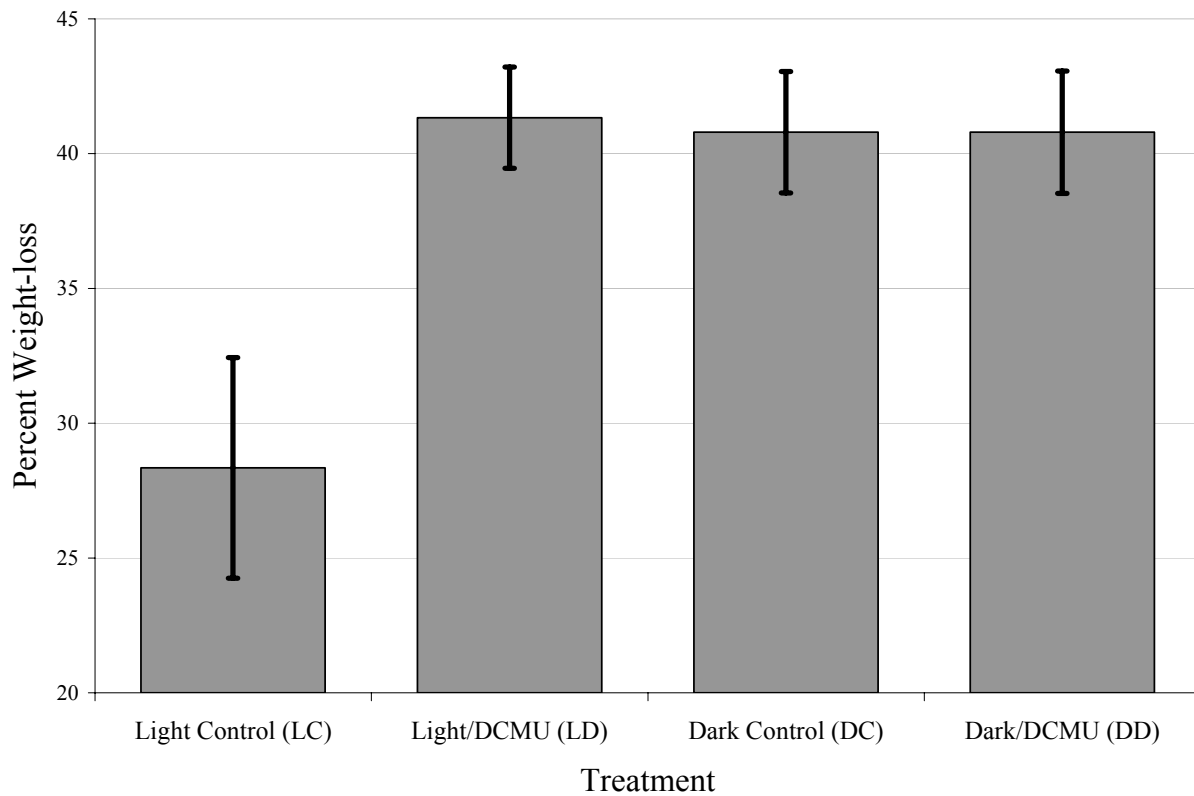


Figure 3.6. Percent weight loss of *Convolutriloba retrogemma* subjected to 4 treatments. Same as previous figure, but with non-photosynthetic effects of DCMU removed from the data corresponding to the treatments utilizing DCMU. Error bars represent 95% confidence intervals. Data clearly show significantly higher weight loss in acoels kept in the dark and those treated with DCMU, indicating a net translocation of photosynthate from symbiont to host.

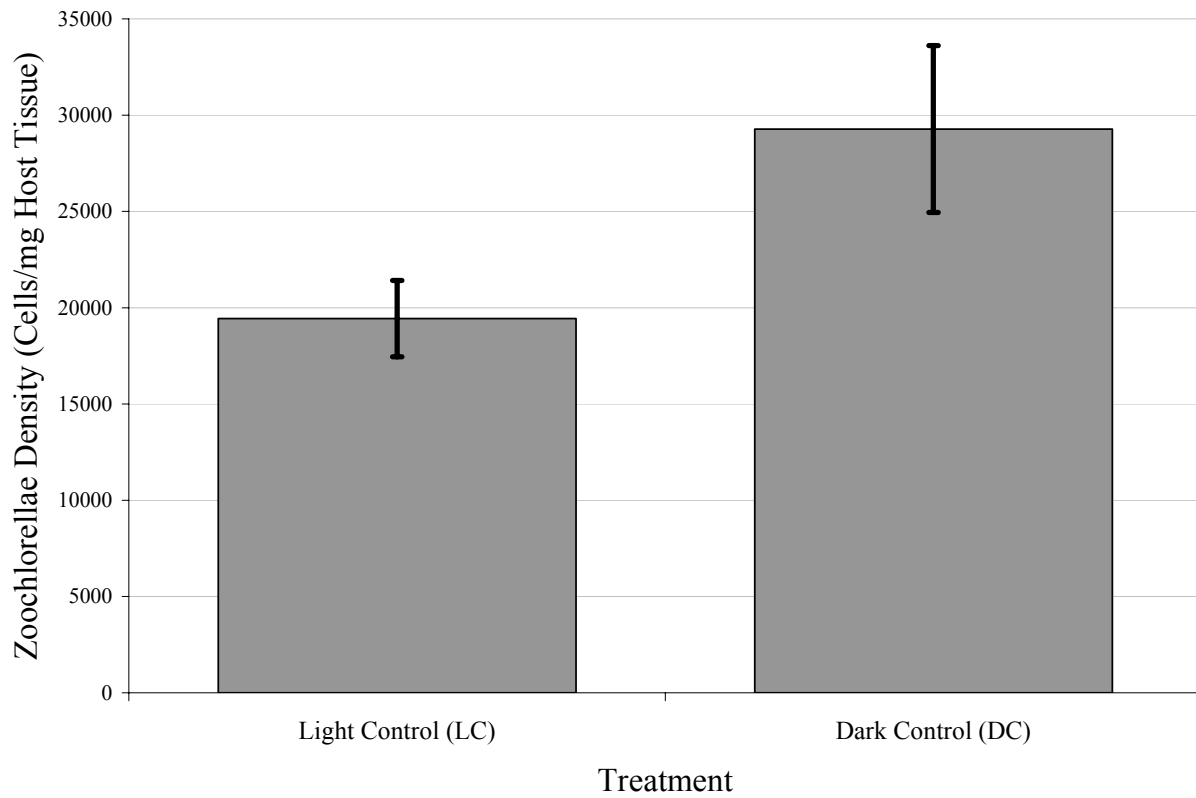


Figure 3.7. Post-test zoothlorellae densities in Light and Dark Control group acoels used in the carbon-translocation experiment. Density was measured as algal cells per milligram of host tissue. Error bars represent 95% confidence intervals.

## CHAPTER 4

### PHOTOMOVEMENTS OF *CONVOLUTRILOBA RETROGEMMA*<sup>1</sup>

---

<sup>1</sup> Shannon, T. To be submitted to *Marine Ecology Progress Series*.



## **Abstract**

Detailed herein are the photomovements and photoreactions of *Convolutriloba retrogemma*. Described are the general basking behaviors of this acoel and explanations as to the qualitative and quantitative nature of light that leads to these behaviors. Specifically detailed are a blue-light-mediated, step-up, photophobic response to sudden increases in light, and a photoaccumulative behavior responsible for observed mass basking formations. The photophobic response is triggered by visual, photic stimuli, whereas the photoaccumulative behavior occurs as a consequence of the symbiotic condition of the host and is regulated by the photosynthetic activity of the algal endosymbiont.

**Key words:** *Convolutriloba*, acoel, photomovements, behavior, light emitting diode, halo, light response

## Introduction

Countless studies of invertebrate responses to photic stimuli can be readily discovered in any literature search, and numerous bodies of work have been devoted primarily to the physical effect of light on invertebrates and the mechanisms by which that light is sensed and translated to discernable animal behavior (e.g., Carthy 1958; Wolken 1971; Warrant & Nilsson 2006). Within this fathomless sea of research can be found an equally daunting collection of studies focusing solely on the vision of marine invertebrates and the role of light on behaviors that affect every facet of their existence from recruitment to navigation to hunting to predator-avoidance to sex (e.g., Land & Nilsson 2006). A small sub-sampling of this latter work is dedicated to invertebrates with algal endosymbionts.

In many of these symbiotic systems, like that of *Symsagittifera (Convoluta) roscoffensis* Graff 1891, and its alga *Tetraselmis (Platymonas) convolutae*, the phototactic behaviors of symbiotic animals are identical to those of aposymbiotic specimens (Keeble 1910), suggesting visual, photoreceptor-mediated, responses. Though one of the phototactic/geotactic responses of this acoel also involves a statocyst (Fraenkel 1929), all occur independent of the algal endosymbiont. This, however, is not always the case in algal-invertebrate systems.

Kawaguti found, in 1940, that zooxanthellate planula larvae of corals exhibited positive phototaxis whereas those without zooxanthellae exhibited no reaction to light whatsoever, suggesting a non-visual response to photic stimuli dependent upon the symbiotic condition of the host. Zahl & McLaughlin (1959) found additional algal-dependent responses in the anemone *Condylactis* whereby a majority of zooxanthellate animals, originally distributed evenly between the shaded and un-shaded regions of a pool, had moved to the shaded area after 12 days. Aposymbiotic *Condylactis* showed no photoresponse and remained randomly distributed over

the same time period. Lastly, Pearse (1974b) discovered in the anemone *Anthopleura elegantissima*, similar symbiont-dependent phototactic behaviors, and further noted that the sign (positive or negative) of phototaxis depended on the light intensity of the habitat from where the animal was collected. These results suggested not only a photosynthetically-related trigger for the behaviors, but a regulator as well (for comprehensive review of algal-invertebrate photobehavior see: Pearse 1974a, b).

*Convolutriloba retrogemma* Hendelberg & Åkesson 1988, a free-living acoel with green-algal endosymbionts, exhibits several behaviors in response to photic stimuli. The animal, when introduced to a lighted environment, will move about the substrate and eventually settle out in one of two “basking” positions. If situated on the substrate, perpendicular to the light source, the animal flattens dorso-ventrally exposing maximum surface area to the light; if situated on the sides of a container, parallel to the light source, the animal will again flatten dorso-ventrally, but will bend in such a way as to project its front half away from the side and into the light-stream. Animals subjected to a sudden increase in light intensity will react in one of several ways; if on a gravel substrate, it will exhibit negative phototaxis and move directly down into the substrate; if on a smooth substrate with a directional light source, it will exhibit negative phototaxis and move away from the light source; in non directional light it will exhibit positive photokinesis, i.e., increased forward speed and increased random turning until an area of lower light intensity is reached. Similar photophobic behaviors can be triggered by mechanical agitation, i.e., tapping on the container. Animals left undisturbed for long periods tend to photoaccumulate, or aggregate, in “halo” formations (Fig. 4.1) around objects arising from the substrate, or along the edges of visible shadows cast on the substrate.

The photophobic behavior of *C. retrogemma* appears to be visually-triggered, whereas the photoaccumulative response is likely regulated non-visually by the photosynthetic activity of the algal endosymbiont. The experiments conducted for, and covered in, this chapter involved both of these photobehaviors and were designed to determine the quality and quantity of light required to elicit and/or maintain the responses.

## **Materials and Methods**

Populations of *Convolutriloba retrogemma* were maintained in trough-style research aquaria in both a mixed-species population with other convolutrilobids (*C. hastifera*, *C. longifissura* & *C. macropyga*) and in a monospecific culture tank separate from other *Convolutriloba* spp. as outlined in Chapter 3.

In an effort to determine substrate-level light intensities experienced by acoels in a halo-formation relative to the distance from the edges of the encircled object, an experiment was designed in which photography was employed to ameliorate the detection of subtle light gradients. To set up the experiment to best mirror the conditions found in the research aquaria where the halo-forming, basking behavior was first discovered, a grey PVC cylinder (6 cm diameter x 7 cm high) was placed into the center of a small glass aquarium (50 cm x 30 cm x 30 cm) containing artificial seawater at a depth of 20 cm. An air-stone was also submerged into the aquarium and charged with low-pressure air to agitate the water's surface with bubbles. The aquarium was then placed on the stage of a photographic enlarger in a dark-room atop a sheet of unexposed photographic paper. In order to diffuse the otherwise omnidirectional light from the enlarger, a sheet of plastic "prismatic" light-fixture covering was placed over the top of the aquarium. Exposure time of the paper through the aquarium was 1.5 seconds. The resulting

photograph was scanned into a computer using SigmaScan (Version 2.0) and grayscale measurements of pixels in the computer image were recorded along eleven 10 cm linear transects radiating out from the center of the cylinder's photographic impression. The grayscale measurements were averaged along the lengths of all transects and the resulting averages normalized to a 0–100 scale. Relative light intensity was determined for the area corresponding to 0–7 cm, relative to the edge of the cylinder, from these normalized averages.

Photomovements/photoresponses of *C. retrogemma* were recorded and quantified using a custom-designed environmentally-controlled light chamber. The light chamber (Figs. 4.2 & 4.4) allowed for the maintenance of temperature, salinity, and light intensity/color over the course of each experiment. The experimental water volume in which the acoels were tested was only 30 ml and was apt to experience detrimental increases in temperature due to heat emission from the light source and increases in salinity due to evaporative losses; as such, water temperature was maintained during experiments by an internal cooling jacket (Fig 4.2) in the lower half of the chamber supplied from an external water source maintained at 25°C. Chamber air was maintained at ~ 26°C with a high moisture content to ensure no evaporative losses and subsequent salinity increase by bubbling pressurized air through the same 25°C external water source and supplying it to the upper half of the chamber at low pressure and velocity. Salinity was maintained at 34 ppt. The light chamber design allowed for the use of a variety of light sources and optical filter configurations.

For the first photomovement experiment, to determine the short-term reaction to sudden increases in light (a “step-up” photobehavior), a fiber-optic, white-light source (Fostec AceI w/ USHIO Halogen EKE-21V-150W bulb) was utilized. Each experimental run consisted of 50 acoels selected at random from individually maintained conspecific cultures. Culture use was

rotated to eliminate pseudoreplication. Acoels were placed in 30 ml of filtered artificial seawater, one half of the surface area was shaded (Fig. 4.2), the light chamber was sealed and the acoels were allowed to dark adapt for 30 minutes. Following dark adaptation, light was applied to the chamber at full intensity with or without optical filters depending on the experimental run. Two white-light treatments were tested, high and low, as were three colored-light treatments. High white-light trials received the halogen/fiber-optic light-source maximum intensity at  $260 \mu\text{mole}\cdot\text{m}^{-2}\cdot\text{s}^{-1}$ . Low white-light trials were illuminated through a neutral density filter (single-ply black fiberglass screen) yielding an intensity of  $145 \mu\text{mole}\cdot\text{m}^{-2}\cdot\text{s}^{-1}$ . Color-light trials were illuminated through either a red, high-pass filter; a blue, narrow band-width filter; or a blue-green, wide band-width filter (Fig. 4.3).

Once light was applied, photographs of the experimental area (Fig. 4.4A inset) were captured every 5 seconds and recorded utilizing Breeze System's PS Remote (Version 1.5) software via a Canon PowerShot A520 digital camera. Time lapse capture for each experimental run continued for 10 minutes. Each white-light run was continued for a total of 18 hours, though without time-lapse capture. Following each run the final (at 18 hrs) number of acoels in the lighted region was determined, sequential photographs were analyzed and the number of acoels in the lighted region of each image was determined and recorded. Results at each time step were calculated as percent of acoels remaining in the lighted region in relation to the number present when the light was first applied. Mean percentage remaining at each time step was determined for  $n = 5$  replicate runs. A 95% confidence interval for each time step was calculated and the results graphed.

For the second photomovement experiment, to determine/verify the wavelengths of light responsible for the step-up photobehavior determined in the previous experiments, a variable-

intensity, narrow band-width, interchangeable light emitting diode array light source was designed and fabricated (Figs. 4.4B&C). The LED light source consisted of 6 lamp sockets in a series-parallel arrangement (2 x 3 in-series), allowing for simple wavelength changes via lamp replacement. Output intensity was determined by the resistance rating of interchangeable series resistors (Fig. 4.4B). A dimmer switch (Holly Solar, Petaluma, CA) allowed for fine control at any given output intensity. LED's used in the experiment trials emitted in the blue, green, yellow, orange, and red (models E7113PBC-J, E7113VGC-J, E7113SYC-J, E7113SEC & E7113SEC-H, eLED.com Corporation, Walnut, CA) at peak wavelengths of 470, 525, 589, 610, and 630 nm respectively. LED output spectra were determined with a CCD Spectrometer (EG&G Princeton Applied Research Model 1235 Digital Triple Grating Spectrograph) and data were normalized to a 0–100 scale for illustrative purposes and plotted (Fig. 4.5). LED array intensity for all trials was selected based on the lowest rated maximum output of any single lamp used, in this instance, the 610 nm orange lamps at 2500 mcd. Maximum array output intensities at each of the five colors was measured using a Li-Cor Model LI-1400 Data Logger with an LI-190SA quantum sensor and an intensity ratio determined using the manufacturer's rated (mcd) maximum output. Using this ratio, an equivalent experimental output for each color array was determined and set using the Li-Cor data logger. Trials were run at each color treatment as outlined in the previous experiment, but with  $n = 6$  runs per experiment instead of 5.

The third and final photomovement experiment, to determine the stimulus/stimuli responsible for the observed, long-term photoaccumulative behavior of *C. retroemma*, was conducted on symbiotic and aposymbiotic acoels subjected to low-intensity white-light over 24 hour trial periods. Symbiotic acoels were chosen at random from the monospecific culture tanks for each experimental trial. Aposymbiotic acoels were obtained by modifying the method of

Trench & Winsor (1987). As such, randomly chosen symbiotic animals were incubated under an irradiance of  $\sim 800 \mu\text{mole}\cdot\text{m}^{-2}\cdot\text{s}^{-1}$  (halogen/fiber-optic light-source) in 5  $\mu\text{M}$  DCMU, 3-(3,4-dichloro-phenyl)-1,1-dimethylurea, for 5 days until algae-free or nearly algae-free. DCMU solutions were mixed according to the method outlined in chapter 3. The same light-chamber and time-lapse photographic equipment used in the photophobia experiments was employed for these experiments. Fifteen acoels were used in each trial, and were dark-adapted for 30 minutes prior to the beginning of each trial. Filtered artificial seawater (34 ppt) was used in all trials; for trials involving aposymbiotic acoels, DCMU was added to 0.01  $\mu\text{M}$  to ensure photoinhibition of any remaining algae. Following dark adaptation, the light chamber was illuminated by white LED's (model E7114PWC-H, eLED.com Corporation, Walnut, CA) at  $1 \mu\text{mole}\cdot\text{m}^{-2}\cdot\text{s}^{-1}$ , and time-lapse photography was initiated. Photographs of the experimental area were captured every 5 minutes for 24 hours,  $n = 5$  trials per treatment. Results at each time-step were calculated as percent of total (15) acoels in the lighted region. Results within each hour of each trial were averaged together and the mean of all 5 trials was calculated for each hour of both treatments; 95% confidence intervals were calculated accordingly and the results plotted.

## Results

As shown in figure 4.6, relative irradiance at substrate level varies with respect to distance from the edge of an object; in this instance, a 6 cm diameter x 7 cm high PVC cylinder. The onset of an exponential increase in light intensity occurs relatively near the object's edge with a maximum slope around 1 cm out; this 1 cm band around a similar object in the research aquaria (see fig. 4.1) corresponds to an area of low acoel density. From this point, light intensity continues to increase and slowly asymptotes towards maximum levels. The area between 1 and



6 cm from the edge of the object corresponds, *in situ*, to the area in which acoels accumulate and exhibit their halo-forming basking behavior.

The initial tests to determine short-term photoresponses of *C. retrogemma* to white-light showed a definite step-up photophobic response (Fig. 4.7) whereby dark-adapted animals exposed to the sudden onset of light exhibited an increase in velocity and direction change until a lower intensity area was encountered. Baseline tests, utilizing high-intensity white light,  $\sim 260 \mu\text{mole}\cdot\text{m}^{-2}\cdot\text{s}^{-1}$ , yielded a sharp decline in animals remaining in the lighted region of the test chamber over the first 4 minutes of exposure with a slower, continuous decline over the remaining 6 minutes of the 10 minute trials. Under lower intensity white light,  $\sim 145 \mu\text{mole}\cdot\text{m}^{-2}\cdot\text{s}^{-1}$ , the acoels exhibited a similar photophobic response though less pronounced and with greater variability at each time-step between trials. After 18 hours of high-intensity illumination, only 1–7 of 50 acoels had settled in the lighted region; under low-intensity illumination nearly all, 47–50, had settled in the light. In the initial experiments utilizing optical filters (Fig. 4.8) in short-term trials, the step-up photophobic behavior was observed in response to blue and blue-green light, but not to red light.

Utilizing the narrow band-width of the LED array light source, it was possible to determine on a finer scale which wavelengths of light mediated the step-up, photophobic response. As shown in figure 4.9, all colors resulted in over-all photodispersal; however slight, of the acoels, but only the blue-light treatment resulted in the pronounced, step-up photophobic response of *C. retrogemma* observed in the white-light experiments.

In prolonged, low intensity, white-light experiments (Fig. 4.10), a photoaccumulative behavior of symbiotic *C. retrogemma* was observed whereby a gradual and steady increase in the number of acoels occurred in the lighted region over a 24 hour period. Under the same

illumination, no such photoaccumulative response was observed in trials involving aposymbiotic acoels.

## Conclusions

The majority of photophobic responses in invertebrates result from a sudden change in photic excitation of a photoreceptor or visual organ (e.g., Carthy 1958; Wolken 1971; Warrant & Nilsson 2006). In rarer instances, as in some ciliates, photophobic stimuli have been attributed to photosynthetic activity of algal symbionts (Reisser & Hader 1984). Given the majority, the observations and findings that the photophobic response of *Convolutriloba retrogemma* was triggered by visually-perceived, sudden changes in light were by no means unexpected.

The step-up photophobic response observed in *C. retrogemma*, however, is not as common amongst marine invertebrates as a step-down response. The step-down photophobic response, like that of sabellid tube worms or tridacnid clams (Land 2003; Land & Nilsson 2006), is triggered by a sudden *decrease* in light intensity, or shadowing. In both of these examples the instantaneous response, of pulling in feeding tentacles by sabellids, or closing of valves by tridacnids, is easily triggered by passing fish or other large marine life and serves the animal well as a means of predator avoidance. From an ecological perspective, no such avoidance is needed by *C. retrogemma*, yet it exhibits a photophobic behavior nonetheless.

The extreme toxicity of the convolutrilobids (Shannon & Achatz 2007) excludes these acoels from the diet of all but one known predator, the shield-head slug *Chelidonura varians* (Sprung & Delbeek 1997). Furthermore, the sudden increase in light intensity required to trigger the photophobic behavior would prove ineffective as a mechanism for the detection of predators. As such, the step-up photophobic response of *C. retrogemma* does not appear to serve the animal

in this manner, but may function as a means of escaping excessive photosynthetically-active radiation (PAR) levels and the potential production of reactive oxygen species (ROS) by its algal endosymbiont (Dykens *et al.* 1992). This assumption is further warranted in that the intensity of the response (Fig. 4.7) increases relative to the intensity of the light; as PAR increases, so does the potential for the production of ROS, oxidative stress, and subsequent loss of algae and/or tissue damage.

Invertebrate responses mediated by photosynthetic activities, such as the photoaccumulative behavior of endosymbiotic *Paramecium bursaria* with *Chlorella* sp. (Niess *et al.* 1981), tend to occur not only in white light, but in blue/blue-green and red light as well since these emit at the wavelengths corresponding to the maximum absorption of chlorophylls and their associated auxiliary photopigments. Most marine invertebrate *visual* pigments utilize the chromophore retinal combined with a variety of opsins to form rhodopsins. Though the wavelength of maximum absorption of these pigments can vary from 300 to 600<sup>+</sup> nm, many tend to absorb primarily blue/blue-green wavelengths (e.g., Cronin 2006; Land & Nilsson 2006). Since these shorter wavelengths travel further and penetrate deeper in seawater – least attenuation at ~ 475 nm – (Tyler & Smith 1970), they are best suited for affording maximum photic stimulation at any ambient light-level. Given this logic, the observation that the photophobic behavior of *C. retroemma* occurs only in blue/blue-green light (Figs. 4.8 & 4.9), and that the onset of the response is instantaneous; the step-up photophobic response is almost certainly visually-mediated.

The tendency of invertebrates with endosymbiotic algae to accumulate in the light is intuitive in that in order to benefit from the symbiosis, the host must situate its symbiont (and in doing so, itself) in an area of optimal PAR irradiance. The mechanisms by which a host searches

for and locates this area, are not so easily defined. Seeking out an illuminated environment (phototaxis and photoaccumulation) has been described as a “simple” visual process in a multitude of phototile organisms (e.g., Carthy 1958), but in order for a symbiotic host to actively locate an area of optimal irradiance for its alga, the process must invariably include the alga lest the host settle in sub-standard photic environments. As mentioned previously, such a system does exist in *Symsagittifera roscoffensis* (Keeble 1910) whereby both symbiotic and aposymbiotic animals exhibit the same photobehaviors. In other systems, however, such as *Condylactis* sp., *Anthopleura elegantissima*, and *Paramecium bursaria* (Zahl & McLaughlin 1959; Pearse 1974a, b; Niess *et al.* 1981), the symbiotic condition of the host not only results in specific photobehaviors, but study results suggest that the photosynthetic activity of the algal symbionts likely determine the extent to which the behaviors progress. In other words, host behavior is regulated by symbiont photosynthesis.

The results of this study clearly show that the photoaccumulative response of *Convolutriloba retrogemma* is mediated by the photosynthetic activity of its endosymbiont. As in *Condylactis* and *Anthopleura elegantissima* (Zahl & McLaughlin 1959; Pearse 1974a, b), the behavior was only observed in symbiotic animals (Fig. 4.10), verifying the obligatory algal role in exacting the behavior. Combining this finding with the results of the halo light intensity experiment (Fig. 4.6) and the observed basking behaviors, indicates that the photoaccumulative behavior occurs as a result of photosynthesis, and suggests that the host behavior is regulated by the photosynthetic activity in such a way as to situate the symbionts in photosynthetically-optimal light conditions.

## **Acknowledgements**

Thanks to Bill Fitt, Walter Hatch, and Gregory Schmidt for their continued support of my work. Special thanks to Mike Hollibaugh of Holly Solar for sharing his expertise in LED technology and aiding me in the design of the LED light source used in these experiments. This research was supported by the U.S. Environmental Protection Agency under STAR Fellowship No. FP-91636501-0

## Literature cited

- Carthy JD (1958) *An Introduction to the Behaviour of Invertebrates*. The MacMillian Company, New York, 380 pp.
- Cronin TW (2006) Invertebrate vision in water. In: Warrant E, Nilsson D-E (eds) *Invertebrate Vision*. Cambridge University Press, Cambridge; New York, pp 211-249
- Dykens JA, Shick JM, Benoit C, Buettner GR, Winston GW (1992) Oxygen radical production in the sea anemone *Anthopleura elegantissima* and its endosymbiotic algae. *Journal of Experimental Biology* 168:219-241
- Fraenkel G (1929) Über die geotaxis von *Convoluta roscoffensis*. *Zeitschrift für vergleichende Physiologie* 10:237-247
- Graff L (1891) *Die Organisation der Turbellaria Acoela*. Verlag Von Wilhelm Engelmann, Leipzig, 90 pp.
- Hendelberg J, Åkesson B (1988) *Convolutriloba retrogemma* gen. et sp.n., a turbellarian (Acoela, Platyhelminthes) with reversed polarity of reproductive buds. *Fortschritte der Zoologie* 36:321-327
- Kawaguti S (1940) On the physiology of reef corals. V. Tropism of coral planulae, considered as a factor of distribution of the reefs. *Palao Tropical Biological Station Studies* 2:319-328
- Keeble F (1910) *Plant-Animals: A Study in Symbiosis*. Cambridge University Press, London, 163 pp.
- Land MF (2003) The spatial resolution of the pinhole eyes of giant clams (*Tridacna maxima*). *Proceedings of the Royal Society of London Series B-Biological Sciences* 270(1511):185-188
- Land MF, Nilsson D-E (2006) General-purpose and special-purpose visual systems. In: Warrant E, Nilsson D-E (eds) *Invertebrate Vision*. Cambridge University Press, Cambridge; New York, pp 167-210
- Niess D, Reisser W, Wiessner W (1981) The role of endosymbiotic algae in photoaccumulation of green *Paramecium bursaria*. *Planta* 152(3):268-271
- Pearse VB (1974a) Modification of sea anemone behavior by symbiotic zooxanthellae: Expansion and contraction. *Biological Bulletin* 147(3):641-651
- Pearse VB (1974b) Modification of sea anemone behavior by symbiotic zooxanthellae: Phototaxis. *Biological Bulletin* 147(3):630-640
- Reisser W, Hader DP (1984) Role of endosymbiotic algae in photokinesis and photophobic responses of ciliates. *Photochemistry and Photobiology* 39(5):673-678

Shannon T, Achatz JG (2007) *Convolutriloba macropyga* sp.nov., an uncommonly fecund acoel (Acoelomorpha) discovered in tropical aquaria. *Zootaxa* 1525:1-17

Sprung J, Delbeek JC (1997) *The Reef Aquarium: A Comprehensive Guide to the Identification and Care of Tropical Marine Invertebrates*, 2. Ricordea Publishing, Coconut Grove, FL, 546 pp.

Trench RK, Winsor H (1987) Symbiosis with dinoflagellates in two pelagic flatworms, *Amphiscolops* sp. and *Haplodiscus* sp. *Symbiosis* 3(1):1-22

Tyler JE, Smith RC (1970) *Measurements of Spectral Irradiance Underwater. Ocean series, 1*. Gordon and Breach, New York, 103 pp.

Warrant E, Nilsson D-E (eds.) (2006) *Invertebrate Vision*. Cambridge University Press, New York

Wolken JJ (1971) *Invertebrate Photoreceptors*. Academic Press, Inc., New York, 179 pp.

Zahl PA, McLaughlin JJA (1959) Studies in marine biology. IV. On the role of algal cells in the tissues of marine invertebrates. *Journal of Protozoology* 6(4):344-352



Figure 4.1. Characteristic halo-formation resulting from the photoaccumulative behavior of basking *Convolutriloba retrogemma*. Aggregations, 2–5 cm wide, of the acoel generally form between 1 and 6 cm surrounding objects on flat substrate.



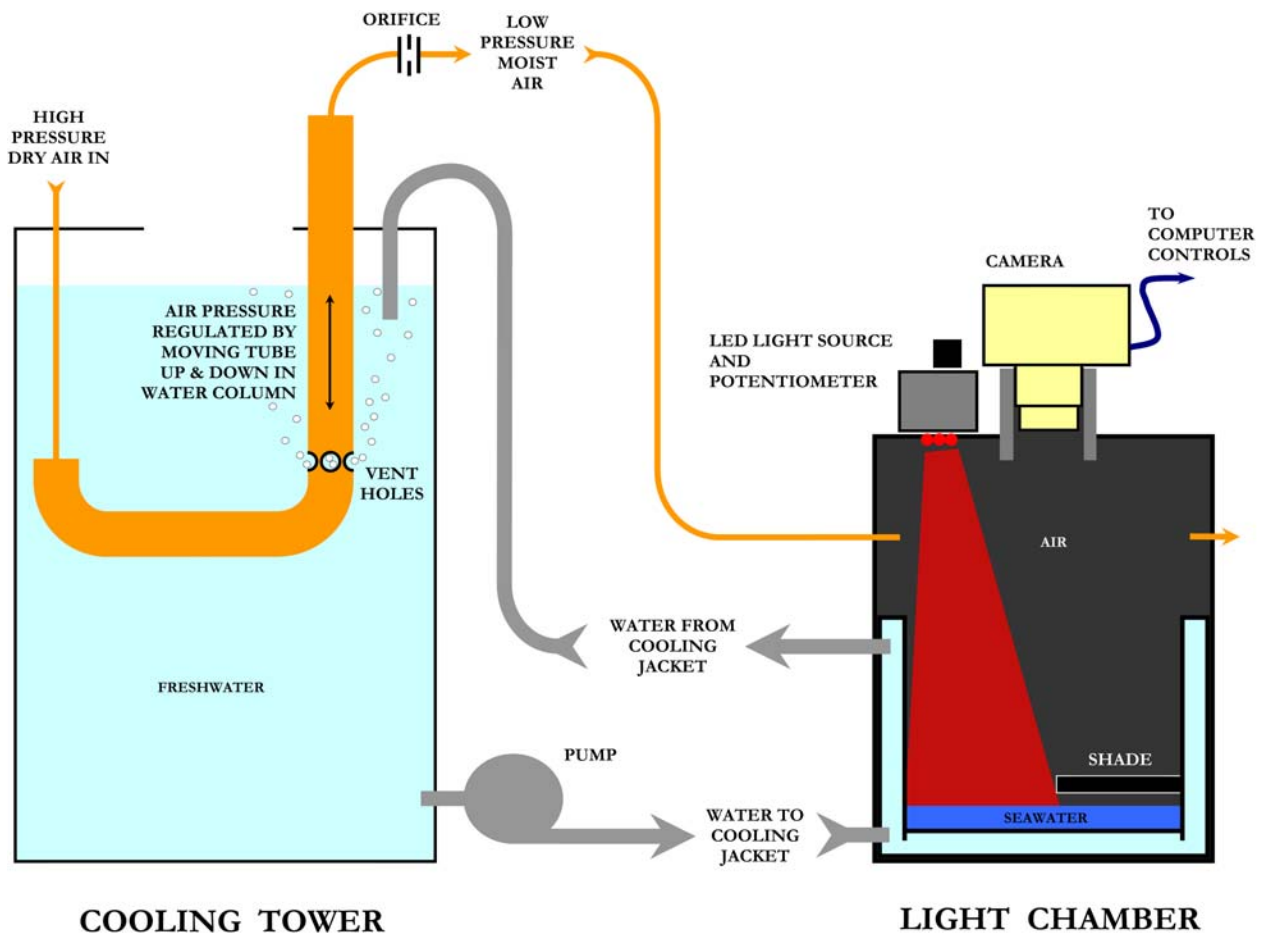


Figure 4.2. Schematic representation of light chamber and time-lapse photography apparatus utilized in the photomovement experiments. Light-source was interchangeable. Experiments used either a halogen/fiberoptic light-source with optical filters or monochromatic, light emitting diode arrays (shown).

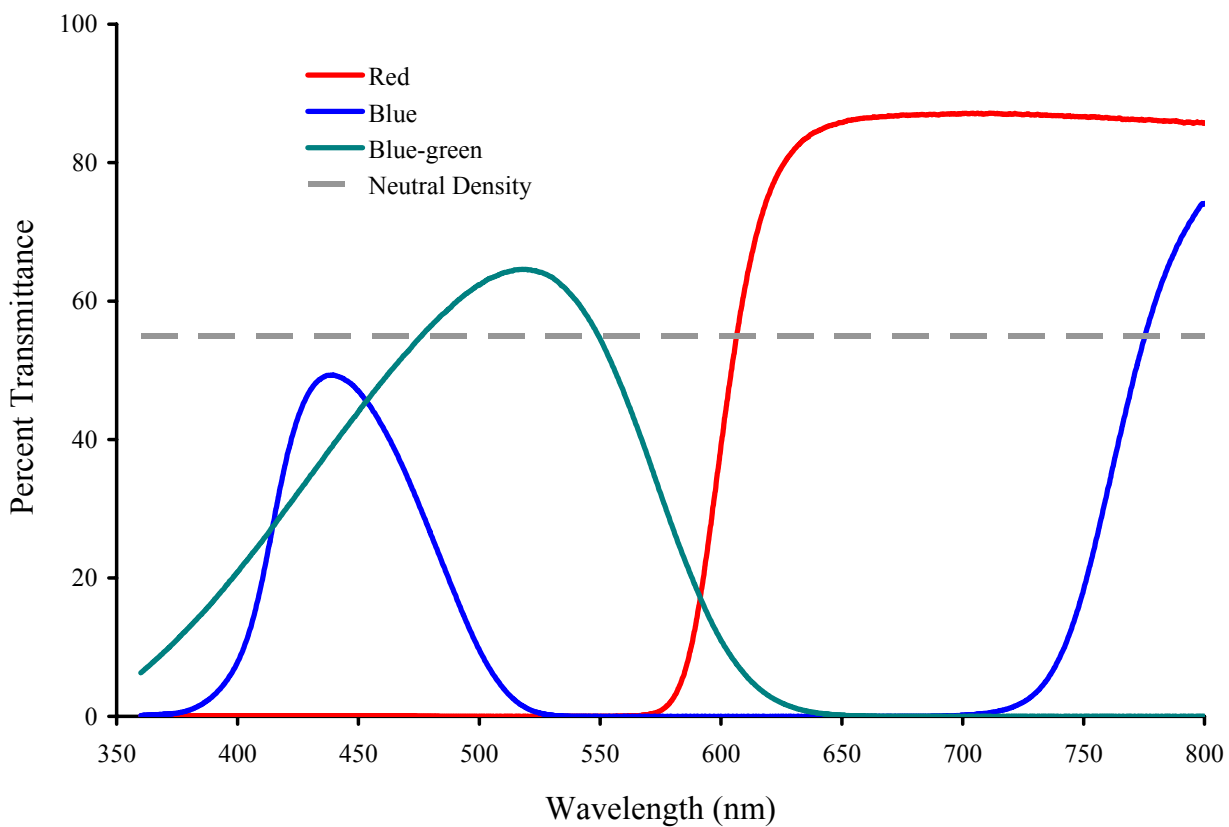


Figure 4.3. Transmittance spectra of the filters used in determining and defining the short-term response of *Convolutriloba retrogemma* to a step-up, sudden increase in light intensity. These filters were used in conjunction with a halogen, fiber-optic light source.

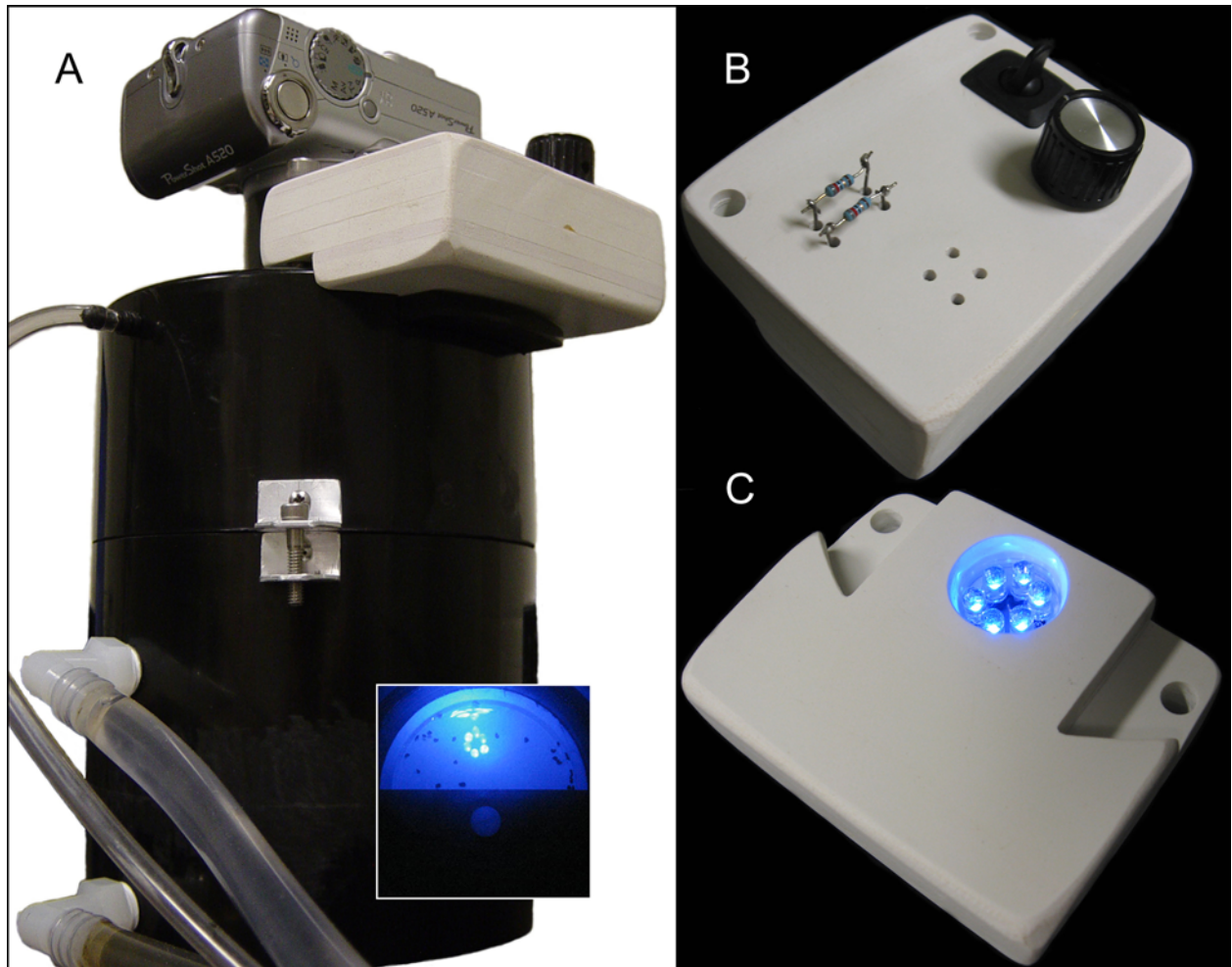


Figure 4.4. Photographs of light chamber used in photomovement experiments. A. Chamber with camera and LED light-source attached. Thin tubing at top left supplies moisture-saturated air; lower penetrations are cooling-water supply and return lines. Inset shows actual photograph taken during the photophobic response experiments. B. Top view of LED light-source showing interchangeable resistors, dimmer control and power switch. C. Bottom view of LED light-source showing array of six interchangeable LED lamps (470 nm peak  $\lambda$  shown).

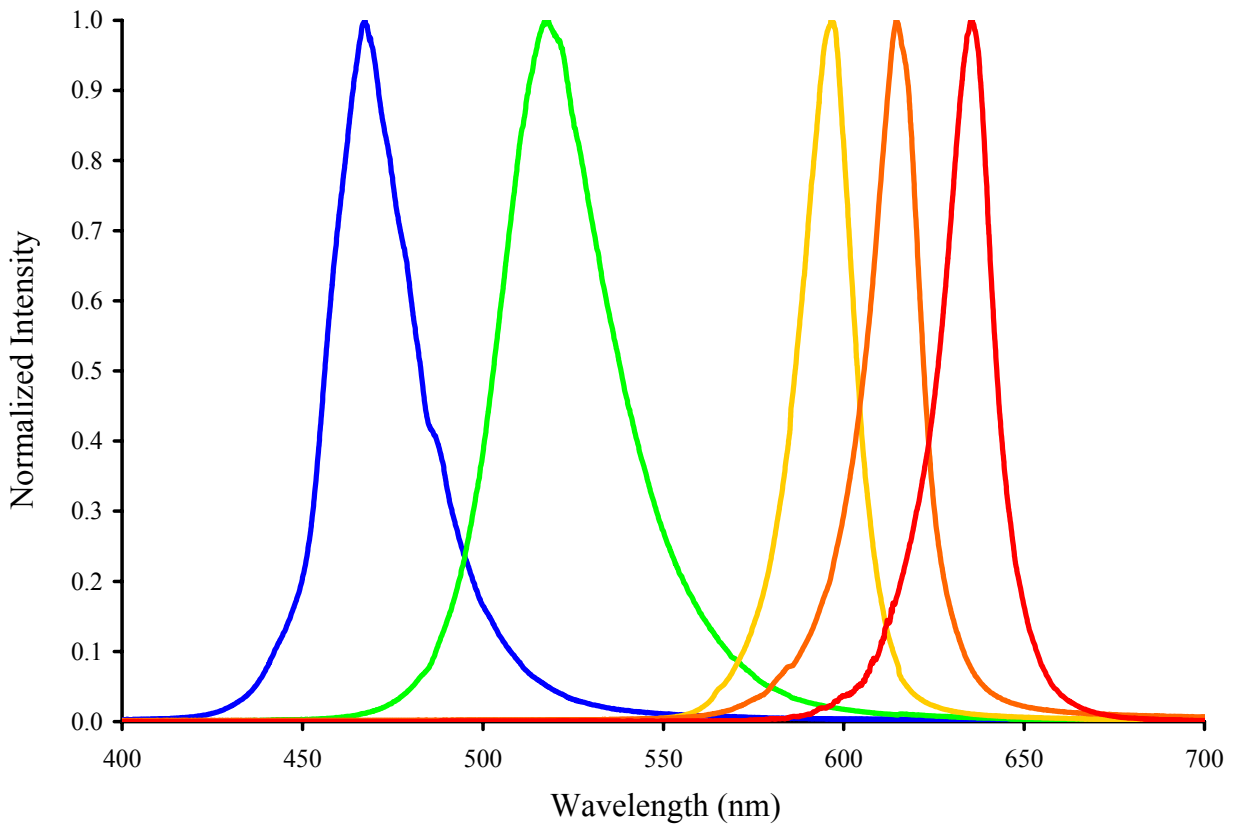


Figure 4.5. Normalized output spectra of the five light emitting diodes used in the photophobic response experiments. Wavelength peaks were at 470, 525, 589, 610, and 630 nm respectively for the blue, green, yellow, orange, and red LED lamps.

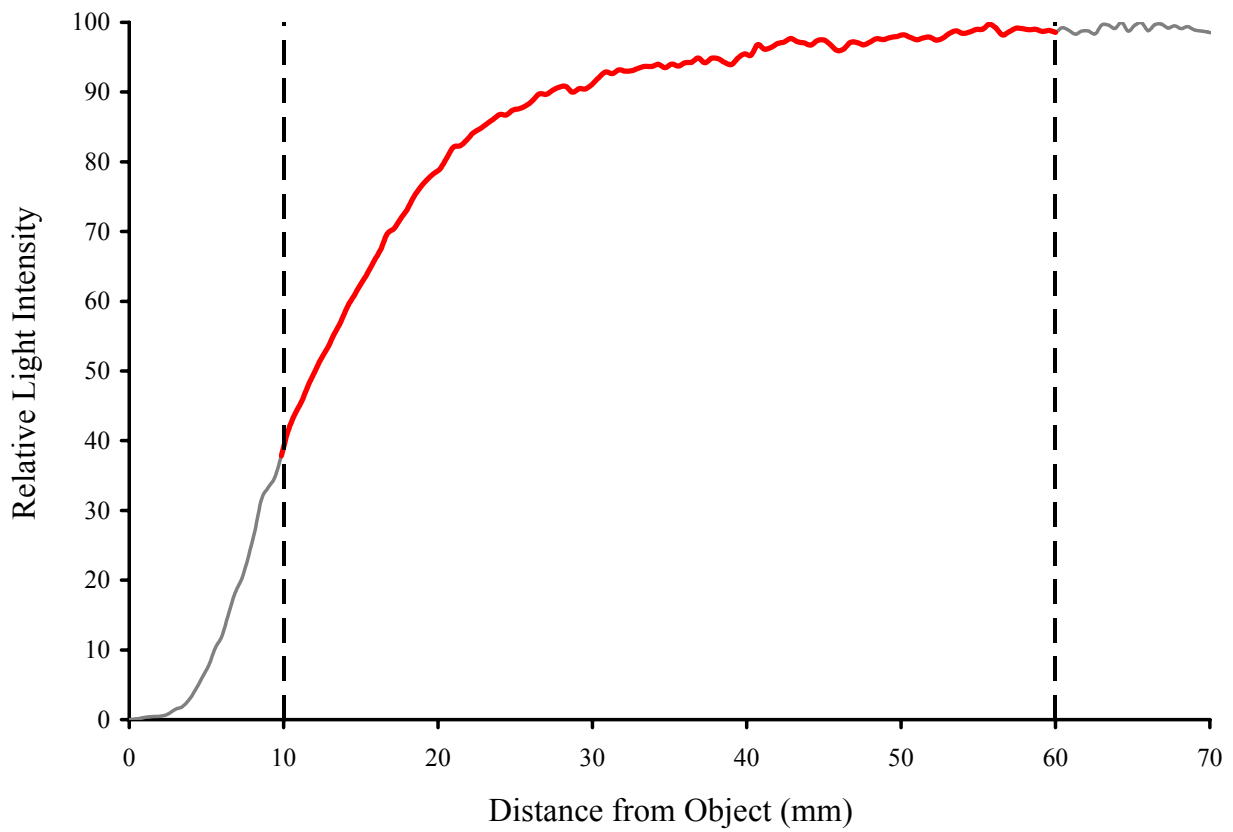


Figure 4.6. Graphic representation of relative light intensity at substrate level with respect to distance from an object. The colored portion of the graph, between the dashed lines, corresponds to the approximate 2–5 cm area surrounding an object in which *Convolutriloba retrogemma* exhibit their halo-forming basking behavior.

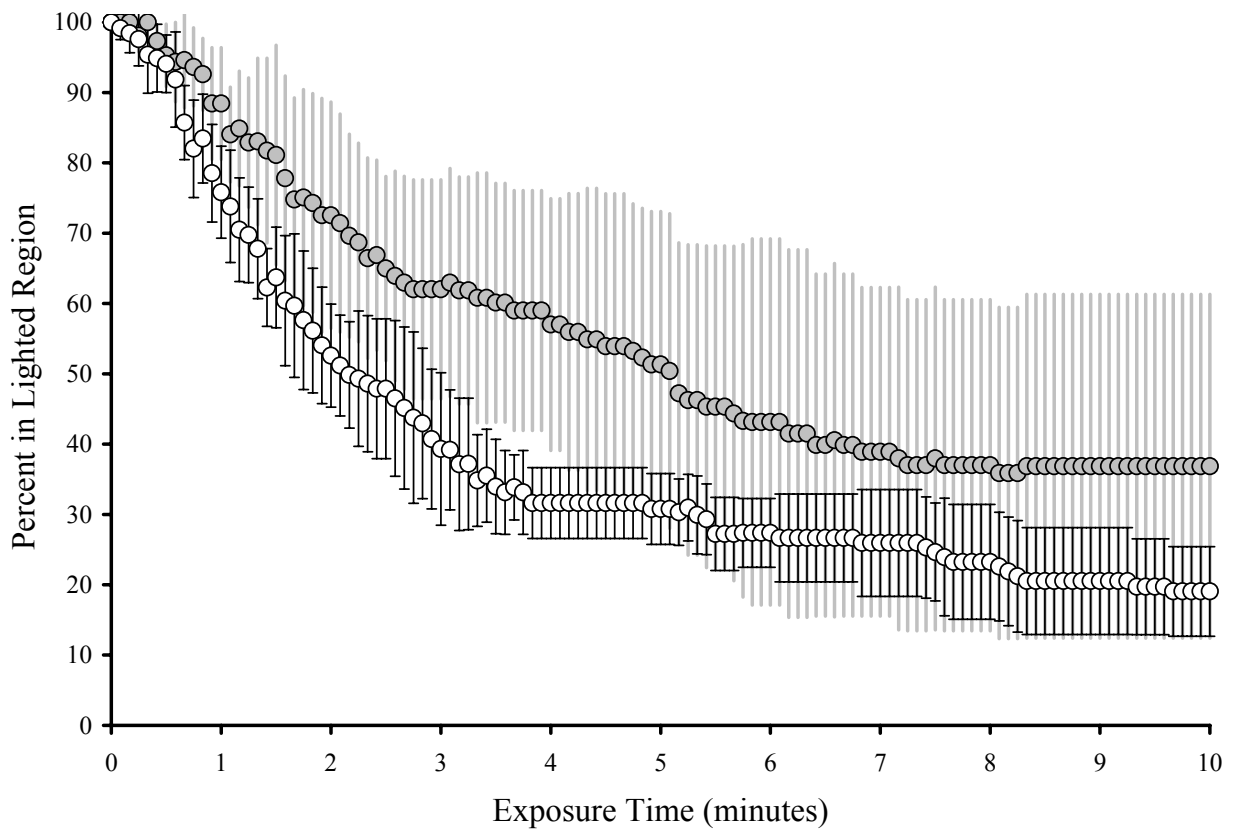


Figure 4.7. Percentage of acoels remaining in lighted region vs. time. Open circles represent means of  $n = 5$  experimental trials under high intensity white-light ( $260 \mu\text{mole}\cdot\text{m}^{-2}\cdot\text{s}^{-1}$ ), shaded circles represent means under low intensity white-light ( $145 \mu\text{mole}\cdot\text{m}^{-2}\cdot\text{s}^{-1}$ ). 50 acoels were used in each trial. Error bars represent 95% confidence intervals at each time step. A marked step-up, photophobic response was evident under both light treatments, though somewhat slower and less-pronounced under low intensity light.

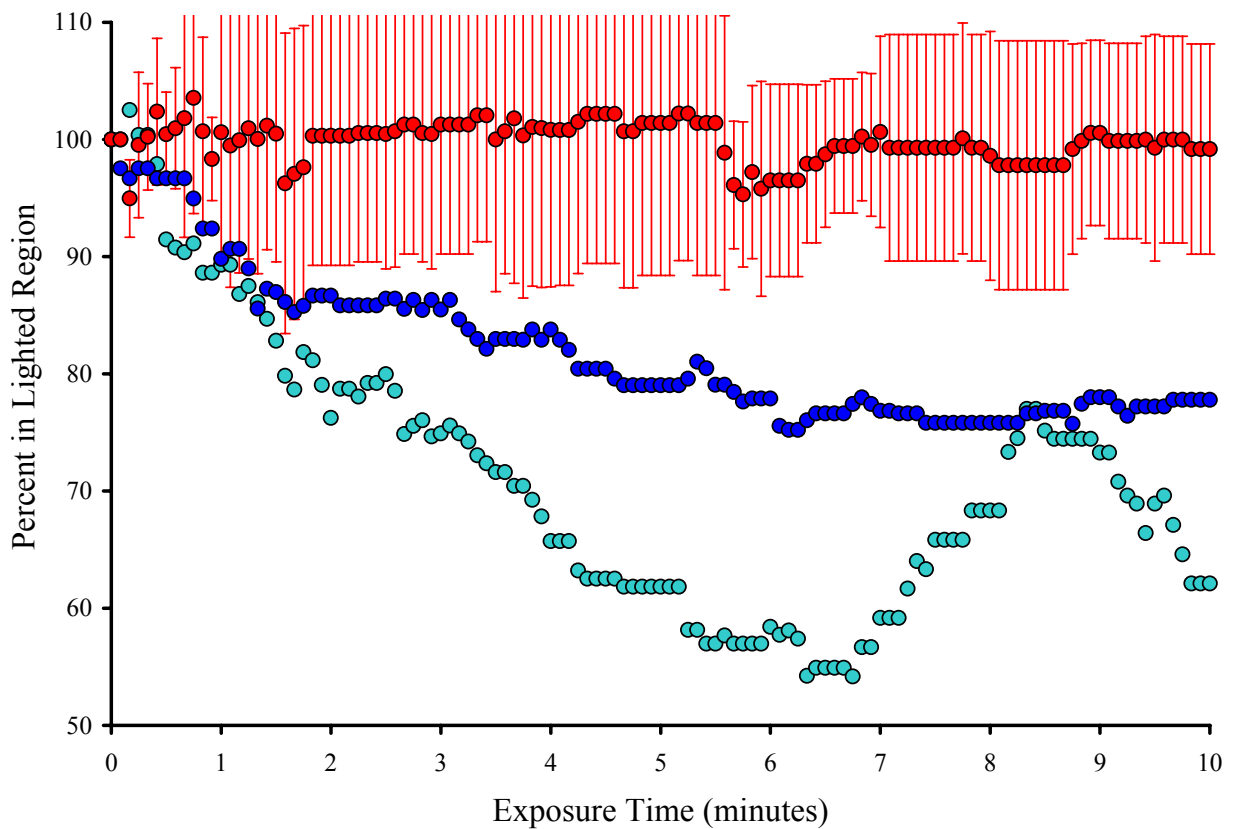


Figure 4.8. Percentage of acoels remaining in lighted region vs. time –photophobic response – Circle color represents color of filter used in each experiment. Each circle represents the mean of  $n = 5$  trials. Light-source intensity was constant over all treatments ( $260 \mu\text{mole}\cdot\text{m}^{-2}\cdot\text{s}^{-1}$ ); actual (colored) intensity at the water surface varied depending on the filter (see fig. 4.4) used. 50 acoels were used in each trial. Error bars represent 95% confidence intervals at each time step. A step-up, photophobic response was evident under both blue and blue-green light treatments, whereas no response was observed under red light.

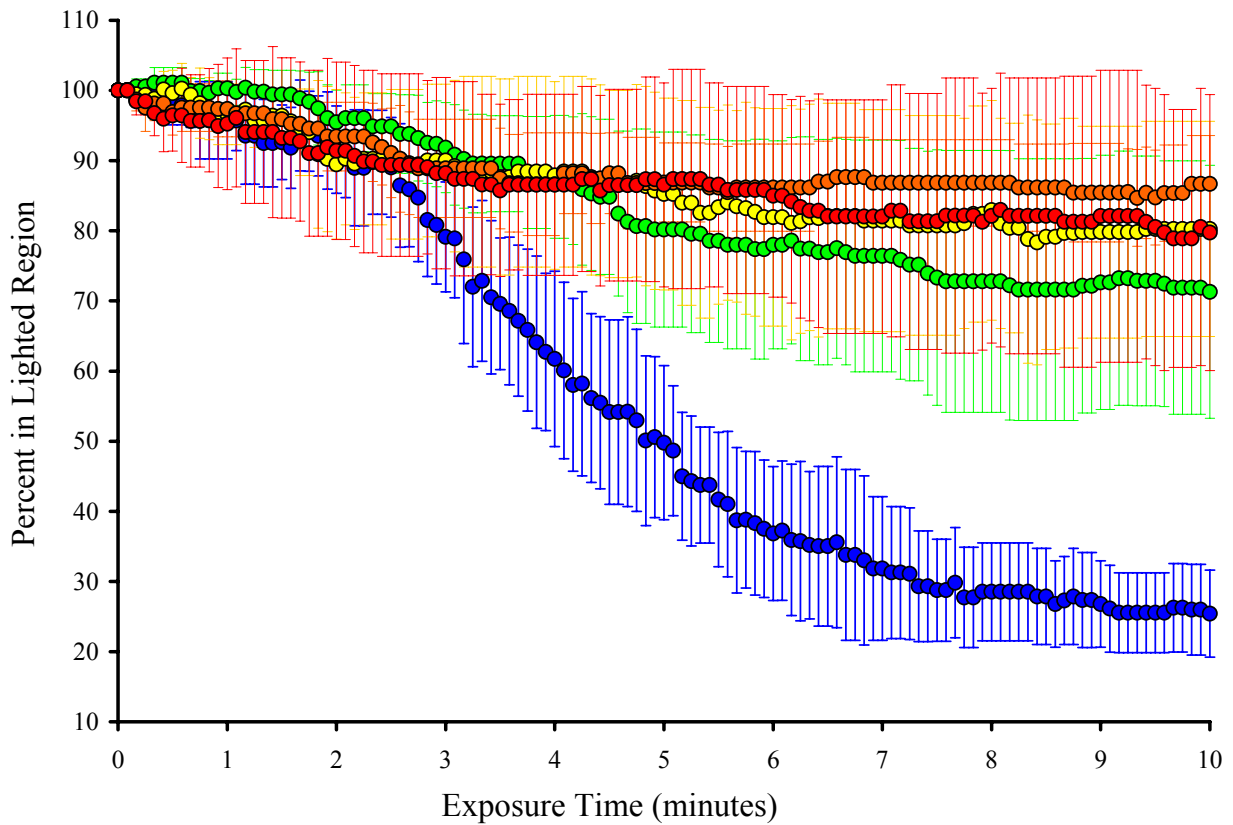


Figure 4.9. Percentage of acoels remaining in lighted region vs. time – photophobic response – Circle color represents LED color used in each experiment. Each experiment consisted of  $n = 6$  trials. 50 acoels were used in each trial. Light intensity was kept equal across all experiments regardless of wavelength. Error bars are 95% confidence intervals at each time step. The data confirm that the step-up photophobic response, indicated in figures 4.5 and 4.6, was blue-light mediated.



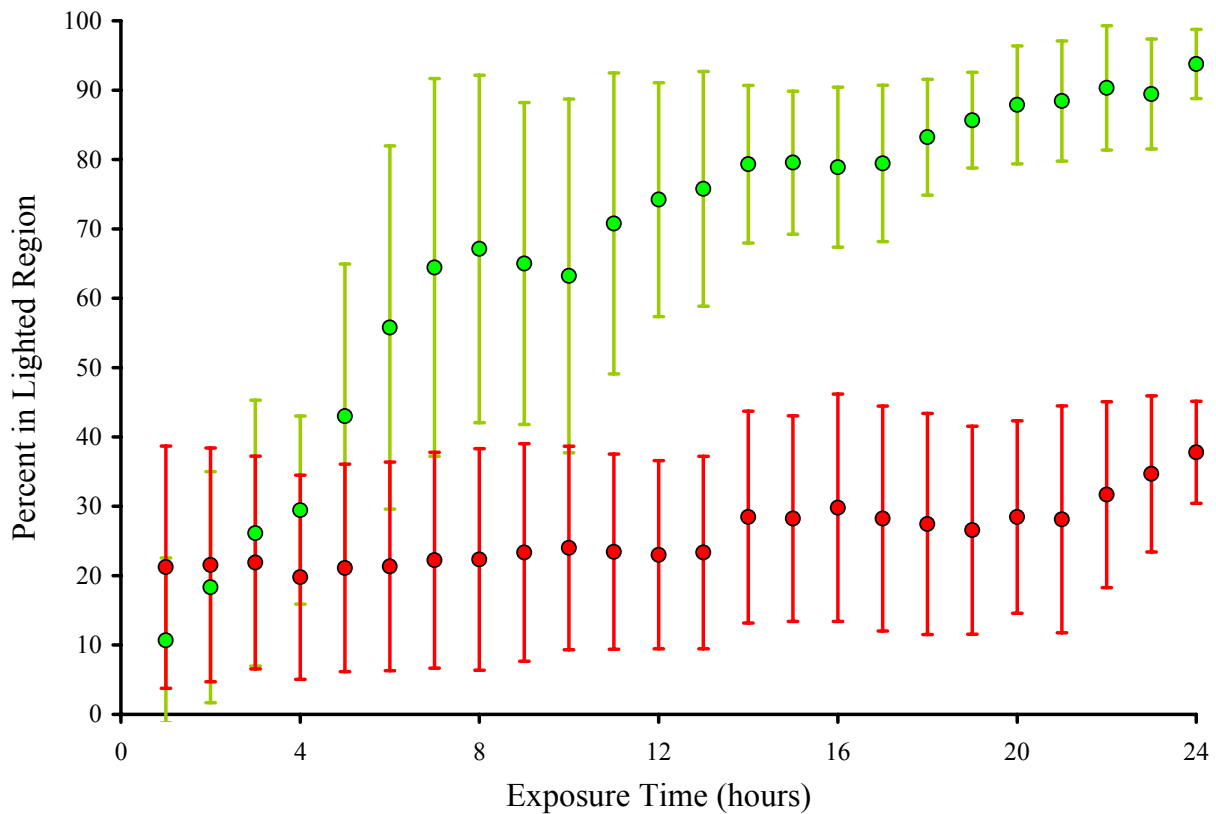


Figure 4.10. Percentage of acoels in lighted region vs. time – photoaccumulative response – Green circles represent means from control trials involving symbiotic acoels. Red circles represent means from trials involving aposymbiotic acoels. 15 acoels were used in each trial,  $n = 5$  trials per treatment. White-light intensity in all trials was  $1 \mu\text{mole}\cdot\text{m}^{-2}\cdot\text{s}^{-1}$ . Error bars represent 95% confidence intervals at each time step. The data indicate that the photoaccumulative response was mediated by a factor related to the photosynthetic activity of the algal endosymbiont.

## CHAPTER 5

### PHOTOREGULATION AS A METHOD OF OSMOREGULATION IN THE SYMBIOTIC SYSTEM OF *CONVOLUTRILOBA RETROGEMMA*<sup>1</sup>

---

<sup>1</sup> Shannon, T. To be submitted to *Marine Ecology Progress Series*.

## **Abstract**

This study examines the effects of holozoic starvation on the symbiotic system of *Convolutriloba retrogemma* and its algal endosymbiont; particularly as it applies to host photobehavior. It is shown that contrary to expected behavior, acoels denied prey for over 20 days do not seek out areas of high intensity light, but instead retreat to low light areas or shadows. The results of this study support a hypothesis that the basking behaviors of these acoels serve as methods of photoregulating their algal endosymbionts. The results further show that starved acoels appear to have diminished capabilities for processing translocated algal photosynthates and that under high-light conditions a build-up of these compounds results in hyposmotic stress in the animals and an influx of osmotic water into the animals' tissues. It is suggested that the photoregulatory basking behaviors of *C. retrogemma* may function as a method of host osmoregulation and that intercellular change in osmotic pressure resulting from photosynthesis is the photoregulatory stimulus. The term "photosmoregulation" is offered to describe the process.

**Key words:** *Convolutriloba*, acoel, photomovements, behavior, photoregulation, osmoregulation, osmotic water gain, holozoic feeding, starvation, chlorophyll, protein, carbon, nitrogen, photosmoregulation

## Introduction

Phototactic and photoaccumulative behaviors are exhibited by a multitude of marine invertebrates with symbiotic algae (see Pearse 1974a,b) as one would expect from animals which stand to benefit from the photosynthetic activities of those symbionts. Though these photobehaviors vary from one animal to the next, they generally fall into one of two categories; sudden responses, or slow responses. In sudden responses, as in the photophobic response of *Symsagittifera (Convoluta) roscoffensis* to a rapid increase in light (Gamble & Keeble 1903), the behavior is an instantaneous reaction to photic stimuli and is generally visually-triggered (e.g., Carthy 1958). Slow responses occur over the course of hours or days.

The result of many slow responses is a net phototactic movement of an animal, and when many like animals are involved, photoaccumulation. Although these photobehaviors are sometimes exhibited by symbiotic *and* aposymbiotic hosts, such as *Hydra viridis* (Whitney 1907) and *Symsagittifera (Convoluta) roscoffensis* (Gamble & Keeble 1903; Keeble 1910), they are most often observed in animals with intact symbioses. Owing to the varying intensities under which some of these animals accumulate, depending on pre-experimental, environmental light levels, it is assumed that these behaviors serve to photoregulate the algal symbionts (Zahl & McLaughlin 1959; Pearse 1974b).

*Convolutriloba retrogemma* exhibits two distinct photobehaviors, photophobia and photoaccumulation (see previous chapter). Sudden increases in light intensity trigger a step-up photophobic response like that exhibited by *Symsagittifera roscoffensis* (Gamble & Keeble 1903). Data show that this behavior is visually-triggered and blue-light mediated. The photoaccumulative response is a much slower response, occurs only in symbiotic animals, and is regulated by either algal photosynthesis or a process/mechanism resulting from algal

photosynthesis. In preliminary experiments conducted while designing methods for the previous study, it was noted that the photoaccumulative behavior of *C. retrogemma* was most pronounced in irradiance levels well below the levels in the culture tanks from which the animals were collected. As the experimental irradiance levels neared and exceeded those of the culture tanks, the behavior became progressively less pronounced. These observations suggest a photoregulatory role of the behavior. The questions remain, however, who does the photoregulation serve; and is the optimal photosynthetic activity of the alga “dictated” by the symbiont, the host, or a combination of both?

This study was designed to verify the photoregulatory function of the photoaccumulative behavior of *C. retrogemma*, to ascertain the requisite factors that would necessitate photoregulation of its algal endosymbiont, and to determine the nature of the photosynthetically-related stimulus that regulates the observed host behavior.

## **Materials and Methods**

Populations of *Convolutriloba retrogemma* were maintained in trough-style research aquaria in both a mixed-species population with other convolutrilobids (*C. hastifera*, *C. longifissura* & *C. macropyga*) and in a monospecific culture tank separate from other *Convolutriloba* spp. as outlined in Chapter 3. All experiments were conducted in a constant temperature room maintained at 25°C. Artificial seawater (ASW, Instant Ocean) used in all experiments was maintained at a salinity of 34±1 ppt as measured with an Atago S/Mill hand-held refractometer.

Six 4-liter tanks were set up to maintain cultures of fed and starved *C. retrogemma* for use in several of the experiments outlined below. Each tank contained several hundred animals

collected from the general-population research aquaria. Tanks were individually supplied with filtered (5 micron) ASW from the research aquaria at ~ 20 L/hr and were illuminated on a light-dark 14L:10D hr cycle by full-spectrum, metal halide bulbs (Hamilton Tech MH175W/U True 10000K) through neutral density screen providing an average irradiance of ~50  $\mu\text{mole}\cdot\text{m}^{-2}\cdot\text{s}^{-1}$  at the water surface. The acoels in three tanks were supplied daily with *Artemia* sp. nauplii *ad libitum* (fed cultures) over the course of all experiments, while those in the other three were denied prey (starved cultures). Fed cultures were not used until at least 20 days after set-up; starved cultures were rotated into and out of service according to the number of days of starvation required for each experiment.

Most of the initial experiments in this study required the body-mass measurement of the same acoel(s) before and after experimental treatments. As such, the relationship between wet weight, dry weight, and ash-free dry weight was calculated. To determine the body-mass relationships, 10 samples of medium-to-large acoels, 4–6 mm, were collected from the general aquaria population and placed in 1.25 ml, pre-tared Durham tubes (unless otherwise stated, all weights in the experiments were obtained using a Mettler AT261 DeltaRange 5-place balance). The first tube contained 5 individuals, the second, 10, etc. with each successive tube containing 5 acoels more than the previous; the tenth tube contained 50. Excess water was carefully absorbed from the tubes using filter paper “points”. Wet weight was then determined for each of the ten sample tubes. Sample tubes were then dried at 105°C to constant weight, cooled in a desiccator and dry weight recorded. Following this, sample tubes were heated at 520°C to constant weight using an NEY 2-525 Series II muffle furnace, cooled in a dissector, and ash-free weight recorded. From the resulting data, dry weight and ash-free dry weight of the samples were

calculated. Wet weight was plotted against dry weight and ash-free dry weight and linear functions were determined by regression analysis.

Light preferences of fed and starved acoels subjected to an irradiance gradient were determined using a procedure modified from Åkesson & Hendelberg (1989). Tests were performed in a 90 cm long trough constructed from 4" I.D. sched-40, white, PVC pipe cut in half along its length and capped on both ends. Filtered (5 micron) artificial seawater (ASW) from the research aquaria was supplied at a rate of approximately 3 l/hr. Water depth in the trough was ~1 cm at centerline. Light was supplied from 2 fluorescent bulbs (Sylvania F40/CWX) powered by an IceCap Model 660 electronic ballast. An irradiance gradient was formed by illuminating the trough through a neutral density filter divided into six equal sections; each section made darker than the preceding by adding layers of black, fiberglass screen. The trough was marked along its length in six equal sections corresponding to the six irradiance levels. Average irradiance measurements in the six sections were 10, 22, 32, 58, 117, and 208  $\mu\text{mole}\cdot\text{m}^{-2}\cdot\text{s}^{-1}$  determined from 10 readings per section using a Li-Cor Model LI-1400 Data Logger with an LI-190SA quantum sensor. Experimental trials were run on acoels following 20 days of either holozoic feeding or starvation as outlined above; the period of 20 days was chosen based on Åkesson & Hendelberg (1989) noting a cessation of reproductive budding after 2 weeks in acoels denied access to prey, indicating a nutritional/metabolic change at that point. Thirty medium-to-large acoels were selected for each test and distributed evenly throughout the trough (5 in each section). A light-dark regimen of L14:D10 hrs was implemented during all trials corresponding to the cycle used on the general cultures in an effort to eliminate any potential variation due to circadian rhythm shifts. Animals were added to the trough at the beginning of the dark cycle and allowed 10 days to settle out according to irradiance preference; preliminary trials showed little

change in individual positions after this time period. Subjects from fed culture were supplied *Artemia* sp. daily during the 10 day trials. Ten experimental trials each were run on fed and starved acoel groups. Water flow direction was alternated (in relation to the irradiance gradient) with each new run to minimize any potential variability due to flow regimen. The number of animals in each section was recorded at the end of each trial. Resulting averages were calculated and plotted with 95% confidence intervals.

“Preliminary”, follow-up experiments were run following the light preference experiments to help ascertain the cause of unexpected results of those experiments. As such, chlorophyll *a*, chlorophyll *b*, protein, carbon, and nitrogen concentrations were determined for fed and starved animals before and after subjecting groups to high or low light levels. Following 20 days in either fed or starved culture, acoels were chosen at random from their respective culture tanks and placed into 8 control groups (4 replicates each for fed and starved cultures) of 20, 20, 10, and 10 individuals for chl*a*, chl*b*, protein, and C/N concentration experiments respectively; this was repeated two more times to select groups for the high-light and low-light trials for each experiment. Animals subjected to high ( $166 \mu\text{mole}\cdot\text{m}^{-2}\cdot\text{s}^{-1}$ ) and low ( $13 \mu\text{mole}\cdot\text{m}^{-2}\cdot\text{s}^{-1}$ ) light treatments were removed from the culture tanks *at* the beginning of the light cycle and subjected to their respective treatments for 12 hours, control animals were removed from the culture tanks ( $50 \mu\text{mole}\cdot\text{m}^{-2}\cdot\text{s}^{-1}$ ) 12 hours *after* the beginning of the light cycle. Replicates for high and low light experiments were placed in individual 4½” glass culture dishes in 200 ml ASW; the culture dishes were then placed, partially submerged in the research aquaria to maintain temperature at ~25°C, under their respective lighting treatments. High and low light treatments were illuminated by the same metal halide light source used on the cultures; desired irradiance levels were obtained by removing or adding neutral density, black, fiberglass screen.



Following all treatments, the wet weight of each replicate group of acoels was measured as outlined above.

Chlorophyll was extracted and collected from designated samples by reversed-phase chromatography and quantified by spectrophotometry. Samples were placed in 3 ml capped centrifuge tubes and air dried in a stream of low pressure, dry air for 2–3 hours. When all remaining water was evaporated, 1.5 ml 100% acetone was added to each tube. All tubes were subsequently vortexed once an hour for 3 hours to fully extract all chlorophyll from the tissues. Following chlorophyll extraction, 330  $\mu$ l de-ionized water was added to each tube resulting in a 75% acetone solvent. Tubes were vortexed then centrifuged in an Eppendorf model 5415 C microfuge at 14,000 rpm for 10 minutes. One ml of supernatant from each tube was loaded onto individual Waters C<sub>18</sub> Sep-Pak reversed-phase cartridges. Polar, non-chlorophyll components of the mixture were eluted from each cartridge with a 5 ml flush of 75% acetone. Elution and collection of the chlorophyll component was performed with a 4 ml flush of 100% acetone. Spectrophotometry of the resulting chlorophyll solutions was performed on a Hewlett Packard 8452A Diode Array spectrophotometer. Chlorophyll *a* & *b* concentrations were quantified according to the formulae of Arnon (1949) using Beer's law, the extinction coefficients of both molecules, and the absorption maximums at 663 and 645 nm respectively. Extracted chlorophyll concentrations were correlated with calculated ash-free dry weights of their respective samples.

Protein concentration per mg acoel/algal tissue was determined utilizing the Bradford (1976) method. Samples were placed in 1500  $\mu$ l microfuge tubes and air dried in a stream of low pressure, dry air for 2–3 hours. Samples were rehydrated with 0.5 ml de-ionized water and homogenized using a pestle and intermittent vortexing. Following centrifugation at 14,000 rpm for 10 minutes, aliquots of 400  $\mu$ l from each sample were pipetted into individual test tubes

containing 5 ml diluted Bio-Rad Protein Assay dye reagent concentrate, and vortexed. Absorbance at 595 nm of each tube was read in a Sequoia-Turner Model 340 spectrophotometer. Concentration of protein in each sample was calculated from a standard curve produced from Bio-Rad Protein Assay bovine serum albumin standard reconstituted in Milli-Q water. Protein concentrations were then correlated with calculated ash-free dry weights of their respective samples.

Both carbon and nitrogen concentration was determined for each designated sample allowing for accurate C:N ratios of samples. Weighed samples were dried on an individual Whatman GF/F filter pads (25 mm; 0.7  $\mu\text{m}$  pore size; pre-combusted at 550°C) at 45°C to constant weight. Samples were then analyzed for carbon and nitrogen content utilizing an Exeter Analytical, Inc. CE-440 Elemental Analyzer. Carbon and nitrogen quantities were then correlated with calculated ash-free dry weights of their respective samples.

To determine the extent to which *C. retrogemma* experiences hyposmotic stress (osmotic pressure of media < osmotic pressure of acoel tissues) as a function of starvation (stress), an experiment was designed to measure individual animal body-mass before and after exposure to high-light irradiance over the course of a starvation regimen. Several hundred medium-to-large specimens were collected from the mixed population of acoels growing in the research aquaria and were distributed evenly between twenty 4½” covered glass culture dishes containing 200 ml ASW each. In order to ensure that all animals were in relatively equal nutritional and physical health at the onset of the experiment, all dishes were subjected to a light-dark regimen of L14:D10 hrs provided by two Philips 5000°K Ultralume and two Philips cool white 40W fluorescent lamps at 70  $\mu\text{mole}\cdot\text{m}^{-2}\cdot\text{s}^{-1}$ , *Artemia* sp. nauplii were added daily in superabundance and water was changed every other day. After 20 days all feeding was stopped and all acoels

were transferred to ten clean glass dishes containing 200 ml filtered (0.45 micron) ASW. From these dishes, 144 animals were chosen at random and placed individually into the wells of six Costar (Corning Inc.) 24-well cell-culture trays (numbered 1–6) in 2.75 ml filtered ASW. Remaining animals were evenly redistributed between the ten glass culture dishes and were used to replace dead or injured test animals over the course of the experiment. At this point, day 0 of the experiment, trays 1 & 2 were placed in the dark for 1 hour. Following dark adaptation, 24 randomly pre-selected animals (of 48 total) were individually dewatered and weighed according to the method described in chapter 3. Once all animals were returned to their original wells, the trays were subjected to an irradiance of  $\sim 800 \mu\text{mole}\cdot\text{m}^{-2}\cdot\text{s}^{-1}$  provided from a fiberoptic light-source (Fostec AceI w/ USHIO Halogen EKE-21V-150W bulb) for 1 hour, after which the previously selected acoels were once again weighed and  $\Delta_{\text{mass}}$  determined for each. This procedure was repeated every other day (with the exception of a three day interval between days 4 and 7) for 32 days. Tray use was rotated throughout the experiment such that each pair of trays was used every 6 days. Animals were randomly pre-selected before each run such that the likelihood of any single acoel being used on consecutive 6 day intervals was 50%. On day 24, 24 acoels were randomly selected from the ten glass dishes, placed individually into wells of a cell culture tray in 2.75 ml ASW with 50  $\mu\text{M}$  DCMU, 3-(3,4-dichloro-phenyl)-1,1-dimethylurea and incubated at  $70 \mu\text{mole}\cdot\text{m}^{-2}\cdot\text{s}^{-1}$ . After 8 hours of incubation, the acoels were subjected to the same procedure outlined above and  $\Delta_{\text{mass}}$  determined for each animal in the group.  $\Delta_{\text{mass}}$  results were averaged for each day and plotted with calculated 95% confidence intervals; additionally, average  $\Delta_{\text{mass}}$ , as measured following dark adaptation, relative to average weight at day 0, was determined for each day of the experiment for comparative purposes.

To aid in understanding unanticipated results in the final days of the  $\Delta_{\text{mass}}$  experiment, fed and starved groups of acoels were subjected to high and low light as outlined in the concentration experiments; and the wet weights, dry weights, and ash-free dry weights measured as outlined in the procedure for determining the body-mass calibration curves at the beginning of this study. Starvation period was extended to 32 days. The percent water content of the organic portion of each sample was determined and treatment averages plotted with calculated 95% confidence intervals.

## Results

In measuring the wet weight, dry weight, and ash-free dry weight of several groups of *C. retrogemma* a functional method for calculating tissue mass from wet weights of live animals was determined by regression analysis (Fig. 5.1). From a known wet weight, dry weight could be calculated as  $0.1111 \times \text{wet weight}$ ,  $R^2=0.98$ . Ash-free dry weight was calculated as  $0.0798 \times \text{wet weight}$ ,  $R^2=0.96$ .

The light preference experiments of fed vs. starved acoels (Fig. 5.2) clearly showed a strong preference for the highest light intensities in the fed groups, and a somewhat less-pronounced preference for the lower intensities in the starved groups. A two-way ANOVA run on these data indicated a highly significant ( $p < 0.001$ ) interaction between the two treatments, nutrition and light intensity. When the results from the three lower intensity treatments (10, 22, and  $32 \mu\text{mole}\cdot\text{m}^{-2}\cdot\text{s}^{-1}$ ) and the three higher intensity treatments (58, 117, and  $208 \mu\text{mole}\cdot\text{m}^{-2}\cdot\text{s}^{-1}$ ) were each combined, the differences in intensity preferences were more readily noticeable between the fed and starved treatment groups (Fig. 5.3). Presented and analyzed in this way, preferences differed significantly between starved and fed treatments within the high and low

intensity groupings, and between intensity groupings within both fed and starved treatments (two-tailed *t*-tests, 8*df*,  $p < 0.001$  in all comparisons).

Comparisons of chlorophyll *a*, protein, carbon, and nitrogen concentrations in fed vs. starved acoels (Fig. 5.4) yielded inconclusive results due to an unforeseen variable, osmotic water movement, which will be explained later in the paper. No statistical differences were found between control group concentrations and low light concentrations in any of the experiments, as such, these data are not included in the figures. Likewise, profiles for chlorophyll *b* concentrations mirrored those of chlorophyll *a*, and are also not included in the figures. Although comprehensive results concerning individual substance concentrations were lacking, an overall trend was observed regardless of the substance tested for. As can be seen in figure 5.4, concentrations of all substances decreased in starved animals when they were subjected to high-light with significant drops observed in all but the protein experiment (one-tailed *t*-tests, 6*df*, *chl a*  $p = 0.006$ , protein  $p = 0.102$ , carbon  $p = 0.036$ , nitrogen  $p = 0.015$ ).

Comparison of carbon/nitrogen ratios (Fig. 5.5) allowed for the elimination of the osmotic water effect/variable on the starved acoel groups. The C:N averages were significantly higher in the starved control group than in the fed control, and remained so following low and high light treatments (one-tailed *t*-tests, 6*df*,  $p < 0.001$  in all comparisons). Comparison of the *differences* in carbon/nitrogen ratios (Fig 5.6) between control and high irradiance treatments on fed vs. starved acoels, however, showed no statistical difference between the two (two-tailed *t*-test, 6*df*,  $p = 0.323$ ).

In comparing the before and after weight of acoels subjected to a 1 hour treatment of high irradiance (Fig. 5.7), no consecutive, significant changes in weight were observed until the 10<sup>th</sup> day of starvation. From this point of the starvation regimen until the 25<sup>th</sup> day, weight gain due to

irradiance increased steadily to a maximum of ~ 13% after which a relatively sharp decline was observed. No weight change was observed on day 31 of the starvation regimen or beyond. On the 24<sup>th</sup> day of starvation, corresponding to the peak of weight gain at day 25, a group of animals were subjected to and tested in 50  $\mu\text{M}$  DCMU to inhibit photosynthesis (red data point in figure 5.7); no significant weight change was observed in this group. The average weight change of acoels over the entire course of the experiment, in relation to average starting weight, was calculated for comparative purposes (Fig. 5.8). These data show a slow increase in average acoel weight (measured pre-light-treatment) corresponding to the decline in light-induced weight gain between days 25 and 31.

A comparison of the percent water-content of fed and starved animals subjected to irradiance treatments of 50  $\mu\text{mole}\cdot\text{m}^{-2}\cdot\text{s}^{-1}$  (control) and 166  $\mu\text{mole}\cdot\text{m}^{-2}\cdot\text{s}^{-1}$  (high-light) following 32 days of starvation (Fig. 5.9) showed no significant differences between irradiance treatments within fed or starved groups (two-tailed  $t$ -tests, 8 $df$ ,  $p = 0.725$  and  $0.621$  respectively). However, a significant difference was found between the fed and the starved treatments with water content of ~91.25% in fed animals, and ~93.5% in starved (one-tailed  $t$ -test, 18 $df$ ,  $p < 0.001$ ).

## Conclusions

*Convolutriloba retrogemma* is a heterotrophic acoel with a green, algal endosymbiont (Hendelberg & Åkesson 1988). Like other such symbiotic invertebrates found amongst the Protista, Porifera, Cnidaria, Mollusca, Ascidia, and Acoelomorpha (e.g., Smith & Douglas 1987; Smith 1991; Douglas 1994), this species feeds holozoically and obtains additional nutrition in the form of translocated photosynthates from its algal symbiont (see chapter 3). One would anticipate, by intuition alone, that in such a symbiotic system, a host deprived of exogenous food

would seek out environmental light conditions conducive to maximizing the photosynthetic output of its symbiont. Such is not the case with *C. retrogemma*.

As was observed by Åkesson & Hendelberg (1989), in their light-preference experiments on *C. retrogemma*, fed animals tested in *this* study gravitated towards settling out in the area of highest irradiance offered (Fig. 5.2). Experiments on starved animals in this study yielded unexpected, counter-intuitive results, though, in that they tended to prefer the three areas of lower light intensities (Figs. 5.2 & 5.3). Such results are not unheard of, however. Zahl & McLaughlin (1959) observed that symbiotic *Condylactis*, when offered full sunlight or shade, tended to accumulate in the shaded area close to the shade/sunlight interface. The authors did not indicate the nutritional status of the test animals. Pearse (1974b) observed similar behavior in *Anthopleura elegantissima* but noted that this only occurred in animals collected from low-light environs; those collected from areas subjected to high PAR intensities preferred like intensities in experimental trials. In both of these studies, and in an additional study involving the expansion and contraction of tentacles by *A. elegantissima* as a function of light intensity (Pearse 1974a), the authors suggest that the behaviors may play a role in “favorably regulating the amount of light to which the zooxanthellae are exposed” (Pearse 1974b). If this is the case in *C. retrogemma*, the hypothesis falls short of explaining why in a well-fed host the “favorable” amount of light to the symbiont is significantly greater than in a starved host.

The comparisons of chlorophyll *a*, protein, carbon, and nitrogen concentrations in fed vs. starved acoels (Fig. 5.4) were conducted in an effort to help determine what change in biological processes within the host, symbionts, and/or between the two partners could result in the observed light preferences. As alluded to earlier, the intended results of all of these experiments were inconclusive due to a “fortunate” oversight in the design of the experimental methods; it

was this oversight that offered the first clue as to why a starved host would seek low light intensities. There was no significant change in any substance concentration as a result of subjecting well-fed acoels to high-intensity light, but when starved acoels were subjected to the same light treatment, substance concentration decreased – significantly in the *chl<sub>a</sub>*, carbon, and nitrogen experiments, but not significantly ( $p = 0.102$ ) in the protein experiment. Based on these results it became apparent that the observed decreases in concentration were not the result of diminished chlorophyll, protein, carbon, or nitrogen, but were likely due to increases in water content. Light-induced change in the osmotic potential of the host/symbiont complex appeared to be the cause; followed by osmotic water influx into the host tissues.

The higher C:N ratio averages in the starved groups (Fig. 5.5) suggest that increased carbon levels were the underlying cause of the osmotic potential increases. Since the increases were light-driven, photosynthates from algal photosynthesis appeared to be the source of the osmolytes. The increase in C:N ratio observed between the control and high irradiance treatments in both fed and starved groups (Fig. 5.5) suggest a build-up of photosynthates as a result of increased algal photosynthetic rates. That there was no significant difference between the change in C:N ratio in both the fed and starved groups (Fig. 5.6), suggests that the build-up of photosynthates was likely due to a “bottle-neck” in the translocation process. In summary, the combined C:N data suggest that temporary osmotic pressure increases occurred in both fed and starved animals, but that the higher starting concentrations in starved animals placed these acoels at a higher risk of experiencing substantial hyposmotic stress.

The results of the starvation experiment (Fig. 5.7) support the hypothesis that an increase in water content was responsible for the observed concentration decreases in the starved acoels in the chlorophyll, protein, carbon, and nitrogen experiments. In these experiments, groups of



acoels were starved over the course of one month and tested every other day for weight changes resulting from exposure to high PAR irradiance. The results clearly show that as starvation progressed, light-induced weight gain increased. The group of acoels subjected to DCMU and tested at day 24, a time corresponding to maximum light-induced weight gain, showed no change in weight thereby inextricably linking the observed weight gain to water influx as a result of endosymbiont photosynthesis.

Over the final 6 days of the starvation experiment (Fig. 5.7) a rapid drop in light-induced weight gain was observed and on the 31<sup>st</sup> day, no significant change occurred. Likewise, the average weight of the acoels, represented as percent of the original weight, appeared to increase over the same 6 day period at the end of the experiment (Fig 5.8). In preliminary experiments, the same phenomenon was observed and was thought to be an indication of host senescence brought about by starvation. Test animals used in this study's experiment were starved for an additional 30 days following the experiment and suffered a less than 1% mortality rate thereby ruling out senescence as a cause of the decline in weight gain.

To date, there have been no in-depth studies done on the nutritional interactions between the convolutrilobids and their algal endosymbionts; therefore, one can only speculate on the mechanisms responsible for the observed, idiosyncratic photoregulatory behavior of *C. retrogemma*. It is well known that most of the platyhelminthes and acoelomorphs are lacking in the ability to produce certain amino acids and synthesize fatty acids and sterols *de novo* (Muscatine *et al.* 1974; Boyle & Smith 1975; Meyer *et al.* 1979), and require an exogenous supply of these substances or their precursors from their prey, environment, parasitized host, or symbiont. Given these dependencies and short-comings, coupled with the sensitive cost/benefit balances required to maintain a healthy invertebrate symbiosis (Muller-Parker & D'Elia 1997) it

is easy to imagine that holozoic starvation of *C. retrogemma* could negatively impact the integrity of its symbiosis.

Bearing this in mind, the results of this study show that the observed photobehaviors of *C. retrogemma*, as outlined in the previous chapter, serve foremost as a method of photoregulating its algal endosymbiont. They show that a healthy, intact symbiosis can accommodate relatively high rates of photosynthesis; and they show that a stressed symbiosis cannot. The symbionts in *C. retrogemma* are intercellular, and photosynthates must be translocated from the algae to the intercellular spaces of the host tissues, and finally transported into the host cells before they can be utilized by the host. The increased C:N ratio observed following high-light irradiance appears to stem from the limitations of the speed of translocation. When an animal is starved, as can be seen in figure 5.5, further restrictions to translocation, or in downstream metabolic processes lead to higher concentrations of unmetabolized photosynthates, and therefore osmotic stress.

Interestingly, there appears to be an upper limit to the osmotic potential of the host tissues, and therefore a limit to the osmotic stress. *C. retrogemma*, like most acoels, has no basement membrane underlying its epidermal cells (Hendelberg & Åkesson 1988; Tyler & Hooge 2004); as such, the weaker intercellular connections of the epidermal cells define the integrity of the whole animal. Since the algal symbionts are also intercellular, photosynthates released from the algae that are not immediately transported into the host cells will accumulate in the intercellular spaces. As photosynthates collect in these spaces, osmotic water influx will result in increased intercellular pressure and the host cells will be pushed apart. As pressure continues to increase against the elasticity of the intercellular connections, openings to the external medium will form allowing for “free-flow” of water and photosynthates across the

epidermis. It is this free-flow point that determines the osmotic limit of the host tissue since the free-flow invariably results in an eventual state of osmotic equilibrium with the external medium. This limit can be seen in figure 5.9 where after 32 days of starvation, the water content of the host tissues no longer increases in response to high-light irradiance and photosynthesis.

In conclusion, the data show that the photoaccumulative behavior of *C. retrogemma* is regulated not by visual photic stimuli, but by the photosynthetic activity of the symbiont; and that the behavior, itself, is a method of host photoregulation of the symbiont. The data further show that the photoregulatory behavior serves as a novel method of non-metabolic osmoregulation of the host tissues, and that change in intercellular osmotic pressure may be the photosynthetically-produced stimulus responsible for determining host light preference. Since the behavior, its stimuli, effectors, and feedback loops can appear somewhat convoluted, the term photosmoregulation is suggested as a descriptor for the behavior and its purpose.

### **Acknowledgements**

Thanks to Bill Fitt, Walter Hatch, Gregory Schmidt, Mark Farmer, and Jim Porter for their continued support of my work. This research was supported by the U.S. Environmental Protection Agency under STAR Fellowship No. FP-91636501-0

## Literature Cited

- Åkesson B, Hendelberg J (1989) Nutrition and asexual reproduction in *Convolutriloba retrogemma*, an acoelous turbellarian in obligate symbiosis with algal cells. In: Ryland JS, Tyler PA (eds) *Reproduction, genetics and distributions of marine organisms*. Olsen & Olsen, Fredensborg, Denmark, pp 13-21
- Arnon DI (1949) Copper enzymes in isolated chloroplasts. Polyphenoloxidase in *Beta vulgaris*. *Plant Physiology* 24:1-15
- Boyle JE, Smith DC (1975) Biochemical interactions between the symbionts of *Convoluta roscoffensis*. *Proceedings of the Royal Society of London. Series B, Biological Sciences* 189(1094):121-135
- Bradford MM (1976) A rapid and sensitive method for the quantitation of microgram quantities of protein utilizing the principle of protein-dye binding. *Analytical Biochemistry* 72(1-2):248-254
- Carthy JD (1958) *An Introduction to the Behaviour of Invertebrates*. The MacMillian Company, New York, 380 pp.
- Douglas AE (1994) *Symbiotic Interactions*. Oxford University Press, Oxford, 148 pp.
- Gamble FW, Keeble F (1903) The bionomics of *Convoluta roscoffensis*, with special reference to its green cells. *Proceedings of the Royal Society of London Series B-Biological Sciences* 72:93-98
- Hendelberg J, Åkesson B (1988) *Convolutriloba retrogemma* gen. et sp.n., a turbellarian (Acoela, Platyhelminthes) with reversed polarity of reproductive buds. *Fortschritte der Zoologie* 36:321-327
- Keeble F (1910) *Plant-Animals: A Study in Symbiosis*. Cambridge University Press, London, 163 pp.
- Meyer H, Provasoli L, Meyer F (1979) Lipid biosynthesis in the marine flatworm *Convoluta roscoffensis* and its algal symbiont *Platymonas convoluta*. *Biochimica Et Biophysica Acta* 573(3):464-480
- Muller-Parker G, D'Elia CF (1997) Interactions between corals and their symbiotic algae. In: Birkeland C (ed) *Life and Death of Coral Reefs*. Chapman and Hall, New York, pp 96-113
- Muscantine L, Boyle JE, Smith DC (1974) Symbiosis of acoel flatworm *Convoluta roscoffensis* with alga *Platymonas convolutae*. *Proceedings of the Royal Society of London Series B-Biological Sciences* 187(1087):221-234
- Pearse VB (1974a) Modification of sea anemone behavior by symbiotic zooxanthellae: Expansion and contraction. *Biological Bulletin* 147(3):641-651

Pearse VB (1974b) Modification of sea anemone behavior by symbiotic zooxanthellae: Phototaxis. *Biological Bulletin* 147(3):630-640

Smith DC (1991) Why do so few animals form endosymbiotic associations with photosynthetic microbes? *Philosophical Transactions of the Royal Society of London Series B-Biological Sciences* 333(1267):225-230

Smith DC, Douglas AE (1987) *The Biology of Symbiosis. Contemporary Biology*. Edward Arnold Ltd, London, 302 pp.

Tyler S, Hooge M (2004) Comparative morphology of the body wall in flatworms (Platyhelminthes). *Canadian Journal of Zoology-Revue Canadienne De Zoologie* 82(2):194-210

Whitney DD (1907) Artificial removal of the green bodies of *Hydra viridis*. *Biological Bulletin* 13(6):291-299

Zahl PA, McLaughlin JJA (1959) Studies in marine biology. IV. On the role of algal cells in the tissues of marine invertebrates. *Journal of Protozoology* 6(4):344-352

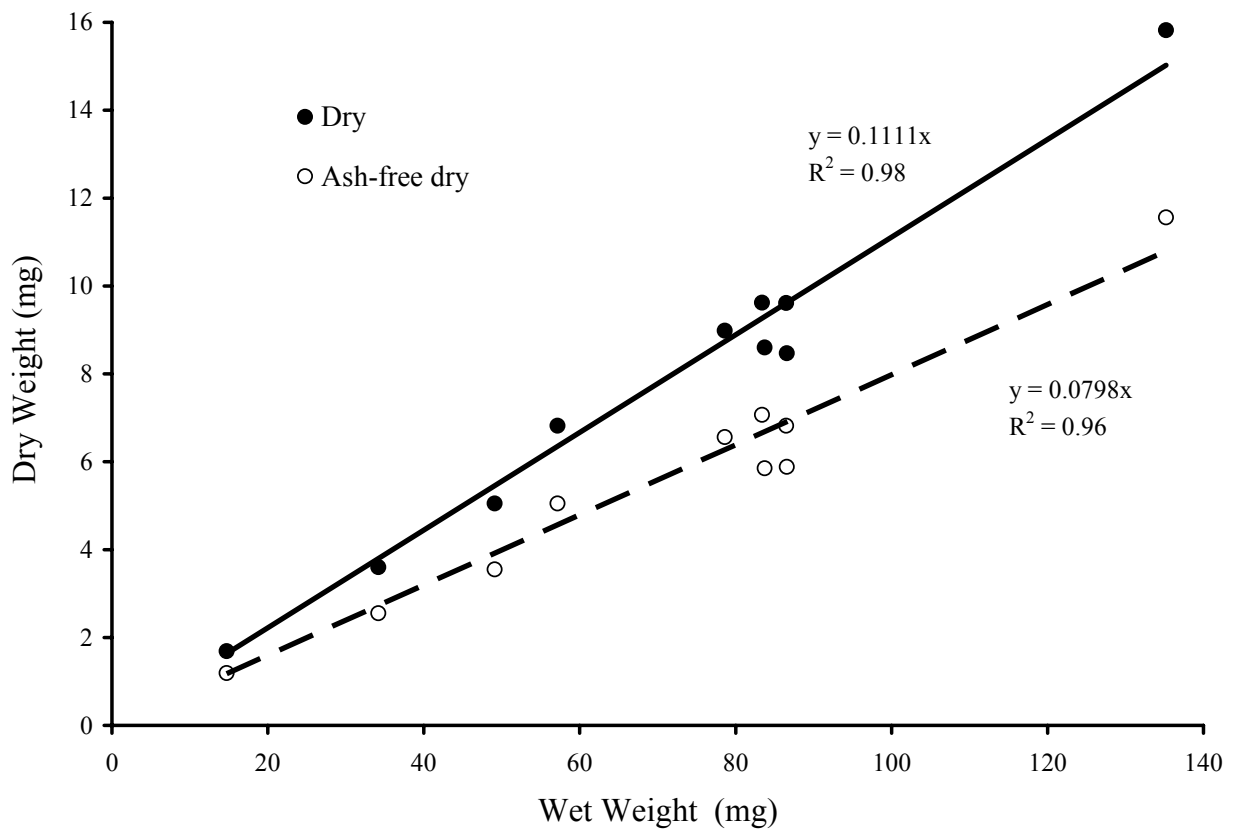


Figure 5.1. Functional relationship between wet weight (ww), dry weight (dw), and ash-free dry weight (afdwt) of *Convolutriloba retrogemma*. The top line (closed circles) represents wet weight vs. dry weight ( $dw = 0.1111 \times ww$ ,  $R^2 = 0.98$ ). The bottom line (open circles) represents wet weight vs. ash-free dry weight ( $afdwt = 0.0798 \times ww$ ,  $R^2 = 0.96$ ).

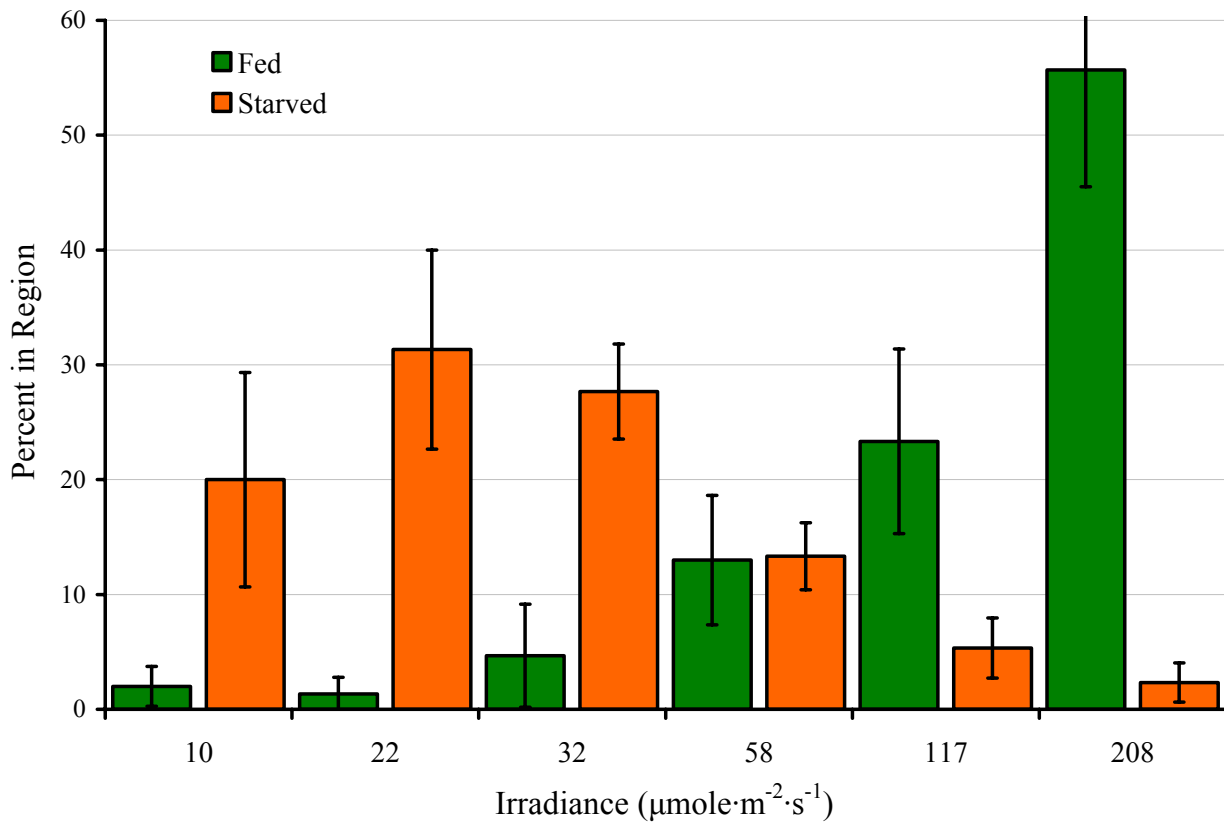


Figure 5.2. Light preference of fed vs. starved *Convolutriloba retrogemma*. Independent axis corresponds to the irradiance levels measured in six sections of a test trough. Acoels were counted in each of the six sections after 10 days. Data were averaged from 10 trials each of fed and starved acoels; 30 individuals were used in each trial. Error bars represent 95% confidence intervals.

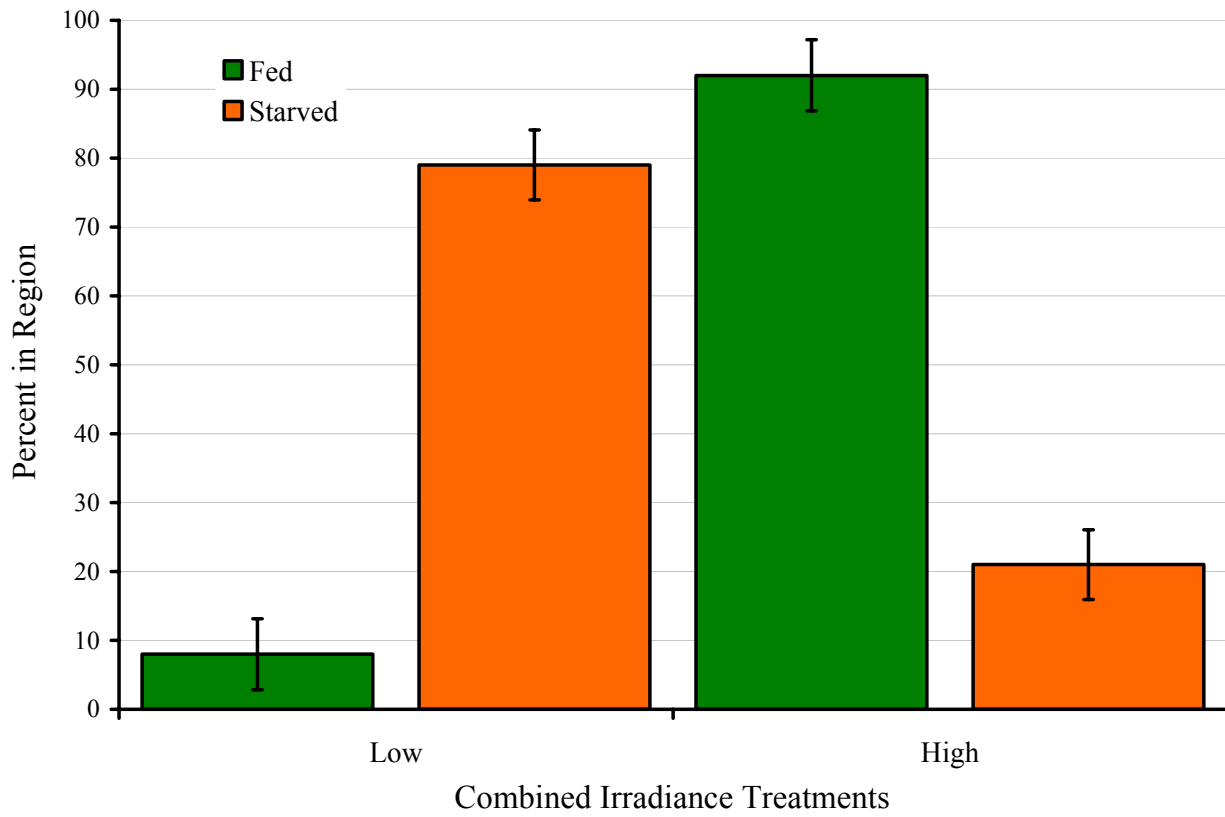


Figure 5.3. Light preference of fed vs. starved *Convolutriloba retrogemma*. Independent axis corresponds to the combined results of the three lowest and the three highest irradiance levels shown in figure 5.1 Error bars represent 95% confidence intervals.



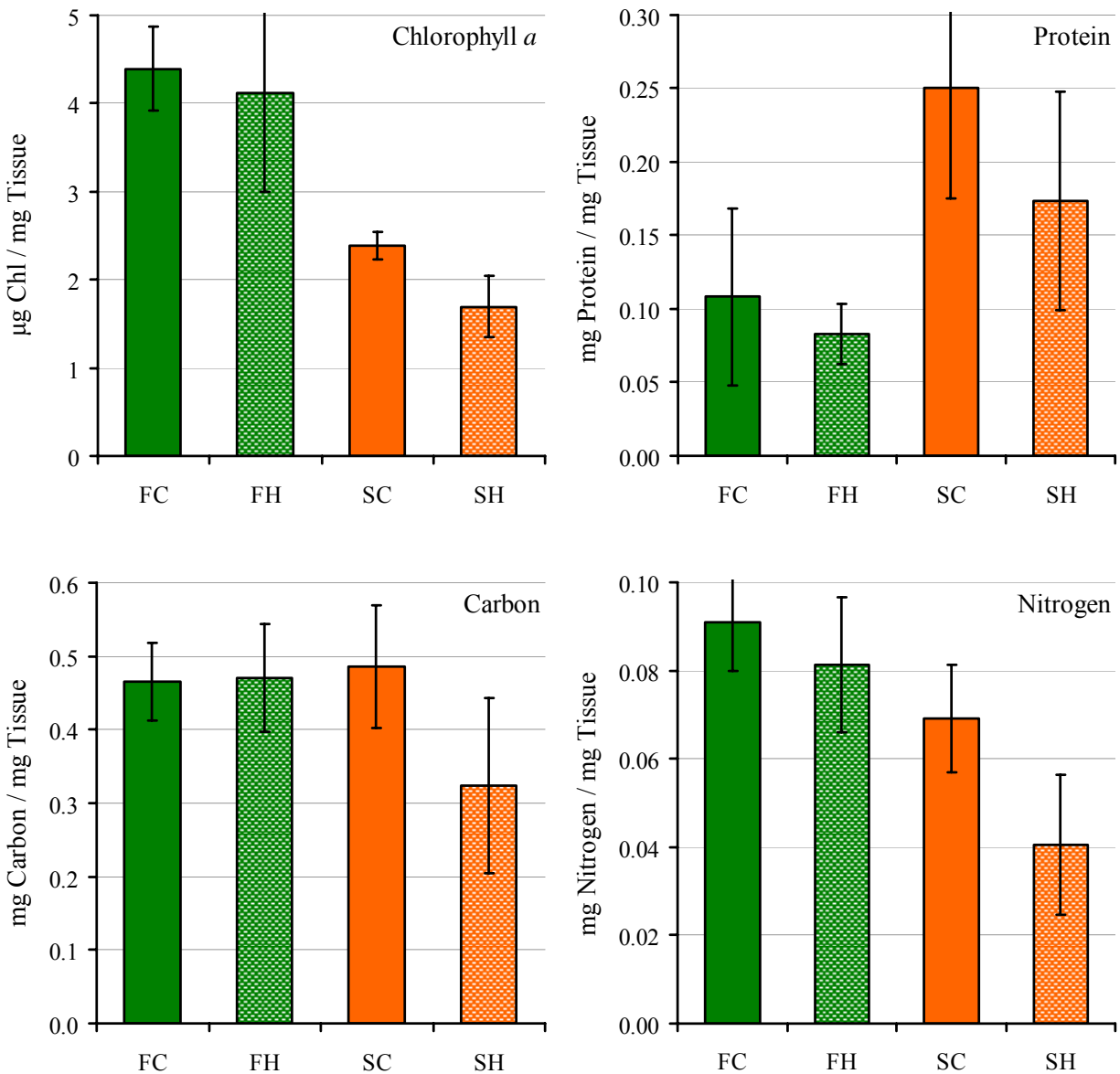


Figure 5.4. Preliminary comparisons of chlorophyll *a*, protein, carbon, and nitrogen concentrations in Fed (F) vs. Starved (S) *Convolutriloba retrogemma* subjected to one of two irradiance treatments for 12 hours. Control (C) irradiance level was  $50 \mu\text{mole}\cdot\text{m}^{-2}\cdot\text{s}^{-1}$ , High (H) irradiance level was  $166 \mu\text{mole}\cdot\text{m}^{-2}\cdot\text{s}^{-1}$ . Error bars represent 95% confidence intervals. Though individual experiment results were inconclusive, concentrations of all substances tested decreased in starved acoels subjected to high light suggesting an influx of osmotic water into the animals' tissues.

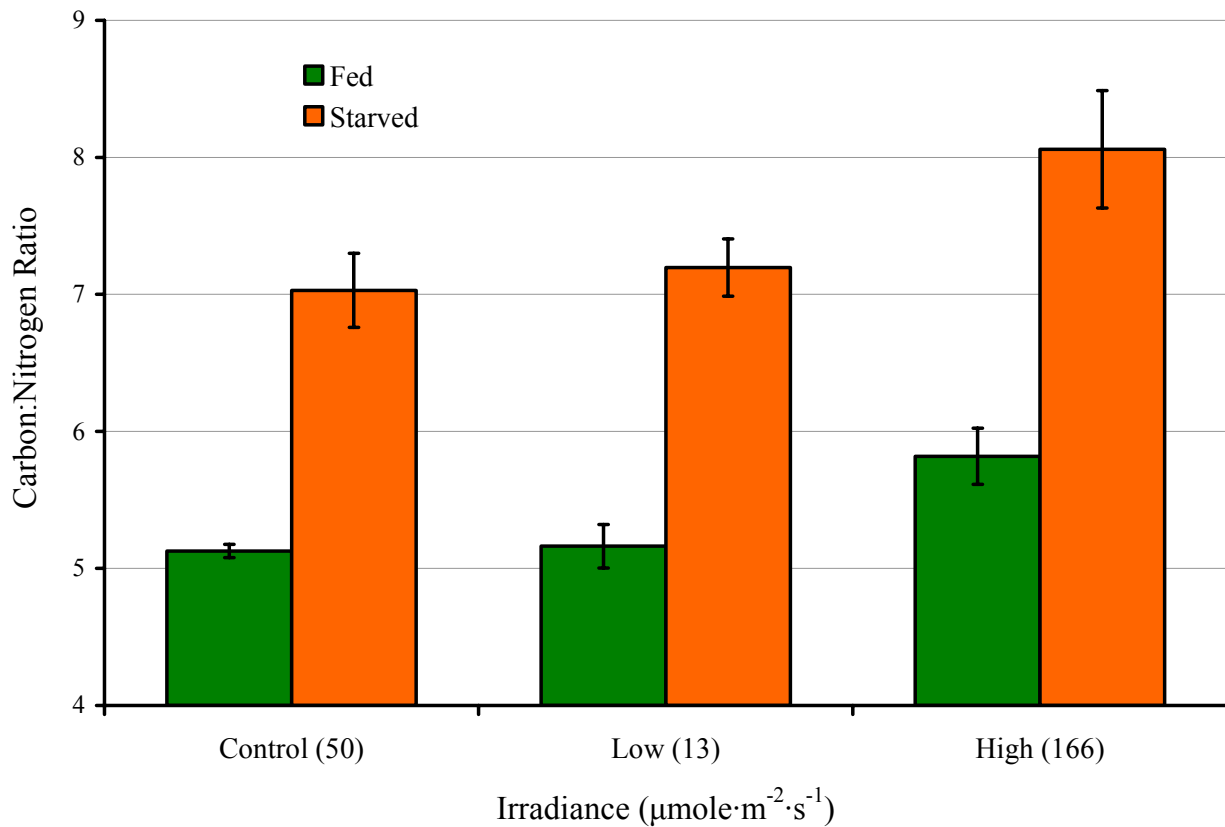


Figure 5.5. Comparison of carbon/nitrogen ratios in fed vs. starved *Convolutriloba retrogemma* subjected to one of three irradiance treatments. Error bars represent 95% confidence intervals. By examining the C:N ratio, the osmotic water effect in the starved groups is eliminated. The over-all higher averages seen in the starved groups suggest increased carbon levels (photosynthates) regardless of light intensity. The increase in C:N ratio in both fed and starved groups suggests an upper limit on the rate at which photosynthate can be transferred into, and metabolized by, host cells.

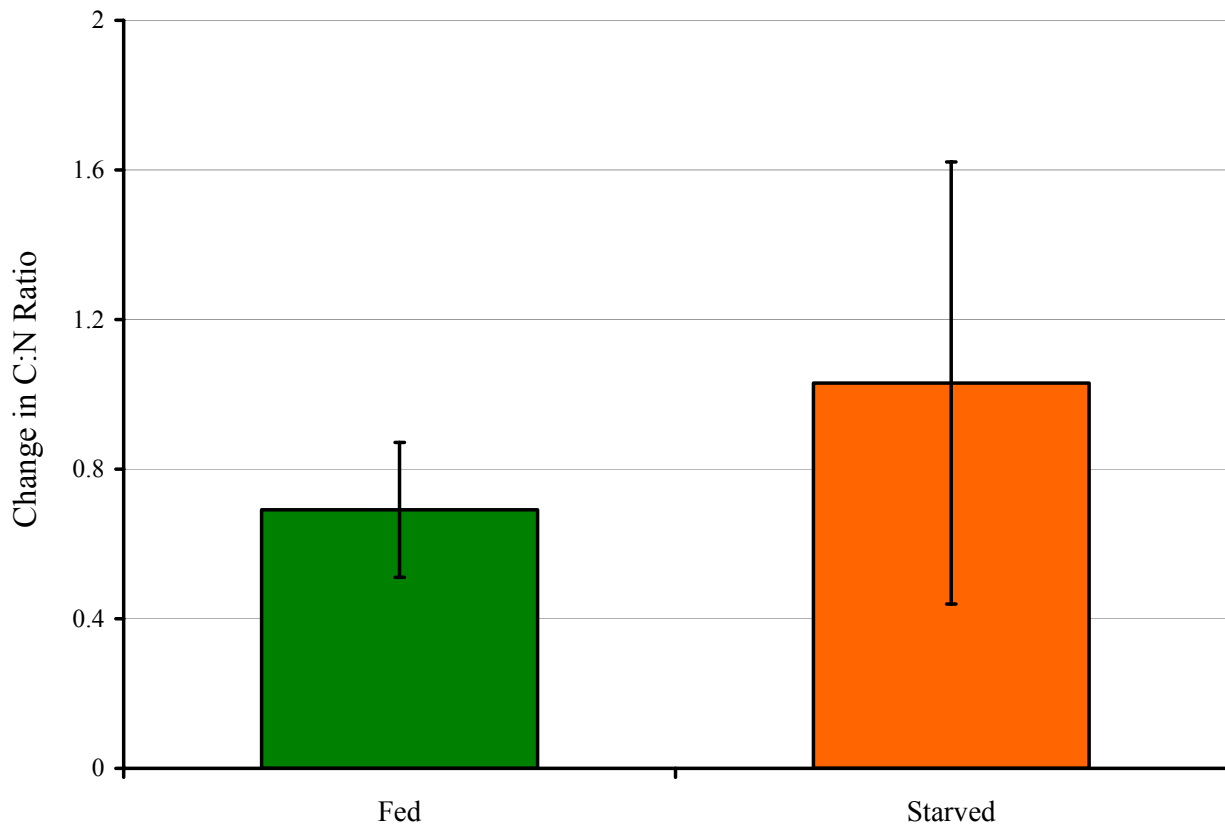


Figure 5.6. Comparison of the differences in carbon/nitrogen ratios between control ( $50 \mu\text{mole}\cdot\text{m}^{-2}\cdot\text{s}^{-1}$ ) and high ( $166 \mu\text{mole}\cdot\text{m}^{-2}\cdot\text{s}^{-1}$ ) irradiance treatments on fed vs. starved *Convolutriloba retrogemma*. Error bars represent 95% confidence intervals. No statistical difference is shown, further suggesting a maximum limit on a host's ability to metabolize or otherwise utilize translocated endosymbiotic photosynthates.

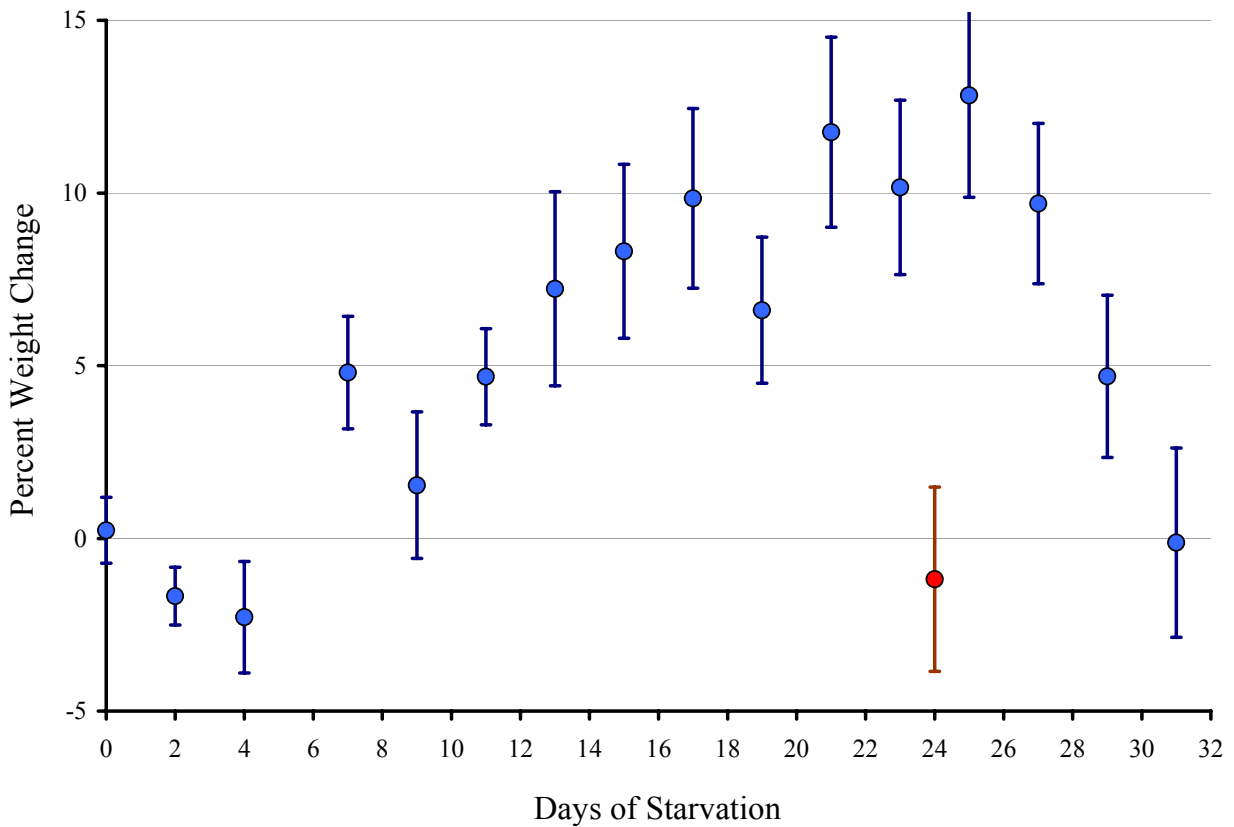


Figure 5.7. Percent weight change in dark-adapted *Convolutriloba retrogemma* weighed before and after being subjected to one hour of PAR irradiance ( $800 \mu\text{mole}\cdot\text{m}^{-2}\cdot\text{s}^{-1}$ ) as measured over a one month starvation regimen. Each point represents the average of 24 acocels tested. Error bars represent 95% confidence intervals. A consistently positive, increasing weight gain was noticed in the animals beginning around the 10<sup>th</sup> day of starvation. A decreasing weight gain trend began after the 25<sup>th</sup> day of starvation, and no weight change was measured on day 31. The red data point at day 24 represents the average weight change of 24 acocels subjected to 50  $\mu\text{M}$  DCMU to inhibit photosynthesis.

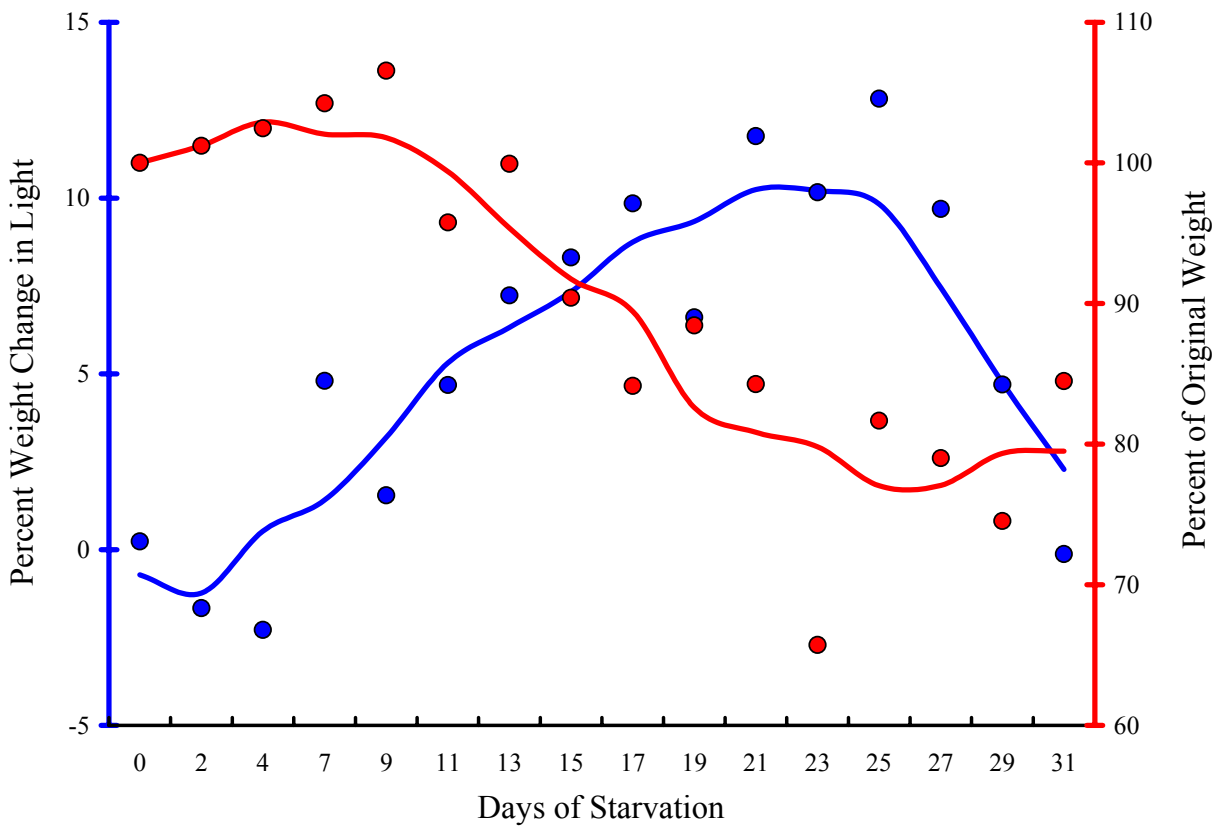


Figure 5.8. Percent weight change in *Convolutriloba retrogemma* as measured over a one month starvation regimen. The left-hand, blue, dependent axis and associated blue data points represent the same data shown in figure 5.5. The right-hand, red, dependent axis and associated red data points represent the average weight of acoels tested on each respective day of starvation as a percentage of the average weights measured on day zero. Pre-light-treatment weights were used. Smoothed lines represent a moving average of the corresponding data to better show the general trends.

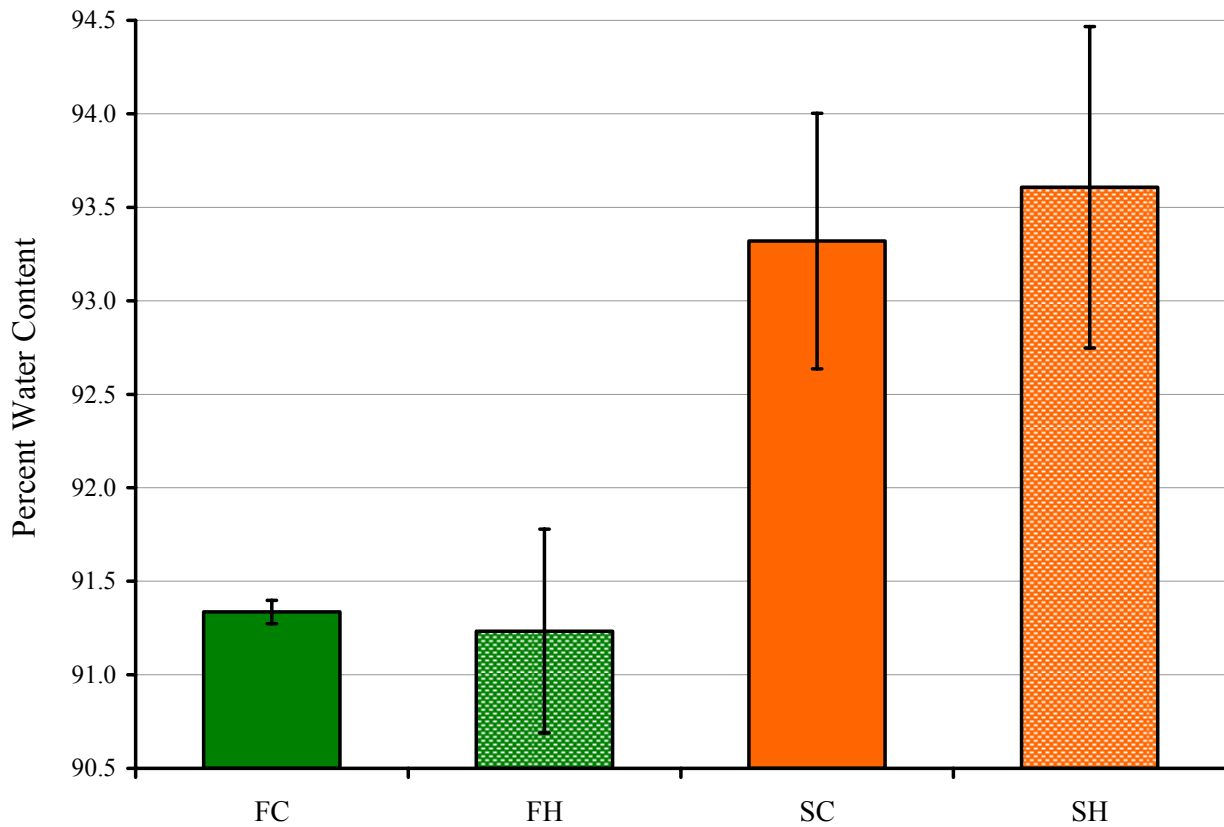


Figure 5.9. Percent water content of Fed (F) and Starved (S) *Convolutriloba retrogemma* subjected to PAR irradiance treatments: Control (C) =  $50 \mu\text{mole}\cdot\text{m}^{-2}\cdot\text{s}^{-1}$  and High (H) =  $166 \mu\text{mole}\cdot\text{m}^{-2}\cdot\text{s}^{-1}$ . Error bars represent 95% confidence intervals. Acoels were tested on the 32<sup>nd</sup> day of the starvation regimen. As shown, a significant difference was found between the fed and the starved treatments; however, no significant differences were found between irradiance treatments within fed or starved groups.

## CHAPTER 6

### *CONVOLUTRILOBA MACROPYGA* SP. NOV., AN UNCOMMONLY FECUND ACOEL (ACOELOMORPHA) DISCOVERED IN TROPICAL AQUARIA<sup>1</sup>

---

<sup>1</sup> Shannon, T. and Achatz, J. G. 2007. *Zootaxa*. 1525:1-17.  
Reprinted here with permission of publisher

## Abstract

A new species of the *Convolutriloba* Hendelberg & Åkesson, 1988, collected from an aquarium in Marietta, Georgia, USA, and cultured at the University of Georgia comprises exceptionally large individuals, up to 10 mm in length. Like other members of the genus, *Convolutriloba macropyga* **sp. nov.** reproduces asexually and possesses symbiotic zoochlorellae, but it also routinely reproduces sexually, laying relatively large eggs that hatch into aposymbiotic juveniles with a statocyst and frontal organ (which are absent in the adults). *C. macropyga* has a narrow tolerance for extremes of temperature and salinity: it cannot survive outside of a temperature range of 18–28°C and suffers 50% lethality at salinity as low as 24 ppt and as high as 44 ppt. It cannot survive total darkness for longer than 23–26 days, even with prey provided, suggesting an obligate symbiosis with its algal endosymbiont. A method for inducing sexual reproduction in other convolutrilobids is presented, as are suggestions for successful shipping of these acoels.

**Key words:** Asexual reproduction, sexual reproduction, reverse budding, symbiosis, anterior-posterior axis, toxicity, acoel, flatworm, shipping.



## Introduction

The genus *Convolutriloba* was erected with the discovery and description of *Convolutriloba retrogemma* Hendelberg & Åkesson, 1988. The authors hesitated to place the genus in a family due to uncertainties about the maturity of the examined animals. Two years later, Winsor (1990) described *Convolutriloba hastifera* from Australia. Winsor had mature specimens at hand and, by comparison, confirmed the maturity of specimens of *C. retrogemma* investigated by Hendelberg & Åkesson. On the basis of the male copulatory organ in these species, he assigned the genus to the family Haploposthiidae Winsor, 1990. *Convolutriloba longifissura* Bartolomaeus & Balzer, 1997, is the third and most recently discovered species of the genus. Gschwentner *et al.* (1999) investigated sagittocysts in this species and, weighting the homology of these micro-organs more heavily than that of the male copulatory organ, which appeared to be secondarily reduced, reassigned the genus to the family Sagittiferidae Kostenko & Mamkayev, 1990.

The genus has attracted attention due to its uncommon modes of asexual reproduction. *C. retrogemma* reproduces by reverse budding, a process in which a daughter individual is released at the posterior end of the mother individual, with its anterior-posterior axis reversed 180° to that of the mother individual (Hendelberg & Åkesson 1988; Hendelberg & Åkesson 1991). In *Convolutriloba longifissura* a longitudinal fission, so far the only described case of such fission in bilaterians, occurs in the posterior daughter individual of a transverse fission (Bartolomaeus & Balzer 1997; Åkesson *et al.* 2001).

These species are particularly amenable to study because of the ease with which they can be maintained in the laboratory. In fact, only one species, *Convolutriloba hastifera*, has been described from natural habitats; the others were originally discovered in aquaria. Because of

their high rate of reproduction through asexual means, all of these species are considered pests in the aquarium trade; they routinely “infest” reef tanks.

Sexual reproduction, on the other hand, has rarely been observed in the genus and has yet to be described. We have discovered a new species in the aquaria of a retail establishment in Marietta, GA, bearing reef organisms collected in the Indo-Pacific. While closely related to *Convolutriloba* species, it reproduces sexually regularly. Its sexually prolific nature, combined with the ease with which it can be cultured under appropriate lighting (for photosynthesis in its algal endosymbiont) and provision of prey, make it an ideal candidate for future studies of development, algal-invertebrate symbioses, and photobiology.

## **Material and Methods**

Specimens were collected between May 2006 and February 2007 from a tropical marine aquarium at Cappuccino Bay Aquarium, Marietta, GA, USA, and cultured at the University of Georgia. Animals were maintained in trough-style research aquaria in both a mixed-species population with other convolutrilobids (*C. retrogemma*, *C. longifissura* & *C. hastifera*) and in a monospecific culture tank separate from other *Convolutriloba* spp. The aquaria were housed in a constant temperature room maintained at 25°C. Artificial seawater (ASW, Instant Ocean<sup>®</sup>) was maintained at a salinity of 34±1 ppt as measured with an Atago S/Mill hand-held refractometer. The mixed-species tank was illuminated by four Philips 40W 5000°K Ultralume fluorescent lamps providing an average PAR irradiance of ~100  $\mu\text{mole}\cdot\text{m}^{-2}\cdot\text{s}^{-1}$  at the water’s surface. Culture tanks were illuminated by two URI Super Actinic and two URI Aquasun-4 VHO 110W fluorescent lamps powered by an IceCap 660 ballast providing ~ 200  $\mu\text{mole}\cdot\text{m}^{-2}\cdot\text{s}^{-1}$ . All tanks were maintained on a 14h:10h light-dark cycle. Irradiance measurements were made with an LI-

190SA quantum sensor and registered with a Li-Cor Model LI-1400 Data Logger. *Artemia* sp. nauplii were provided daily in superabundance to supplement the acoels' diet of rotifers, copepods, and crustacean larvae already present in the aquaria.

Live animals were viewed with an Olympus SZ40 stereomicroscope and an Olympus CX41 compound microscope and photographed with a DFK 31AF03 fire-wire camera and an Olympus C-5050 digital camera (University of Maine). Live animals were alternatively viewed with a Wild M3Z stereomicroscope and a Zeiss Axioskop-2 phase-contrast compound microscope and photographed with a Sony DSC-P71 digital still camera and a Canon PowerShot A520 digital camera (University of Georgia).

Specimens processed for serial sectioning were relaxed with magnesium sulfate isotonic to seawater and fixed for 1 hour in 4% glutaraldehyde in 0.2 M cacodylate (pH 7.2) containing 0.1 M NaCl and 0.35 M sucrose. Specimens were washed in cacodylate buffer, postfixed in cacodylate-buffered 1% (v/v) osmium tetroxide, dehydrated in acetone, and embedded in EMBed/Araldite epoxy resin. Serial thick sections of 2  $\mu\text{m}$  were made according to Smith and Tyler (1984) using a diamond knife mounted in a Butler trough (Butler 1979) and stained with Heidenhain's hematoxylin according to Smith and Tyler (1984) or toluidine blue.

Musculature was revealed through F-actin staining of whole mounts with fluorescently labeled phalloidin (Alexa 488; Molecular Probes, Eugene, OR) according to Hooge (2001) and examined with a Leica TCS SP2 confocal laser scanning microscope.

Salinity tolerance was determined by subjecting animals to ASW with salinities ranging from 20 to 50 ppt in increments of 1 ppt. Salinity arrays were arranged in Costar (Corning Inc.) 24-well cell-culture trays selecting six randomly chosen wells per salinity (2.5 ml/well). One adult specimen from culture was then added to each well (186 specimens total). Trays were

maintained at 25°C on a 14h:10h light-dark cycle with a surface irradiance of 70  $\mu\text{mole}\cdot\text{m}^{-2}\cdot\text{s}^{-1}$  provided by two Philips 5000°K Ultralume and two Philips cool white 40W fluorescent lamps. Surviving numbers for each salinity were recorded every 12 hours concomitant with water changes and removal of asexual progeny. Exposure was continued until the numbers were stable for at least two successive 12-hour periods.

Temperature tolerance was determined in a water tray thermally regulated by a Savant RWC825 constant-temperature circulator. Each experimental trial consisted of 20 adults from culture placed in 15 ml Erlenmeyer flasks immersed in the water tray, one animal per flask. Experimentation commenced at 35°C with successive trials run following an increase or decrease of 1°C. Twenty fresh specimens were tested in each trial. Experimental specimens were maintained in 15 ml ASW at 34 ppt on a 14h:10h light cycle as described for the salinity-tolerance experiments. Numbers surviving were recorded every 24 hours for 3 days at each temperature. Incremental temperature changes continued until any 24-hour exposure resulted in 0% survival.

Release rates of asexual progeny by *C. macropyga* **sp. nov.** were measured under a range of light regimens to determine the effect of irradiance intensity on asexual reproduction. Seventy-two asexually active adult specimens were collected from culture and placed in three 24-well culture plates as previously outlined. Each tray was subjected to one of three light treatments for 15 days: Dark (0  $\mu\text{mole}\cdot\text{m}^{-2}\cdot\text{s}^{-1}$ ), Low (70  $\mu\text{mole}\cdot\text{m}^{-2}\cdot\text{s}^{-1}$ ), and High (200  $\mu\text{mole}\cdot\text{m}^{-2}\cdot\text{s}^{-1}$ ). Low flux was provided from the same system used in the salinity and temperature experiments. High flux was provided from the culture tanks' lighting system. Asexual progeny, i.e., released buds, were counted daily for each individual concomitant with water change, addition of *Artemia* sp. nauplii, and removal of counted progeny. Dark trays were serviced under

green light provided from a laptop computer LCD screen (all-green jpeg file viewed in full-screen mode) at  $<0.01 \mu\text{mole}\cdot\text{m}^{-2}\cdot\text{s}^{-1}$  in an effort to minimize algal photosynthesis. Presence of egg clusters was also recorded and clusters were removed for observation and measurements of egg and cluster sizes.

Dark-survival experiments were conducted with all four species of *Convolutriloba* for comparative purposes. Twenty-four specimens per species were collected from their respective monospecific culture tanks and randomly placed in 24-well culture plates (one animal per well in 2.5 ml, 34 ppt ASW). Trays were then placed in total darkness. Numbers surviving for each species were recorded daily concomitant with water change, addition of *Artemia* sp. nauplii, and removal of egg clusters and asexual progeny. The maintenance tasks were completed in less than 5 minutes and were conducted under the same green-light conditions as outlined above.

Egg comparisons and general observations were conducted on over 200 egg clusters including those collected in the progeny-release experiments and clusters obtained from *C. retrogemma*, *C. longifissura*, and *C. hastifera*. Adult individuals of these three species possessing visible ovaries and false seminal vesicles were selected from their respective culture tanks and placed in 4½” culture dishes in 200 ml ASW, 10 specimens per dish. Sexual reproduction was induced by subjecting these animals to the lower light regimen of  $70 \mu\text{mole}\cdot\text{m}^{-2}\cdot\text{s}^{-1}$ . Egg-laying generally commenced within 24 hours. Twelve egg-clusters per species were collected. Each cluster was placed on a Neubauer brightline hemacytometer (Fisher Scientific) and digitally photographed with a Canon PowerShot A520 on a Zeiss Axioskop-2 phase-contrast compound microscope. Length and width measurements of three randomly selected eggs per cluster were determined in Adobe Photoshop 6.0 using the hemacytometer markings as a linear standard reference.

Permanent cultures of *C. macropyga* **sp. nov.** have been established at the University of Georgia, Athens, GA; the University of Maryland, College Park, MD; and St. Mary's College, St. Mary's City, MD, to ensure availability for future studies.

### **List of Abbreviations**

**bn**, bursal nozzle; **cgc**, gland cell containing cyanophilic vesicles; **cm**, circular muscles; **ds**, digestive syncytium; **ef**, eye field; **fgp**, female gonopore; **fsv**, false seminal vesicle; **g**, ganglion; **lm**, longitudinal muscles; **m**, mouth; **mgp**, male gonopore; **mm**, muscle mantle; **nc**, nerve cord; **o**, oocyte; **pc**, pigment cell; **pg**, prostatoid gland cells; **rh**, rhabdoid gland cell; **sb**, seminal bursa; **sg**, sagittocyte; **sv**, seminal vesicle; **t**, male follicle; **v**, vagina; **ve**, vestibulum; **vg**, vesicula granulorum; **vp**, vacuolated parenchymal cell; **zc**, zoochlorellae.

### **Results**

#### **Family Sagittiferidae Kostenko & Mamkaev, 1990**

#### **Genus *Convolutriloba* Hendelberg & Åkesson, 1988**

#### ***Convolutriloba macropyga* sp. nov.**

**Diagnosis.** *Convolutriloba* with sparsely but widely distributed concrements on the dorsal surface; one type of rhabdoid gland cell with 3- $\mu$ m long rhabdoids. Male copulatory organ consists of paired, lateral, sclerotized canals leading into a seminal vesicle. Seminal vesicle opens into a vesicula granulorum, which is filled with prostate secretion in its proximal part and cyanophilic vesicles in its distal part. Animals have 1 to 3 bursal nozzles. The mouth is

positioned at 31 U of total body length (percent, measured from anterior tip to edge of posterior lobe); the female gonopore is at 52 U; the male gonopore is at 75 U.

**Type material.** Holotype: USNM 1100318, one complete set of 2- $\mu$ m-thick serial cross sections. Paratypes: USNM 1100329, one partial set of 2- $\mu$ m-thick serial sagittal sections, USNM 1100330, USNM 1100331, two partial sets of 2- $\mu$ m-thick serial cross sections.

**Type repository.** Smithsonian Natural History Museum, Washington D.C., USA.

**Type locality.** Tropical marine aquarium at Cappuccino Bay Aquarium, Marietta, GA, USA.

**Etymology.** Specific epithet is a derivation of the Greek *macro-* (large) and *pyga* (rump), and reflects the extensive expansion of the posterior region of the body, especially while basking.

**Other material examined.** Living specimens and eggs in squeeze preparations; 12 whole-mount specimens for fluorescence microscopy; four partial serial sections stained with toluidine blue.

**External morphology & behavior.** *Convolutriloba macropyga* **sp. nov.** is flat and shield-shaped, its body rounded anteriorly and indented at the anterior tip, broadening to auricular apices set off by a transverse constriction ~2 mm behind the anterior tip, and broadening toward two rounded lateral caudal lobes and a longer, slender median caudal lobe (Figs. 6.1A-C, 6.2A). Immature specimens always possess the three caudal lobes (Fig. 6.1C), but adults often develop multiple median lobes — usually 2 or 3, and up to 9 (Fig. 6.1A). Individuals are often observed lying stationary with their anterior end erected into the water column in well-illuminated areas. When basking like this, the body is dorso-ventrally flattened to a thickness of 200–360  $\mu$ m along the lateral margins and 550  $\mu$ m along the median line. Mature basking specimens are up to 8 mm long and 6 mm wide.

When motile, adult specimens measure up to 10 mm in length and, apart from slight indentations in the lateral margins at the transverse constriction, are uniformly 1.5–2.5 mm wide along the entire length as the body is held tube-like, with the lateral margins curled ventrally. The animal glides by ciliary action.

A sudden increase in light intensity triggers a negatively phototactic, or photophobic, behavior. Mechanical disturbance of specimens in glass culture dishes trigger rapid, forward motion. Similar disturbances in more natural environments cause the animal to move to the shaded undersides of objects or into the substrate.

When food is present, as when *Artemia* sp. are added to the cultures, animals lift the anterior body tip from the substrate and curl the lateral edges and the two ventral flaps (Fig. 6.2B) anterior to the transverse constriction ventrally, forming a “capturing funnel” (Fig. 6.1B) *sensu* Hendelberg & Åkesson (1988). The funnel leads to the mouth, which is located medially on the ventral side ~2 mm behind the anterior tip (Figs. 6.2B, 6.3A). Though some animals will move in the direction of the prey, most remain relatively motionless with their posterior lateral margins attached to the substrate. When prey moves into the funnel, the animal traps it by pressing down flat against the substrate and moving forward to bring the prey into its mouth.

Body coloration is green, tinged with red, due to symbiotic zoochlorellae and scattered, red rhabdoid gland cells and a diamond-shaped red spot comprised of pigment cells in front of the caudal lobe. The dorsal body surface appears bluish in reflected light due to refractive concretions (Figs. 6.2A-F).

**Epidermis.** The epidermis is entirely ciliated. The cilia are commonly ~8  $\mu\text{m}$  long, but can measure up to 12  $\mu\text{m}$  in some areas. On the ventral side of the capturing funnel, the cilia are often sparse or shorter. The epidermal nuclei are sunken beneath the body-wall musculature.



Small refractive epidermal concretions occur in large fields. The density of these fields increases gradually from the anterior to the posterior end. The concretions give the surface a bluish sheen under incident light and appear dark purple in transmitted light (Figs. 6.2C-E). The sheen vanishes when animals are relaxed in magnesium sulfate. Dorsally at the transverse constriction, three to five small white spots of concretions occur in a transverse row. Similar spots occur along the lateral margins in some individuals.

**Sensory organs & nervous system.** A pair of eye fields (Fig. 6.2A) appearing colorless due to the absence of symbiotic algae occurs ~650  $\mu\text{m}$  behind the anterior tip. Paired, insunk ganglia lie ventral to them. The ganglia are connected transversally by a commissure. From each ganglion, two nerve cords run frontally, one runs laterally and one runs latero-caudally. A pair of median longitudinal nerve cords originates at the commissure (Fig. 6.3A) and can sometimes be seen in live animals as two colorless stripes due to the absence of zoochlorellae. A statocyst is absent in all adult specimens examined, but present in juveniles (Fig. 6.7A).

**Musculature.** The body-wall musculature is stronger on the ventral than on the dorsal side. The dorsal musculature consists of outermost circular, diagonal, and longitudinal muscles. The ventral musculature consists of outermost circular muscles (Fig. 6.5B), a layer of muscles that arc across the body in curves centered on the mouth (Fig. 6.5C), and an innermost layer of longitudinal muscles and muscles radiating from the mouth (Fig. 6.5D). Circular muscles near the lateral posterior edge of the mouth bend around its anterior rim in a U-shaped path. Some of these do not bend fully around the mouth but run anteriorly and terminate lateral to it. The next layer inward consists of muscles surrounding the mouth and constituting the wall of the capturing funnel. They bend around the posterior rim of the mouth and run straight and oblique anteriorly, crossing each other in front of the mouth (Figs. 6.4A, 6.5C). In the posterior half of the

body are corresponding longitudinal cross-over muscles (Figs. 6.4B, 6.5C). The innermost layer consists of special pore muscles, which fan out from the mouth to the anterior rim and the lateral edges of the capturing funnel (Figs. 6.4A, 6.5D), and longitudinal muscles at the posterior end (Figs. 6.4B, 6.5D). These longitudinal muscles insert slightly in front of the posterior rim of the capturing funnel (Fig. 6.3A). Dorso-ventral muscles are abundant, especially laterally.

**Gland cells.** Numerous adhesive papillae are distributed along the posterior lateral margin. They comprise the distal tips of glands protruding through the body wall and are ~5  $\mu\text{m}$  long and 2  $\mu\text{m}$  wide.

Two sorts of rhabdoid gland cells, whose cell bodies lie in the parenchyma, protrude on the body surface. The cells of the first type are highly flexible in shape but are commonly ~45  $\mu\text{m}$  long and ~15  $\mu\text{m}$  wide and contain ~250 rhabdoids measuring 2–3  $\mu\text{m}$  long and ~1  $\mu\text{m}$  wide, the contents of which are reddish-orange (Fig. 6.2F). Some of these rhabdoid gland cells bear similarly shaped translucent rhabdoids instead. The rhabdoids and the cytoplasm of these cells are cyanophilic. The cells are distributed on the dorsal and ventral side, with the exception of the ventral side of the capturing funnel, including the inner side of the ventral flaps. In non-sexual juvenile specimens the red rhabdoid gland cells are sparsely distributed. As an animal matures, cell densities increase body-wide with higher densities emerging both dorsally and ventrally adjacent to the developing ovaries. In sexually mature adults rhabdoid gland cells are highly numerous along the posterior, lateral margins, the lobes, around the male copulatory organ, and in the region of the gonads on the ventral side (Figs. 6.2A, B). The second rhabdoid gland cell type occurs solely on the dorsal side, about 20 cells in a specimen. Each cell contains ~18 refractive rods, which are ~20  $\mu\text{m}$  long, 1  $\mu\text{m}$  wide (Fig. 6.2F), and strongly cyanophilic.

Mucous gland cells are absent. Adults lack a frontal organ, but freshly hatched juveniles have an easily recognized frontal organ with a reservoir, all lying in front of the statocyst (Figs. 6.7A, B).

Red pigment cells are densely packed on the dorsal side in a diamond-shaped red spot ~1.4 mm long and ~0.9 mm wide in front of the median caudal lobe (Figs. 6.1C, 6.2A, B). The cells lie dorsal to the male copulatory organ and ventral to the body-wall musculature and the rhabdoid gland cells, they do not protrude to the surface, and measure 40–50  $\mu\text{m}$  in diameter (Fig. 6.3B). In histological sections the cells are filled with a grayish meshwork and their cytoplasm is not stained.

Sagittocysts occur in two sizes. Large sagittocysts occur in abundance and measure ~40  $\mu\text{m}$  long and ~2.5  $\mu\text{m}$  wide. Small sagittocysts, distributed mainly at the anterior lateral margins, measure ~20  $\mu\text{m}$  long and ~1  $\mu\text{m}$  wide. The sagittocysts are formed in sagittocytes which lie ventral to the dorsal body-wall musculature and rhabdoid gland cells. The sagittocytes generally contain a bundle of 8–12 sagittocysts. Each sagittocyst moves towards the distal tip of the sagittocyte, which lies within the body wall. A muscle cell, or muscle mantle, enwraps the sagittocyst within the distal tip of the sagittocyte. This arrangement is connected with a sensory cell and altogether is called an extrusion apparatus *sensu* Gschwentner *et al.* (2002). The muscle mantles enwrapping the small sagittocysts are ~50  $\mu\text{m}$  long and ~6  $\mu\text{m}$  wide, those enwrapping the large sagittocysts are ~75  $\mu\text{m}$  long and ~9  $\mu\text{m}$  wide. The extrusion apparatus are distributed over the entire dorsal surface and the lateral sides of the ventral flaps, with higher densities found on the lateral margins. Ventral distribution is limited to the area between the female gonopore and the caudal end with high densities in a broad region between the gonopores.

**Parenchyma & zoochlorellae.** The parenchyma consists of dense peripheral parenchyma and parenchyma cells with large vacuolated spaces. The dense parenchyma occurs primarily in the periphery of the body, but is also found centrally surrounding nervous tissue and often forms extensions into the vacuolated parenchyma. Numerous zoochlorellae, 5–14  $\mu\text{m}$  wide, are distributed throughout the parenchyma. In squeeze preparations and motile specimens, zoochlorellae appear to be arranged in rows, mirroring the overlying musculature (and sometimes the longitudinal nerves, as well); a random distribution is observed in specimens at rest. The algal endosymbiont has been isolated using the  $\text{CO}_2$  bubbling method of Boyle & Smith (1975) and cultured in L1 media. We have not yet identified the algal species.

**Testes & male reproductive system.** The paired testes lie dorsal and lateral to the ovaries. Follicles and sperm pass caudally and sperm accumulate in paired false seminal vesicles, which measure  $\sim 170$   $\mu\text{m}$  in diameter and converge toward the body-midline (Fig. 6.3A). Mature spermatozoa measure  $\sim 280$   $\mu\text{m}$  long, have a thin  $\sim 50$   $\mu\text{m}$  long tail, and a stepped,  $\sim 20$   $\mu\text{m}$  long tip.

The male gonopore lies about 1 mm in front of the posterior end, slightly less than 2 mm behind the female gonopore, and opens into a vesicula granulorum. The vesicula granulorum,  $\sim 50$   $\mu\text{m}$  in diameter and  $\sim 75$   $\mu\text{m}$  high, lies within a plug of peripheral parenchyma, which is 450  $\mu\text{m}$  long, 300  $\mu\text{m}$  wide, and 150  $\mu\text{m}$  high. Dorso-ventral muscles, sagittocytes, extrusion apparatus, and two types of gland cells are embedded in this plug. The first type of gland cell contains small cyanophilic vesicles with a diameter of 300–500 nm, and protrudes through the body wall around the male gonopore and into the distal part of the vesicula granulorum. The second type, prostate gland cells *sensu* Winsor (1990), produce basophilic vesicles with a diameter of  $\sim 1$   $\mu\text{m}$ , and protrude exclusively into the proximal part of the vesicula granulorum.

A seminal vesicle, measuring ~100  $\mu\text{m}$  in diameter when filled with sperm, opens into the proximal end of the vesicula granulorum (Fig. 6.3B). One lateral canal on each side connects the seminal vesicle with the caudal end of the corresponding false seminal vesicle. Each canal is ~300  $\mu\text{m}$  long and has a diameter of 22  $\mu\text{m}$ . The paired canals and the seminal vesicle are surrounded by sclerotized tissue and parenchymal musculature.

**Ovaries & female reproductive system.** The paired ovaries lie ventral and medial to the testes (Fig. 6.3A). Early oocytes contain numerous translucent granules, have a cell diameter of ~50  $\mu\text{m}$ , a nucleus measuring ~10  $\mu\text{m}$ , and a nucleolus measuring 2–5  $\mu\text{m}$  in diameter. The nucleus is surrounded by dense homogeneous cytoplasm measuring 25  $\mu\text{m}$  in diameter. During cellular growth the size and morphology of the nucleus and nucleolus remain constant as the cell becomes larger and lobulated. In living specimens one can observe the appearance of orange-brown granules in the cytoplasm of oocytes at about the level of the mouth. At the same level, basophilic granules with a diameter of 500–800 nm start to appear in histological sections. As oocytes mature the cytoplasm stains progressively darker.

The female gonopore lies ~1.5 mm behind the mouth (Fig. 6.3A). The vagina is an invagination of the body wall ~100  $\mu\text{m}$  long, ciliated, and lined with weak musculature (Fig. 6.3C). The vagina connects with the distal part of the seminal bursa, which is lined with weakly sclerotized tissue and often filled with spongy tissue. The proximal part is surrounded by bursal nozzle tissue. Bursal nozzles range in size from 55  $\mu\text{m}$  to 150  $\mu\text{m}$  and vary in number from 1 to 3 (Figs. 6.6A, B). Of 26 specimens examined, 15 had one nozzle, 7 had two, and 4 had three. All sectioned animals had two bursal nozzles lying in close proximity, sharing one common seminal bursa. The bursal nozzles are directed antero-ventrally, and curve frontally. The

vestibula are extraordinarily large and contain many rounded nuclei, cyanophilic vacuoles, and a weakly stained granular plasma.

**Sexual reproduction.** Although we have not yet witnessed copulation, sexual reproduction is evident in our populations and sexually mature animals routinely produce eggs. One third of the adults in the *progeny-release* trials laid eggs after being individually isolated at the onset of the experiment. Egg laying was most common in the first five days but continued until the ninth day of isolation. Most animals laid eggs on three or four different days; one animal produced eggs on seven consecutive days.

Eggs are commonly laid in a flat cluster measuring no more than 2 mm in diameter and are suspended in a transparent matrix that adheres the cluster to the substrate. Of fifty clusters collected for egg counts, average number of eggs per cluster was 78; the smallest cluster contained 31 eggs, and the largest contained 181. Eggs are ovoid in shape with a thin, transparent shell  $\sim 170 \times 130 \mu\text{m}$ . Embryos in freshly laid eggs bear a reddish-orange color, have no readily identifiable morphological features, and occupy  $\sim 90\%$  of the egg. After 36–48 hours, a darkening, dense, red spot appears within each embryo. The embryos' surfaces are entirely ciliated, and they rotate within the eggs. By the third day the embryos are folded over ventrally, continue to rotate, have fully developed red rhabdoid gland cells concentrated centro-caudally and laterally, and a statocyst. Juveniles begin to hatch on the third day and most have emerged by the end of the fourth. Hatchlings are  $\sim 230 \mu\text{m}$  long and  $\sim 120 \mu\text{m}$  wide, dorso-ventrally flattened, rounded anteriorly and taper caudally to a rounded point (Fig. 6.7A). They harbor no algal symbionts, but have a frontal organ, a statocyst with a statolith, and approximately 100 red rhabdoid gland cells (Figs. 6.7A-D). The statocyst is  $\sim 22 \mu\text{m}$  and the statolith  $\sim 12 \mu\text{m}$  wide (Fig. 6.7C). Four-day-old hatchlings already possess small sagittocysts at the anterior end.

Hatchlings glide along the substrate using their cilia; unlike adult animals they routinely swim freely in the water column by cilia. They appear to consume bacteria, as evidenced by large numbers of live bacterial cells sequestered in the central parenchyma, and have been observed preying on small ciliates.

**Asexual reproduction.** This species reproduces asexually by reverse budding (Hendelberg & Åkesson 1988) whereby the main axis of the progeny is reversed 180° relative to that of the mother. Budding begins as a thickening, slight protrusion anywhere along the caudal margin lateral to the median lobe(s), up to and including the lateral lobes. Concomitant with the thickening is a migration of zoochlorellae to the protrusion rendering it a darker green, and the emergence of red pigment cells medial to, and forward of the protrusion in the mother. Within 24 hours the bud has elongated disto-caudally from the mother and the newly formed red pigment spot has expanded and elongated to span the marginal interface between mother and daughter as can be seen in figure 6.1A. Within the following 24–36 hours a head has developed, eye fields are evident, and in some cases the daughter begins feeding holozoically. Shortly thereafter, the bud is not released but torn from the mother when it attaches itself to the substrate and pulls away. At any one time, we have observed upwards of 4–5 daughter individuals in various stages of development on a mother individual.

Released progeny size is directly proportional to the size of the mother animal. Newly released progeny ranges from 1 to 3 mm in length. Larger progeny can produce buds within 24 hours. Sexual maturity is reached within 8–10 days under optimal environmental conditions. Growing buds and newly released progeny exhibit the characteristic refractive blue sheen of their mother. Soon after release, however, the concrement densities decrease to a sparse distribution primarily in the caudal half of the juvenile animal. As the animal matures the concrement

distribution expands and becomes denser such that sexually mature adults have the refractive blue sheen over the entirety of their dorsal surface.

**Progeny release rates.** Rates appear to vary in response to many environmental factors including, but not limited to, prey availability, diversity of prey, water quality, water flow, and light quality. Of the abiotic variables, light intensity appears to have the greatest influence on asexual budding (Fig. 6.8A). Control animals kept in darkness released about one bud every 10 days; those in high light released one bud every 6.4 days; and those under optimal light conditions released one bud every 2.9 days.

**Environmental limitations.** Salinity-tolerance experiments on adult specimens revealed 50% lethality concentrations at 24 ppt and 44 ppt over a three-day exposure with an optimal salinity (100% survival) of 34 ppt (Fig. 6.9A). Temperature experiments showed a 100% survival range of 18–28°C. Unlike the relatively gradual decreases in survival observed in the salinity experiments, abrupt drops to zero-survival occurred immediately outside this range (Fig. 6.9B).

**Comparative data.** We found few pronounced differences among species of *Convolutriloba* in their sexual reproduction. Egg size was statistically larger in *C. hastifera* than in the three other species (180 x 125µm in *C. hastifera* vs. 170 x 130 µm; one-way ANOVA with length:width ratio as the independent variable,  $\alpha = 0.05$ ,  $p < 0.001$ , post-hoc Tukey HSD test verified statistical difference of *C. hastifera* egg size), but there was no difference in embryo size. Embryos developed similarly in all species and hatched within the same 3-to-4-day window. All species' hatchlings were aposymbiotic and possessed a frontal organ and statocyst. Aposymbiotic hatchlings maintained their size for about one week, then gradually decreased in size and died within two weeks. We do not know how any of the species obtains algal symbionts



in the wild, but one-day-old hatchlings of *C. macropyga* were successfully infected with symbionts when algal (previously isolated from *C. macropyga*) culture was added to dishes containing the hatchlings.

Our comparative dark-survival data (Fig. 6.8B) show that *Convolutriloba macropyga* **sp. nov.**, *C. retrogemma*, and *C. longifissura*, experience 100% mortality after approximately 23–26 days in total darkness with access to prey. *Convolutriloba hastifera*, however, survives for 8 days more. In all species, as zoochloellae density decreased, density of red rhabdoid gland cells increased. Prior to death, all animals, regardless of species, were primarily red-orange in color and were a fraction of their original size despite having captured and consumed *Artemia* sp.

### **Taxonomic remarks**

One major feature that *Convolutriloba macropyga* and *Convolutriloba retrogemma* have in common is the mode of asexual reproduction by reverse budding, but the number of buds at any one time is generally greater in *C. macropyga*. *Convolutriloba hastifera* reproduces by transversal fission (personal observation of populations in Georgia and Maryland, USA, by Shannon, Sikes, and Hatch, and of populations in Innsbruck, Austria by Achatz, Gärber, and Gschwentner), *Convolutriloba longifissura* by transversal fission with a subsequent longitudinal fission (Åkesson *et al.* 2001).

Secondly, *C. macropyga* and *C. retrogemma* share similarities of the male copulatory organ. Both species possess lateral sclerotized canals leading to a vesicula granulorum, or “vesicle filled with granular secretion” *sensu* Hendelberg & Åkesson (1988). In our sections it is evident, especially in Paratype USNM 1100331 that the two canals unite before opening into the vesicula granulorum. In some specimens the appearance of these canals is different than

described above. Instead of a uniform diameter along the entire length, they may have constricted and extended sections, always in a bilaterally symmetrical pattern. This indicates that the canals may transport sperm actively. By contrast, no sclerotized canals are described in *C. hastifera*, and the terminal vesicle is filled with glandular secretions and sperm (Winsor 1990).

The new species shares with *C. hastifera* and *C. longifissura* the distribution of sagittocysts at the anterior end and on the dorsal side.

Like all other species of the genus, *C. macropyga* lacks a statocyst in the adult. As pointed out by Hendelberg & Åkesson (1988) caution should be exercised in declaring the absence of a statocyst since statocysts are absent in asexually produced individuals of *Amphiscolops langerhansi* von Graff, 1882 (Hanson 1960). Though we have found statocysts in the hatchlings of all four convolutrilobids, we have yet to successfully raise a hatchling (and its statocyst) through to adulthood. *Convolutriloba hastifera* and *C. retrogemma* have a frontal organ, which is lacking in *C. macropyga* and *C. longifissura*. Again, *C. macropyga* hatchlings have a frontal organ, though whether it is retained in sexually produced adults is unknown.

*Convolutriloba macropyga* stands distinct from the other species by having up to three bursal nozzles. The multiplication of bursal nozzles could be an adaptation to the high rate of oocyte production — that is, to facilitate higher rates of fertilization. The variable number of bursal nozzles could indicate that this character has not yet stabilized genetically. Another explanation could be that our population is genetically degraded (see *significance of sex* section below).

Concrement spots, which occur in different patterns over the entire dorsal surface in all other species of the genus, are restricted to a transverse distribution above the mouth and along the

lateral margins in the new species. The uniform, scattered distribution of concrement and the blue refractive sheen it affords the animal is exceptional.

*Convolutriloba macropyga* further differs from the other species by having more pronounced ventral flaps and possessing shorter orange-red rhabdoids (2–3  $\mu\text{m}$ ) than the other species (5–6  $\mu\text{m}$ ).

The length of spermatozoa varies significantly within the genus, ranging from 280  $\mu\text{m}$  in *C. macropyga* to 200  $\mu\text{m}$  in *C. retrogemma* (Hendelberg & Åkesson 1988), and 130  $\mu\text{m}$  in *C. longifissura* (Åkesson *et al.* 2001).

Unpublished molecular data of 18S-rDNA and COI sequences further corroborate that *C. macropyga* is distinct from all other convolutrilobids (personal communication, James Sikes, University of Maryland).

**Body-wall musculature.** Our findings on the arrangement of elements in the ventral body-wall musculature differ in various points from the pattern described in *C. longifissura* by Gschwentner *et al.* in 2003. First, circular muscles that bend around the anterior rim of the mouth are absent in *C. longifissura*. Second, the muscles around the mouth are all concentric in *C. longifissura* but in *C. macropyga* just the most inner ones follow this pattern; more eccentrically they cross each other in front of the mouth. In our specimens special pore muscles fan out from the mouth, too, but there are no intermediate muscles between those that run perpendicular to the anterior-posterior axis and those that run caudally. Contrary to the finding of Gschwentner *et al.* (2003) in *C. longifissura*, the posterior longitudinal muscles of *C. macropyga* do not converge towards the mouth but run parallel to the lateral body margin and attach to the body wall in front of the posterior rim of the capturing funnel (compare our figs. 6.5A–D with figs. 5A–D in Gschwentner *et al.* 2003). The differences found can be explained as

modifications due to the larger body size of *C. macropyga*, but it should be mentioned that posterior longitudinal muscles arising at the level of the mouth are described in *Picola renei* Achatz & Hooge, 2006 and *Wulguru cuspidata* Winsor, 1988 (see Hooge 2003), whereas special pore muscles that fan out from the mouth and cover the entire ventral side of the body are unique to *C. longifissura* within the Acoela.

**Endemism.** Although the natural habitat of the new species is unknown, we can deduce that it is likely indigenous to tropical Pacific or Indian Ocean reefs. *Convolutriloba hastifera* was collected in waters off Magnetic Island, Australia (Winsor 1990). *C. longifissura* came from an aquarium with material from Indonesia (Bartolomaeus & Balzer 1997), and we have collected it in Kaneohe Bay, Hawaii. Most interestingly, Ishikawa & Yamasu (1992) report a species similar to *C. retrogemma* — and even more similar to *C. macropyga* — in Japan. The Indo-Pacific origin is further warranted in that the vast majority of corals (the most common vector responsible for convolutrilobid infestations) in the retail market are imported from this area. No evidence exists, scientific or anecdotal, for a Caribbean *Convolutriloba*. Furthermore, our data show *C. macropyga* to be relatively stenohaline and stenothermal, thereby eliminating all temperate waters and estuaries as potential sources.

**Importance of light.** Åkesson & Hendelberg (1989) and Bartolomaeus & Balzer (1997) cited the inability of *C. retrogemma* and *C. longifissura* to survive indefinitely in the dark as evidence of the obligate nature of algal symbioses to these acoels. Bartolomaeus & Balzer (1997) determined that *C. longifissura* was more dependent on its algae than *C. retrogemma* in that it survived a mere 4 days in darkness while *C. retrogemma* survived 34–36. Our own experiment on dark-survival included all four species, allowing for comparison under identical conditions (Fig. 6.8B). The differences between our results and those of Åkesson & Hendelberg

(1989) and Bartolomaeus & Balzer (1997), specifically in *C. longifissura* which survived 23 days in our tests, indicate that some other factor(s) may have influenced the experiments (see *Toxicity* section below).

**Significance of sex.** Sexual reproduction appears to be necessary in this genus to maintain a healthy population. An isolated population of *C. longifissura* in a hobbyist's aquarium yielded "robust" asexual individuals over a one-year span in 2005–2006. We harvested 500–750 individuals every 3 months until June 2006 when only about 100 small specimens could be found. All of these last individuals were similarly deformed in ways affecting the transverse fission phase; both the adult and still-attached daughter usually died, but some simply failed to complete longitudinal fission. Throughout our studies of the convolutrilobids, we have witnessed several crashes in populations from otherwise pristine aquaria. Judging from the case of *C. longifissura*, we surmise that the genetic process known as *Muller's ratchet* (Muller 1932; Gordo & Charlesworth 2000) — the accumulation of deleterious mutations within an asexual population — is responsible for these sudden local extinctions. As in other asexual populations, the process could be reversed through sexual reproduction and genetic recombination.

**Toxicity.** Hendelberg & Åkesson (1988) and Bartolomaeus & Balzer (1997) both noted a coalesced "secretion" from the red gland cells of squeezed *C. retrogemma*, and *C. longifissura* specimens respectively. We find similarly, in the red rhabdoid gland cells of *C. macropyga*, that the red-orange contents of ruptured rhabdoids not only coalesce into a yellow-orange secretion, but that the secretion diffuses through the animal tissue fueling a chain reaction of further gland cell rupture and even lysis of zoochlorellae. Once a rupture occurs, a rapid disintegration of the entire animal ensues, accompanied by a distinct, bromine-like odor. In studying all four species

we found that when multiple animals were maintained in small volumes of water, such as culture dishes, the death of any individual resulted in a discoloration (yellowing) of the water, the bromine-like odor emission, and the subsequent death of the remaining acoels as well as of any live prey (*Artemia* sp.) present. To minimize the impact of this apparent toxic effect, we found it prudent to isolate individuals during experiments. We further found that residual secretions on insufficiently cleaned glassware can affect animals and confound experimental results. We recommend acid cleaning of glassware used to hold Convolutrilobids. Plasticware appears to retain higher residual concentrations and should not be re-used. During experiments in small volumes of water, we find it best to remove released progeny since wounds at the point of separation can leak toxins.

Because of its high fecundity and ability to produce offspring both asexually and sexually, *C. macropyga* could prove to be a good model organism for studying stem cells, reproduction, and development. The basal position that these worms occupy as members of the Acoelomorpha, now widely seen as the most primitive phylum of the Bilateria (Ruiz-Trillo *et al.* 1999; Ruiz-Trillo *et al.* 2004), makes such studies especially significant for understanding the most fundamental aspects of these processes. To encourage use of these animals we recommend the culturing methods described above, and, for shipping animals, we offer the following tips: Thermal extremes are an obvious concern, but death during shipment is more often caused by mechanical agitation. Through extensive trial and error, we have determined that specimens are best shipped in leak-proof plastic or Nalgene containers of at least 100-ml size, at low density (~10 animals per 100 ml maximum), and with no air bubbles. (Containers should be fully immersed in clean seawater as the animals are loaded to ensure all air bubbles are removed from the container and lid prior to sealing it. The container should remain immersed while being

sealed). Containers should be packed in Styrofoam shipping-boxes with sufficient insulating Styrofoam to minimize movement.

### **Acknowledgments**

We are grateful to Seth Tyler, Walter Hatch, and Bill Fitt for their support of this project. We wish to thank James Sikes for sharing his unpublished 18S and COI data. Special thanks go to Cappuccino Bay Aquarium for opening their store to our repeated collecting. This research was supported by the U.S. Environmental Protection Agency under STAR Fellowship No. FP-91636501-0 and by the National Science Foundation under Grant No. 0118804.

## Literature cited

Achatz JG, Hooge MD (2006) Convolutidae (Acoela) from Tanzania. *Zootaxa* 1362:1-21

Åkesson B, Gschwentner R, Hendelberg J, Ladurner P, Muller J, Rieger R (2001) Fission in *Convolutriloba longifissura*: asexual reproduction in acoelous turbellarians revisited. *Acta Zoologica* 82(3):231-239

Åkesson B, Hendelberg J (1989) Nutrition and asexual reproduction in *Convolutriloba retrogemma*, an acoelous turbellarian in obligate symbiosis with algal cells. In: Ryland JS, Tyler PA (eds) *Reproduction, genetics and distributions of marine organisms*. Olsen & Olsen, Fredensborg, Denmark, pp 13-21

Bartolomaeus T, Balzer I (1997) *Convolutriloba longifissura*, nov. spec. (Acoela) - first case of longitudinal fission in Plathelminthes. *Microfauna Marina* 11:7-18

Boyle JE, Smith DC (1975) Biochemical interactions between the symbionts of *Convoluta roscoffensis*. *Proceedings of the Royal Society of London. Series B, Biological Sciences* 189(1094):121-135

Butler JK (1979) Methods for improved light-microscope microtomy. *Stain Technology* 54(2):53-69

Gordo I, Charlesworth B (2000) On the speed of Muller's ratchet. *Genetics* 156(4):2137-2140

Graff L (1882) *Monographie der Turbellarien. I. Rhabdocoelida*. Verlag von Wilhelm Engelmann, Leipzig, 442 pp.

Gschwentner R, Baric S, Rieger R (2002) New model for the formation and function of sagittocysts: *Symsagittifera corsicae* n. sp (Acoela). *Invertebrate Biology* 121(2):95-103

Gschwentner R, Ladurner P, Salvenmoser W, Rieger R, Tyler S (1999) Fine structure and evolutionary significance of sagittocysts of *Convolutriloba longifissura* (Acoela, Platyhelminthes). *Invertebrate Biology* 118(4):332-345

Gschwentner R, Mueller J, Ladurner P, Rieger R, Tyler S (2003) Unique patterns of longitudinal body-wall musculature in the Acoela (Platyhelminthes): the ventral musculature of *Convolutriloba longifissura*. *Zoomorphology* 122(2):87-94

Hanson ED (1960) Asexual reproduction in acoelous Turbellaria. *Yale Journal of Biology and Medicine* 33:107-111

Hendelberg J, Åkesson B (1988) *Convolutriloba retrogemma* gen. et sp.n., a turbellarian (Acoela, Platyhelminthes) with reversed polarity of reproductive buds. *Fortschritte der Zoologie* 36:321-327

Hendelberg J, Åkesson B (1991) Studies of the budding process in *Convolutriloba retrogemma* (Acoela, Platyhelminthes). *Hydrobiologia* 227:11-17



- Hooge MD (2001) Evolution of body-wall musculature in the platyhelminthes (Acoelomorpha, Catenulida, Rhabditophora). *Journal of Morphology* 249(3):171-194
- Hooge MD (2003) Two new families, three new genera, and four new species of acoel flatworms (Acoela, Platyhelminthes) from Queensland, Australia. *Cahiers De Biologie Marine* 44(3):275-298
- Ishikawa K, Yamasu T (1992) An acoel flatworm species related closely to the species *Convolutriloba retrogemma* Hendelberg & Åkesson occurs in Okinawa Island, Ryukyu Archipelago. *Zoological Science* 9:1281
- Kostenko AG, Mamkayev YV (1990) The position of green convolutas in the system of Turbellaria (Acoela) .2. Sagittiferidae Fam N. *Zoologicheskyy Zhurnal* 69(7):5-16
- Muller HJ (1932) Some genetic aspects of sex. *American Naturalist* 66:118-138
- Ruiz-Trillo I, Riutort M, Fourcade HM, Baguna J, Boore JL (2004) Mitochondrial genome data support the basal position of Acoelomorpha and the polyphyly of the Platyhelminthes. *Molecular Phylogenetics and Evolution* 33(2):321-332
- Ruiz-Trillo I, Riutort M, Littlewood DTJ, Herniou EA, Baguna J (1999) Acoel flatworms: Earliest extant bilaterian metazoans, not members of Platyhelminthes. *Science* 283(5409):1919-1923
- Smith JPS, Tyler S (1984) Serial sectioning and staining of resin-embedded material for light microscopy: recommended procedures for micrometazoans. *Mikroskopie* 41(9-10):259-270
- Winsor L (1990) Marine Turbellaria (Acoela) from North Queensland. *Memoirs of the Queensland Museum* 28(2):785-800
- Winsor L (1988) A new acoel (Convolutidae) from the north Queensland coast, Australia. *Fortschritte der Zoologie* 36:391-394

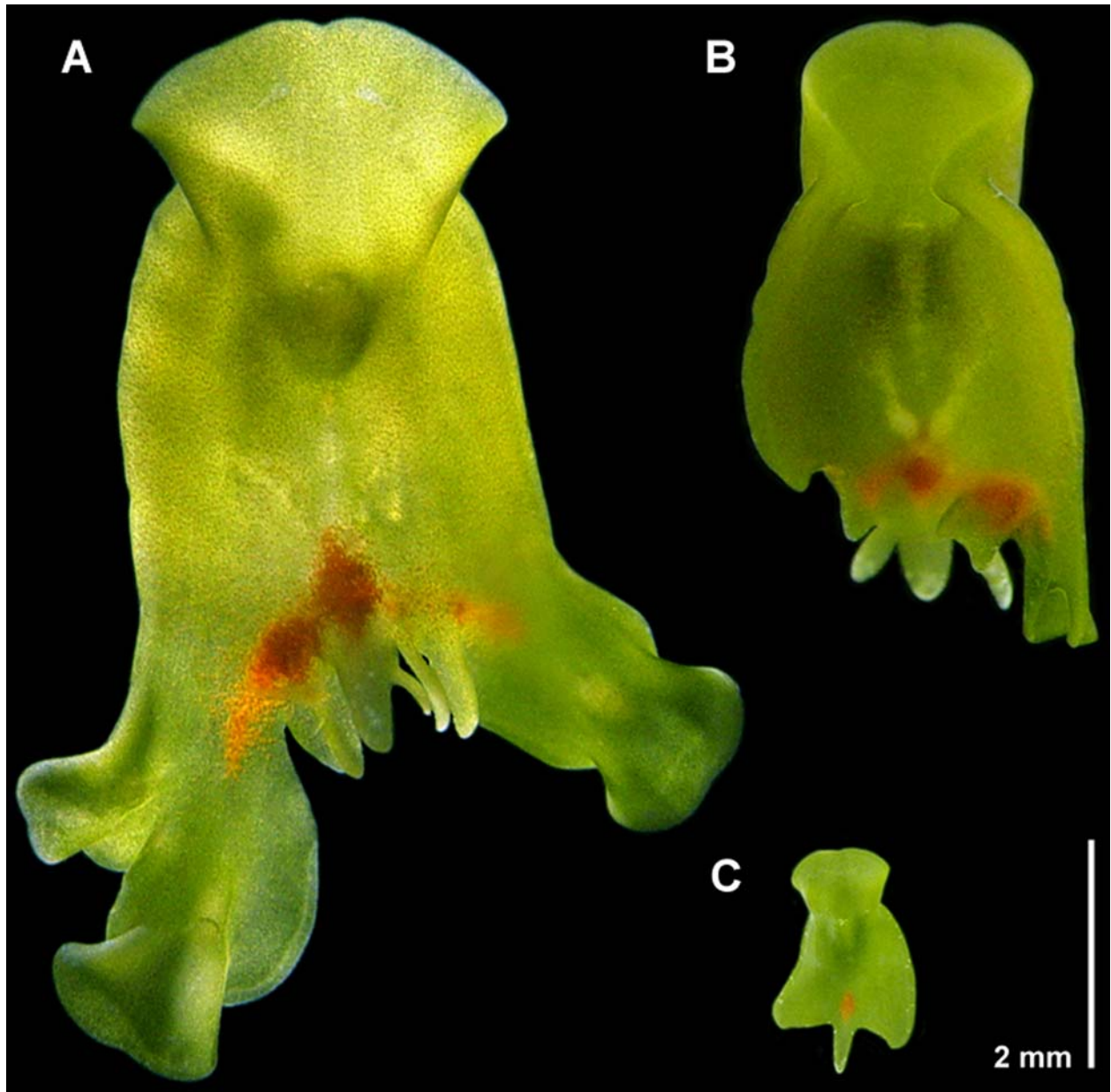


Figure 6.1. *Convolutriloba macropyga* **sp. nov.**; photomicrographs of living, non-anaesthetized, non-squeezed specimens. A. Dorsal view of a large sub-adult with asexual buds and multiple median caudal lobes. B. Ventral view of smaller sub-adult exhibiting the characteristic “capturing funnel” leading to the mouth. Visible are the maturing false seminal vesicles terminating at the male gonopore forward of the central red-pigment spot. C. Dorsal view of an immature, asexually-produced progeny showing the characteristic two rounded lateral caudal lobes and single, longer, slender median caudal lobe.

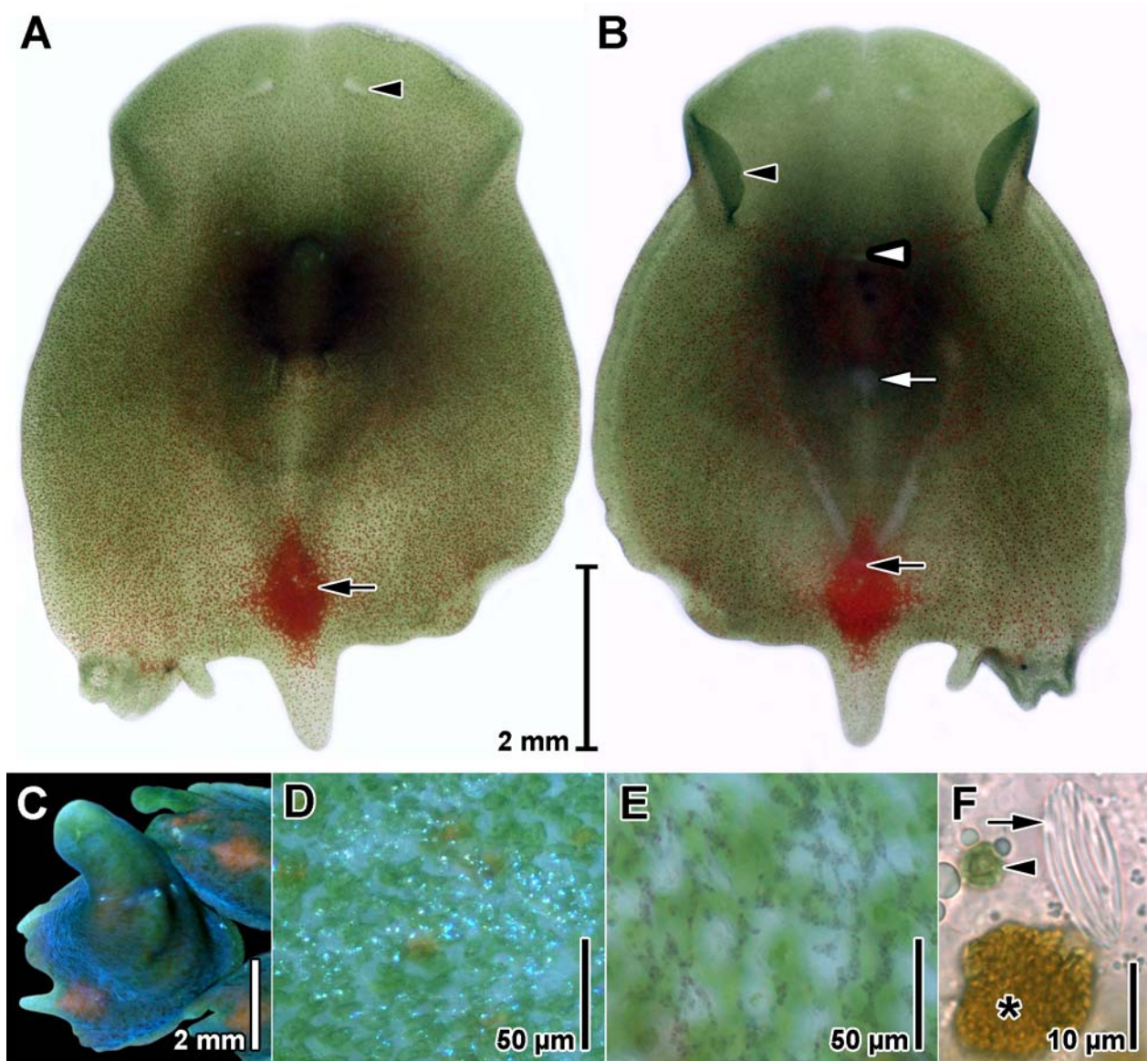


Figure 6.2. *Convolutriloba macropyga* sp. nov.; photomicrographs of living specimens. A. Dorsal view of whole anaesthetized specimen. Black arrowhead points to eyespot, black arrow to diamond-shaped spot of pigment cells. B. Ventral view of whole anaesthetized specimen. White arrowhead indicates mouth, white arrow seminal bursa and bursal nozzle tissue, black arrowhead ventral flap, and black arrow male gonopore. C. Dorsal view of cluster of three specimens showing refractive blue sheen. D. Dorsal body surface with blue concretions in incident light. E. Dorsal body surface with concretions in transmitted light. F. Rhabdoid glands of dorsal body wall. Arrow indicates refractile, uncolored rhabdoids; asterisk marks red rhabdoid gland cell; arrowhead indicates symbiotic algal cell.

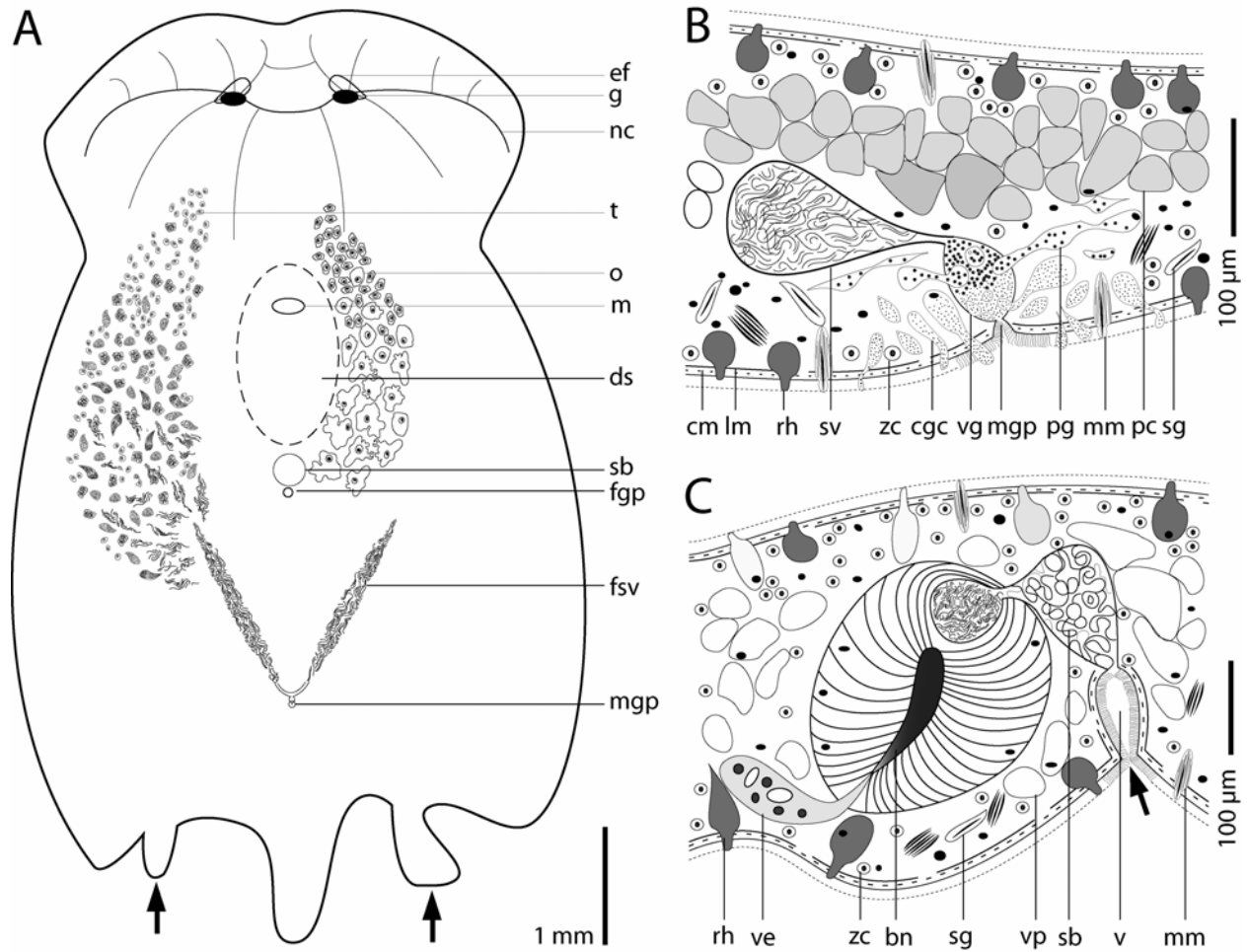


Figure 6.3. *Convolutiloba macropyga* sp. nov.; reconstructions to show arrangement of organs. A. Dorsal view. The gonads are paired but for clarity just the left testis and right ovary are shown. Arrows point to buds on lateral caudal lobes, arrowheads to paired ganglia and eyefields. B. Sagittal reconstruction of male copulatory organ. Peripheral parenchyma not shown. C. Sagittal reconstruction of female copulatory organ. Arrow points to female gonopore. Peripheral parenchyma not shown.

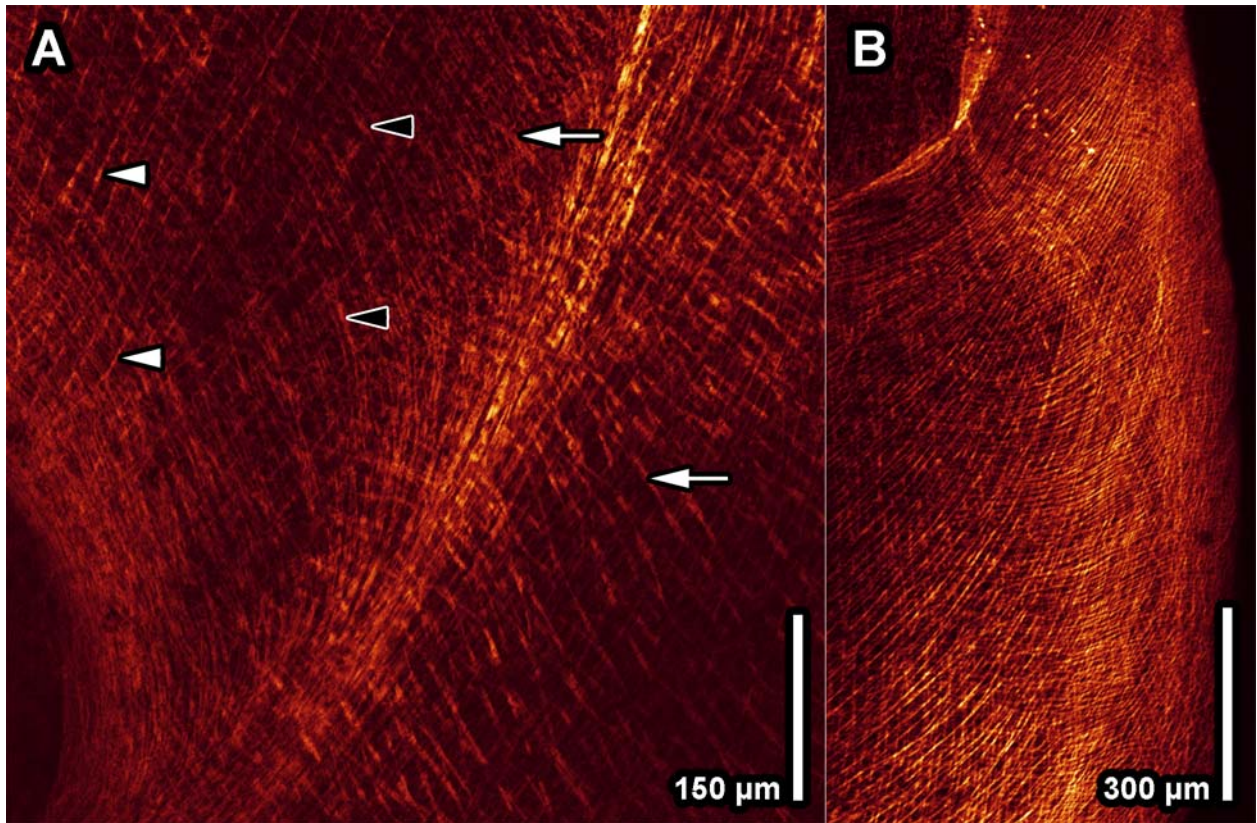


Figure 6.4. *Convolutriloba macropyga* sp. nov.; whole mount stained with Alexa-488-labeled phalloidin and viewed with confocal microscopy. A. Optical section of ventral body-wall musculature. Anterior toward upper left corner. White arrows point to longitudinal muscles, white arrowheads to radial muscles, black arrowheads to U-shaped muscles. B. Projection of ventral and lateral body-wall musculature adjacent to the mouth (in upper left corner).

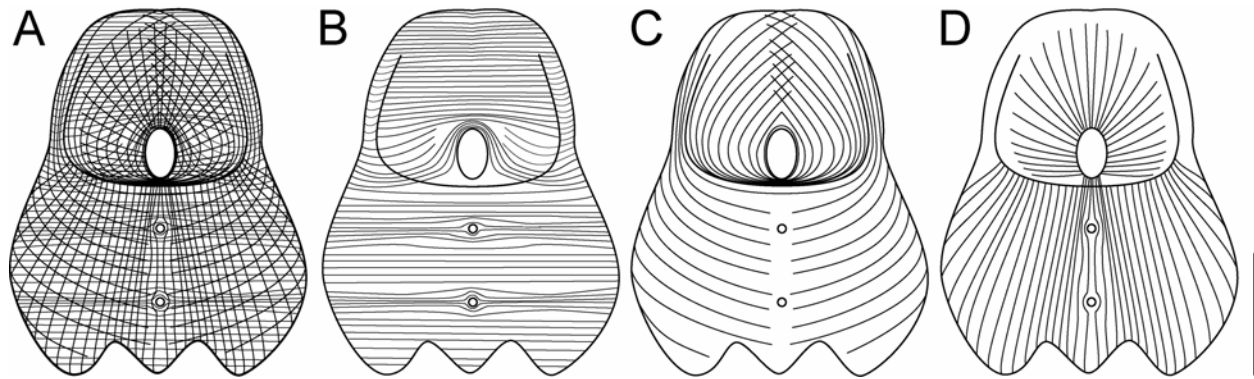


Figure 6.5. *Convolutriloba macropyga* sp. nov.; reconstructions to show ventral body-wall musculature. For clarity just a few muscles are shown. Scale bar: 1 mm. A. All muscle components. B. Circular muscles. C. U-shaped muscles and longitudinal cross-over muscles. D. Special pore muscles and longitudinal muscles.

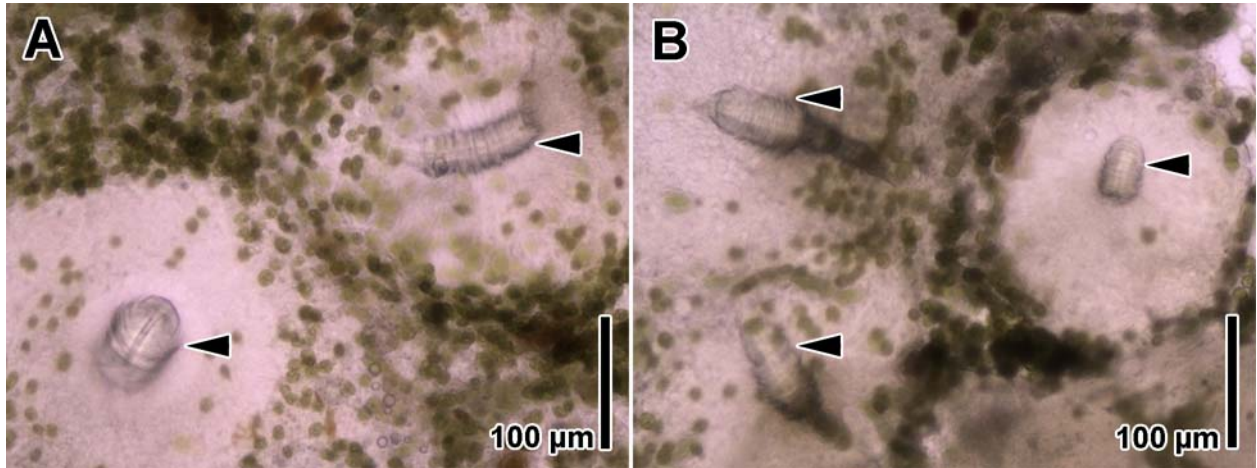


Figure 6.6. *Convolutriloba macropyga* sp. nov.; photomicrographs of living specimens. A. Dorsal view of female copulatory organ with two bursal nozzles. Black arrowheads point to bursal nozzles. B. Dorsal view of female copulatory organ with three bursal nozzles. Black arrowheads point to bursal nozzles.

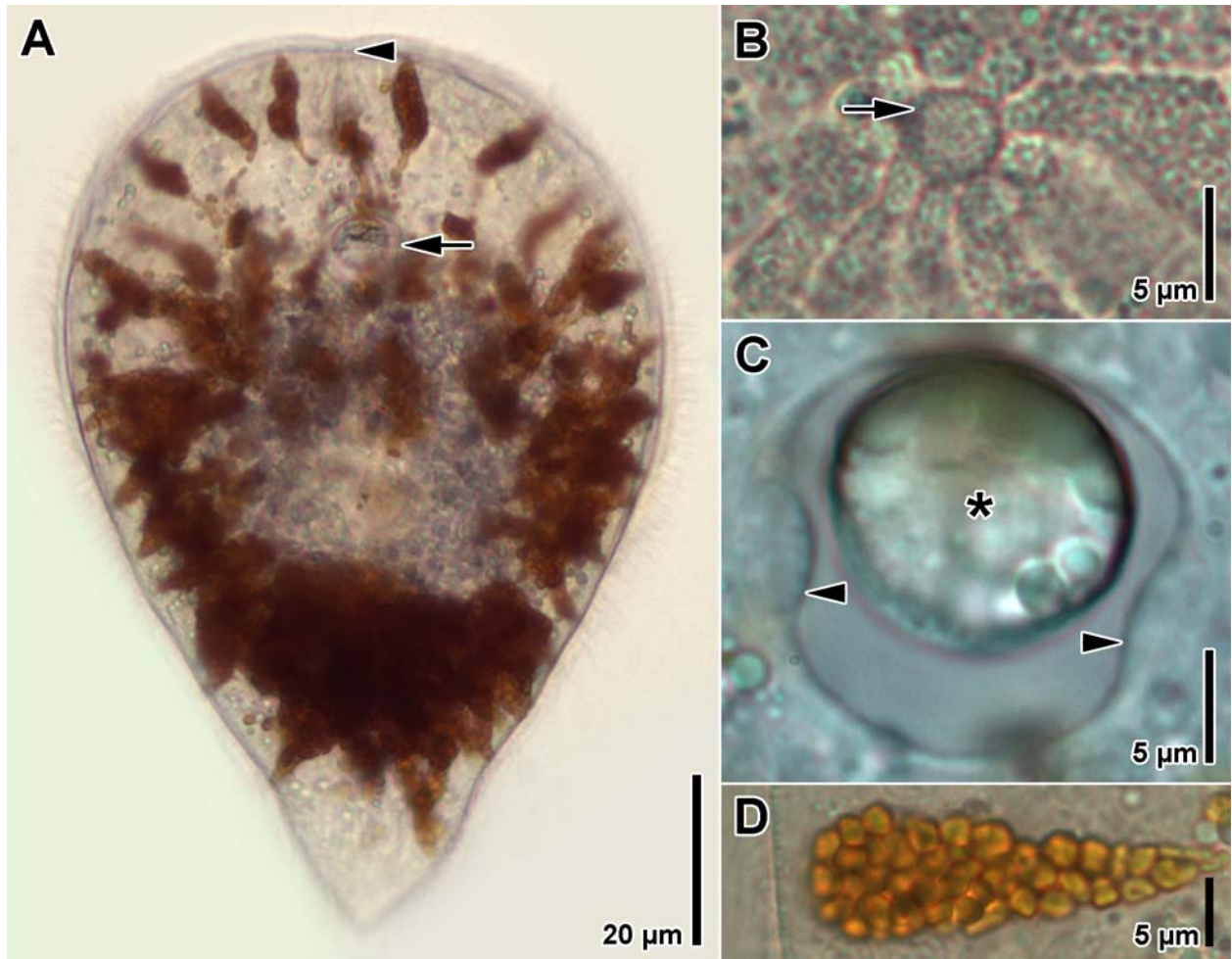


Figure 6.7. *Convolutriloba macropyga* sp. nov.; photomicrographs of live juvenile. A. Dorsal view of whole specimen. Arrow points to statocyst, arrowhead to frontal pore. B. Frontal organ. Arrow points to frontal pore. C. Statocyst. Arrowheads point to nuclei of parietal cells; asterisk marks statolith. D. Rhabdoid gland cell.



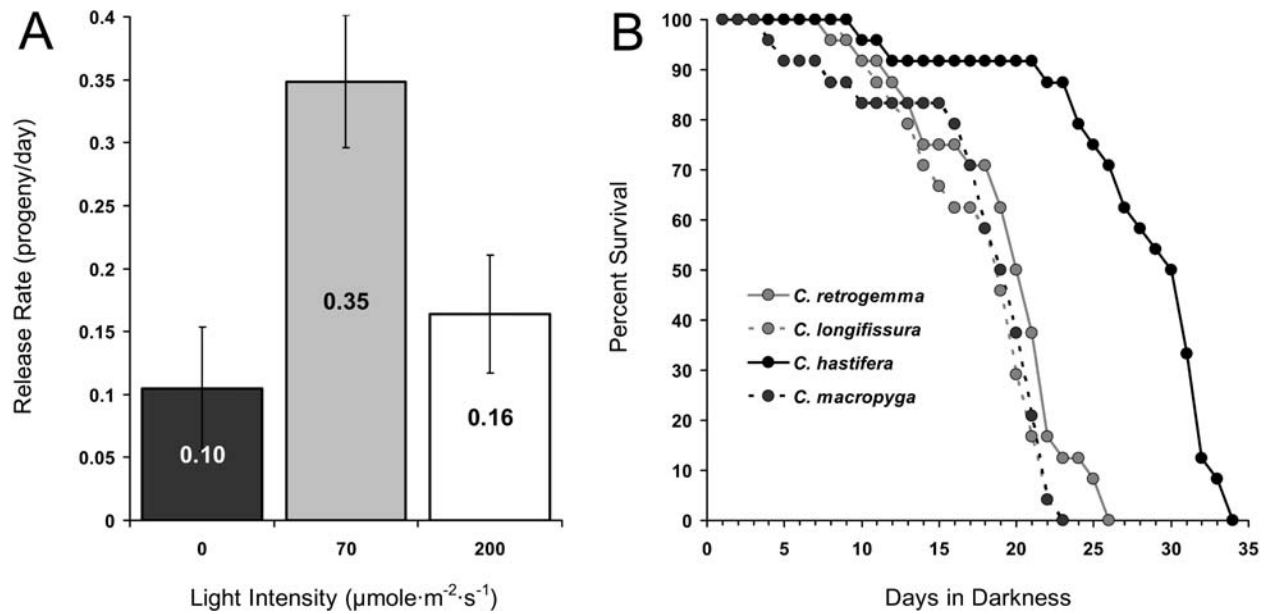


Figure 6.8. Light experiments in *Convolutriloba macropyga* sp. nov. and the *Convolutriloba* genus. A. Progeny release rates of *Convolutriloba macropyga* sp. nov. in response to light intensity. The experiment involved 24 adult specimens each in one of three light treatments: dark, low light, and high light. Trials ran for 15 days. Results are presented as average number of asexual progeny released per individual per day. Error bars are 95% confidence intervals. B. Comparison of dark-survival of species within the genus. Twenty-four adult animals of each species (*C. retrogemma*, *C. longifissura*, *C. hastifera*, and *C. macropyga*) were subjected to total darkness to determine and compare the extent of the obligate nature of algal symbiosis between the different host species. *Artemia* sp. prey was provided daily in superabundance to minimize the variable of holozoic starvation. Results are presented as percent survival over time.

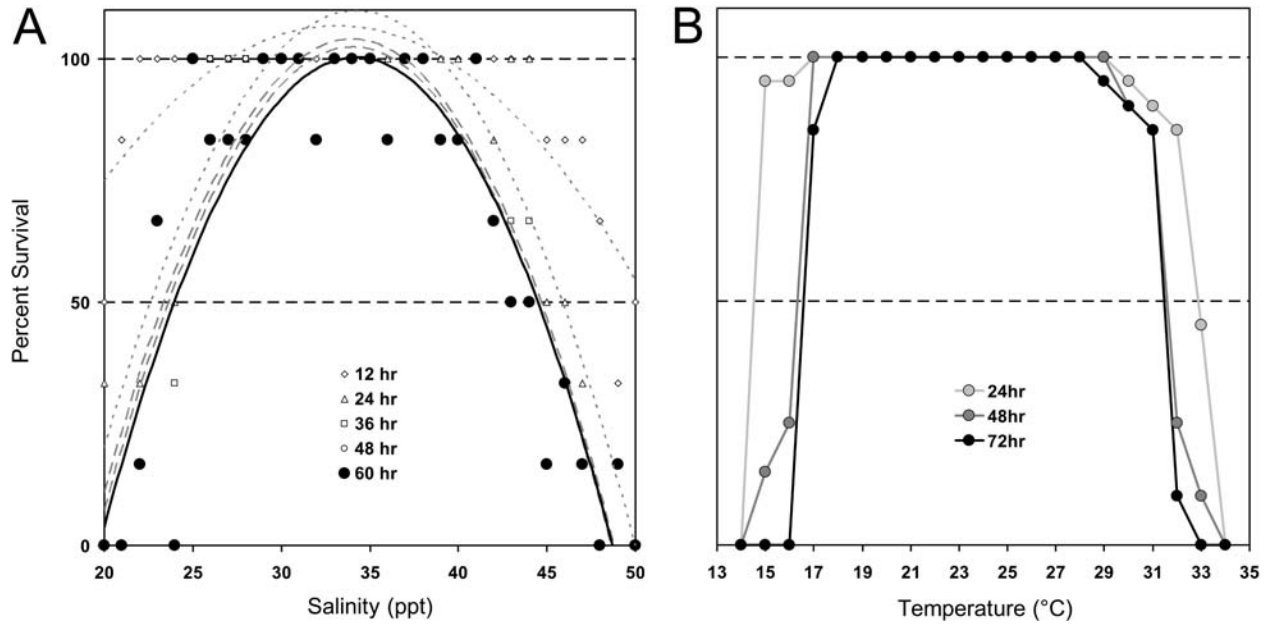


Figure 6.9. Environmental tolerances of *Convolutriloba macropyga* sp. nov.; A. Salinity tolerance. Animals were subjected to a range of artificial seawater salinities,  $n = 6$  per salinity. Surviving numbers were recorded every 12 hours for three days. No change in survival percentages was noted after 60 hours. Second order polynomial regressions were fit to each data set;  $r^2 = 0.81$  for 60-hour regression line. Fifty percent lethality occurred at 24 and 44 ppt. B. Thermal tolerance. Animals were subjected to a range of temperatures,  $n = 20$  at each temperature tested. Surviving numbers were recorded every 24 hours for three days.

## CHAPTER 7

### CONCLUSION AND FUTURE DIRECTION

## Conclusion

Looking back at the arduous academic journey that has lead me to this definitive point, I can now, from a retrospective vantage ask the eternally poignant question... “Would I do it again?” I’m not sure I have the answer.

The introduction of the genus *Convolutriloba* with the discovery of *C. retrogemma* by Hendelberg and Åkesson in 1988 , makes this animal and its congeners relative new-comers to the world of science. As with any new faces in the scientific crowd, these species were met by those they intrigued, with questions. Being one of the intrigued, I familiarized myself with the animals over countless hours of observation. I wondered at their behaviors. I developed hypotheses to explain their behaviors, and I set about to test these hypotheses.

E.O. Wilson laments in his 2006 book *The Creation* that as the scope of scientific knowledge has expanded over time, the focus of the individual scientist has consequentially narrowed. In order to continue a tradition of discovery, the world of science must explore the unknown; and as technology has advanced over the last two centuries, the once-grandiose hiding places of natural mystery have disappeared into the recesses of the sub-microscopic. As a result, Wilson points out, the major biological break-throughs of today center on genetics and biotechnologies, while studies at the organismal and population level are no longer at the cutting edge. The days of the adventurous, natural historians, like Alfred Russel Wallace and Charles Darwin, are dead; but a resurrection, he portends, is nigh. In reading *The Creation* and considering my own scientific direction, I had to agree.

Though I would never rank myself among the naturalists of old, the essence of the research I conducted on *C. retrogemma* categorically isolated me from the core scientific

pursuits of my cohorts and colleagues around me. At the onset of my graduate work, as my peers utilized and perfected the latest in molecular technologies to unravel the mysteries they sought to solve, I found myself, in comparison, poking at a poorly-understood animal with a metaphorical stick. I quickly discovered, in working with this “scientifically virgin” animal and its endosymbiont, that the established methods I had intended to employ in testing my hypotheses did not work when applied to the *Convolutriloba*. To overcome these obstacles and succeed in my research, I had to adjust the direction of my experimental inquiries into the zoological realm to better understand the animal and ascertain why tried & true methods proved ineffective. Only from the vantage point of an organismal biologist – giving dumb-luck and accidental discoveries their due – was I able to design experiments and novel methods that would allow me to succeed.

An inordinate percentage of my five years spent pursuing this degree was spent in the throes of trial and error. Experimental design is a topic usually presented as a progression of *just* the ideas and steps taken by a researcher that led him/her to a successful resolution. Rarely ever does one present in their articles, theses, or dissertations the reams of data collected from the trials that ended in *error*; hence, what is presented is trial and *success*. For those who have never undertaken the task of producing *de novo* methods, the laborious nature of the process is seldom understood and the polished method and results presented may seem intuitively obvious. I ask of anyone who actually reads this body of work, to bear in mind that most of the experiments detailed herein were designed from the ground up. Most required the design and fabrication of detailed, custom apparatus. Several involved novel methods. All resulted from untold numbers of preliminary or failed experiments, and from far more data than is presented.

Of the hypotheses tested, all were supported by this work. Though there never was any actual doubt as to whether photosynthates were translocated from the algal endosymbiont to the host in *C. retrogemma*, the novel qualitative method for determining translocation, utilized in chapter 3, verified what everyone already knew but which was not prudent to assume. Translocation did occur. The step-up photophobic behavior exhibited by *C. retrogemma* was hypothesized to be visually-mediated. Experiments in chapter 4 showed that the response was visually triggered by blue wavelengths, and was intensity dependent in that it was more pronounced in higher light intensity. The photoaccumulative behavior of *C. retrogemma* was hypothesized to be dependent on algal photosynthesis. Experiments in chapter 4 verified that the behavior was exhibited in symbiotic acoels, but not in aposymbiotic acoels. Experiments in chapter 5 showed that host light-preference varied depending on the nutritional status of the host, and that osmotic pressures in the host tissues due to light irradiance and photosynthate translocation increased as starvation progressed. These results suggested that the observed photoaccumulative/phototactic behaviors of *C. retrogemma* appeared to serve both photoregulatory and osmoregulatory functions, and were responsible for the observed basking aggregates of the animal.

### **Future Direction**

I have been working on the same little animal for eight years. Most of the world's six billion plus people have never heard of it, and in the grand scheme of things, it doesn't do much but irritate the occasional aquarist by making a bunch of clonal copies of itself in a reef tank every now and then. Friends have often asked me how it is that I have spent so much time on something so seemingly insignificant, a question I have asked, myself, at times. I don't know

how to answer the question except to say that I'm a scientist. I never intended to dedicate a goodly chunk of my existence to the *Convolutriloba*, but I asked a question... and it was all downhill from there. To those who respond with the quizzical head-tilt of a cocker spaniel, I offer my own skewed definition of science – the art of producing a perpetual series of questions in the pursuit of answers.

In working so closely with this animal, and in answering the few questions I asked, I have found along the way an amazing symbiosis, and many more questions. Much work remains in properly defining the symbiosis, in particular, the exact nature of the nutritional interactions and how they change in response to environmental and internal stresses. The four known species of *Convolutriloba* are asexually prolific and relatively easy to culture in captivity, making them ideal research subjects. These qualities, coupled with their fragile nature and sensitivity to environmental stress, makes them ideal candidates for studies aimed at developing potential biomarkers. As interesting as pursuing this line of research may seem, however, my current interests lie in the newest of the species, *Convolutriloba macropyga*.

All four convolutrilobids produce toxins (Shannon & Achatz 2007), and a collaborative effort is already in progress to identify the molecular structure of the toxin(s) in each species. In working with *C. macropyga*, I noticed immediately that juveniles and sexually-immature adults produced far less toxin than sexually mature adults. No such differences occur in the other three species as can be seen in figure 1.2 on page 10 – toxins are contained in red rhabdoid gland cells and render the animal a brownish-red color (instead of green from the algal symbiont) as gland cell densities increase. Preliminary experiments on the toxicity of the animals using a microwell method with *Artemia salina* (Solis *et al.* 1993), indicates that the toxicities of mature *C.*

*macropyga* and the other three species,  $LC_{50}$  determined per mg of worm tissue, were similar. The toxicity of juvenile *C. macropyga* was between one and two orders of magnitude less.

*Convolutriloba macropyga* reaches sexual maturity rather rapidly, and unlike the other species, reproduces sexually on a regular basis. This reproductive difference, when viewed in the light of the toxicity differences, suggests two significantly different life strategies within the genus. A working hypothesis has been proposed that a cost/benefit trade-off has been made by *C. macropyga* whereby toxin production – a metabolic cost – has been sacrificed at the expense of leaving juveniles susceptible to predation in an effort to reach sexual maturity sooner. In the other three species, sexual reproduction is rare, and toxins are maintained at high levels suggesting that asexual reproduction in juveniles is the preferred life strategy. An additional observation of morphology lends further credence to this hypothesis when viewed in conjunction with the results from chapter 4 of this dissertation.

In testing the photophobic response in *C. retrogemma*, it was determined that the acoel responds to photic stimuli of blue wavelengths; though not yet tested, it is assumed that the same is true of all 4 species. *C. macropyga* is unique among the convolutrilobids in that it bears epidermal concretions that refract a noticeable blue sheen. The granules occur in aggregates on the dorsal surface of the animal and increase in density as the animal matures, whereby juveniles have very few, and the entire back of sexually-mature adults is covered with them. Given that the animal can detect blue light and that concretion densities are maximized in sexually-mature adults, it stands to reason that these granules may provide a visual cue of “readiness” to potential mates.

It is the dynamics behind these differing strategies that intrigue me the most at this juncture. My primary desire, before continuing this work, is to identify and verify the natural



habitats to which these species are endemic – all but *C. hastifera* were discovered in aquaria. Based on my life/reproductive strategy hypothesis, I predict that *C. macropyga* will inhabit waters with greater seasonal temperature and or salinity fluctuations than the other three species... oh, and I'll get to travel.

## Literature cited

Hendelberg J, Åkesson B (1988) *Convolutriloba retrogemma* gen. et sp.n., a turbellarian (Acoela, Platyhelminthes) with reversed polarity of reproductive buds. *Fortschritte der Zoologie* 36:321-327

Shannon T, Achatz JG (2007) *Convolutriloba macropyga* sp.nov., an uncommonly fecund acoel (Acoelomorpha) discovered in tropical aquaria. *Zootaxa* 1525:1-17

Solis PN, Wright CW, Anderson MM, Gupta MP, Phillipson JD (1993) A microwell cytotoxicity assay using *Artemia salina* (brine shrimp). *Planta Medica* 59(3):250-252

Wilson EO (2006) *The Creation: An Appeal to Save Life on Earth*. W. W. Norton & Company, New York, 175 pp.